12-2021

Computational Analysis of the Spin Trapping Properties of Lipoic Acid and Dihydrolipoic Acid

Matthew Bonfield
East Tennessee State University

Computational Analysis of the Spin Trapping Properties of Lipoic Acid and Dihydrolipoic Acid

---

A thesis

presented to

the faculty of the Department of Chemistry

East Tennessee State University

In partial fulfillment

of the requirements for the degree

Master of Science in Chemistry

---

by

Matthew G. Bonfield

December 2021

Dr. Scott J. Kirkby, Chair

Dr. Marina Roginskaya

Dr. David Close

Keywords: spin trap, antioxidant, spin adduct, computational, ALA, DHLA, lipoic acid, Density Functional Theory, Hartree-Fock Self-Consistent Field, geometry optimization

ABSTRACT

Computational Analysis of the Spin Trapping Properties of Lipoic Acid and Dihydrolipoic Acid

by

Matthew G. Bonfield

While the spin trapping properties of thiols have been investigated through EPR analysis and kinetics studies, few groups have studied these properties using strictly computational methods. In particular, α-lipoic acid (ALA) and its reduced form, dihydrolipoic acid (DHLA), one of the strongest endogenously produced antioxidants, show potential for being effective, naturally occurring spin traps for the trapping of reactive oxygen species. This research covers electronic structure calculations of ALA, DHLA, and their corresponding hydroxyl radical spin adducts, performed at the cc-pVDZ/B3LYP/DFT level of theory. The effects on DHLA introduced by other radicals such as ·OOH, ·OCH_3, and ·$OOCH_3$ are reported. Explicit solvation was carried out using open-source molecular packing software and was studied using MOPAC PM6 semi-empirical geometry optimizations. Complete Basis Set (CBS) limit extrapolations were performed using cc-pVXZ (X = D, T, Q) Dunning basis sets under the DFT/B3LYP level of theory, and results are compared to the literature.

DEDICATION

I dedicate this work to my father, Kenneth, and my mother, Rhonda, for their demonstrable, everlasting support. This work also goes out to my brothers Adam, Sage, Tyler, and Greyson, and my sister Allie. I love you all.

I also dedicate this to my friends who have had to put up with me complaining, time and time again, about my workload as a chemistry major for the past several years. You know who you are; this one is for you.

ACKNOWLEDGEMENTS

I have received financial support for my research from the ETSU Graduate School's 'Graduate Student Research Grants program.

I would like to thank Dr. Scott Kirkby for his mentorship and guidance throughout my research and his willingness to allow me to choose my own path, which ultimately has made me a better scientist and critical thinker. His ability to make his students consider all sides of a question is unmatched and is a crucial trait for mentors to demonstrate. I also want to thank my committee members, Dr. Marina Roginskaya and Dr. David Close.

We are scientists who use computers, but we are not computer scientists.

-Dr. Scott Kirkby

I am grateful to Dr. Reza Mohseni and Dr. Ismail Kady for providing me with the support I needed to become an effective teaching assistant for undergraduate chemistry labs as part of my graduate assistantship.

My sincere appreciation goes to Maria Kalis, our executive aid, who is always happy to strike up an interesting conversation, go out of her way to provide snacks and coffee for the graduate students, assist us with course and conference registration, and be just an all-around great person.

TABLE OF CONTENTS

ABSTRACT 2
DEDICATION 4
ACKNOWLEDGEMENTS 5
LIST OF TABLES 8
LIST OF FIGURES 9
LIST OF ABBREVIATIONS 10
CHAPTER 1. INTRODUCTION 12
Free Radicals 12
Spin Traps 13
Lipoic and Dihydrolipoic Acid 16
Research Aims and Goals 20
CHAPTER 2. QUANTUM MECHANICS 22
Introduction to Computational Chemistry 22
Common Methodologies of Computational Chemistry 23
Schrödinger Equation 25
Hamiltonian Operator 27
Atomic Units 29
Born-Oppenheimer Approximation 30
The Hartree-Fock Self-Consistent Field Theory 31
Slater Determinants 33
Variational Principle 34
The Hartree Procedure 35
Density Functional Theory 39
DFT Exchange-Correlation Functionals 43
Basis Sets 46
Solvation Models 51
Conformer Analysis 55
CHAPTER 3. RESULTS AND DISCUSSION 59
Computational Details 59
Energies and Geometries of ALA and DHLA 60

Determining Primary Binding Sites 65
Proposing a Mechanism 67
Radical Delocalization in Doublet and Triplet States 70
Optimizations of Various Radical Adducts 73
Explicit Solvation Study 80
CHAPTER 4. CONCLUSIONS AND FUTURE WORK 85
REFERENCES 88
APPENDICES 101
Appendix A: ALA and DHLA 101
Appendix B: DHLA-OH Adducts 106
Appendix C: ALA-OH Adducts 133
Appendix D: Side Products Following H Abstraction 150
Appendix E: DHLA Hydrogen Abstractions 154
Appendix F: DHLA Adducts with Various Radicals 176
Appendix G: Various Tested Radicals 194
Appendix H: ALA Explicitly Solvated by Water 198
Appendix I: DHLA Explicitly Solvated by Water 211
Appendix J: DHLA-OH Explicitly Solvated by Varying Number of Water Molecules 225
VITA 239

LIST OF TABLES

Table 1: Calculated Geometries for DHLA and ALA, Optimized at DFT/B3LYP/cc-pVDZ 61

Table 2: Geometry Optimized Energies of ALA and DHLA Under HF and DFT/B3LYP 63

Table 3: Gas-phase Energies of DHLA-OH Adducts at DFT/B3LYP/cc-pVDZ..... 63

Table 4: Gas-phase Energies of ALA-OH Adducts at DFT/B3LYP/cc-pVDZ..... 64

Table 5: Gas-phase Energies of HT from DHLA Calculated at DFT/B3LYP/cc-pVDZ 67

Table 6: Gas-phase Energies of DHLA-rad(S1) Adducts at DFT/B3LYP/cc-pVDZ..... 73

Table 7: Optimized Energies and Dipole Moments of Various Free Radicals..... 74

Table 8: Energies of Other Products as a Result of HT at DFT/B3LYP/cc-pVDZ..... 75

Table 9: Sulfur S1-radical Bond Length in DHLA Adducts and C3-S1-rad. Bond Angles 79

Table 10: PM6 Analysis of ALA Explicitly Solvated by Water 81

Table 11: PM6 Analysis of DHLA Explicitly Solvated by Water..... 81

Table 12: PM6 Analysis of DHLA-OH Explicitly Solvated by Water 82

LIST OF FIGURES

Figure 1: Formation of both DMPO-OH and DMPO-O_2^- spin adducts..... 14

Figure 2: Melatonin reacting with $^1O_2$ to form AFMK..... 16

Figure 3: *(R)* enantiomeric structures of ALA and DHLA..... 16

Figure 4: Proposed mechanisms of thiol compounds; HAT, SPLET, SET-PT..... 17

Figure 5: Homologues of ALA and DHLA..... 18

Figure 6: Role of ALA and DHLA in lipid peroxidation pathway..... 20

Figure 7: Schematic of Self-Consistent Hartree Procedure..... 38

Figure 8: Representation of two 1s-type orbitals with different orbital exponents..... 49

Figure 9**:** Labeling scheme for DHLA and ALA..... 61

Figure 10: Avogadro 3-D representation of DHLA and ALA..... 62

Figure 11**:** HOMO in DHLA (top) and ALA (bottom)..... 66

Figure 12**:** Visual representation of HT study; lone electron is transferred from free radical..... 69

Figure 13**:** Spin density surfaces DHLA-OH(S1), ALA, and DHLA..... 71

Figure 14**:** 3-D representations of optimized spin adducts of DHLA with different radicals..... 76

Figure 15**:** ChemDraw® structures of tested DHLA-radical adducts..... 77

Figure 16**:** Molecular energy of (a) ALA, (b) DHLA, and (c) DHLA-OH(S2)..... 83

LIST OF ABBREVIATIONS

AFMK	N(1)-acetyl-N(2)-formyl-5-methoxykynurenine
ALA	α-Lipoic acid
AM1	Austin Model 1
AMBER	Assisted Model Building and Energy Refinement
ASA	Accessible Surface Area
CBS	Complete Basis Set
CC	Coupled Cluster
CoQ10	Coenzyme Q10
DEPMPO	5-(Diethoxyphosphoryl)-5-methyl-1-pyrroline-N-oxide
DFT	Density Function Theory
DHLA	Dihydrolipoic Acid
DMPO	5,5-dimethyl-pyrroline-N-oxide
DNA	Deoxyribonucleic acid
DPPH·	2,2-diphenyl-1-picrylhydrazyl
EPR	Electron Paramagnetic Resonance
GB	General Born
GGA	Generalized Gradient Approximation
GO·	Geometry Optimization
GSH	Glutathione
GTO	Gaussian-type Orbital
HAT	Hydrogen Atom Transfer
HF	Hartree-Fock
HT	Hydrogen Transfer
IST	Immuno Spin Trapping
IST	Immuno Spin Trapping
KS	Kohn-Sham
LDA	Local Density Approximation
LSDA	Local Spin Density Approximation
MD	Molecular Dynamics
MM	Molecular Mechanics
MMFF	Merck Molecular Force Field
MNDO	Modified Neglect of Diatomic Overlap
MP2	Möller-Plesset Second-order Perturbation
NADPH	Nicotinamide Adenine Dinucleotide Phosphate
NDDO	Neglect of Diatomic Differential Overlap
PBE	Poisson-Boltzmann equation
PES	Potential Energy Surface
PM	Parametric Method
RNS	Reactive Nitrogen Species
ROS	Reactive Oxygen Species
SCF	Self-Consistent Field

SE	Semi-empirical
SET-PT	single electron transfer then proton transfer
SPC	Simple Point Charge
SPLET	Sequential Proton Loss Transfer
STO	Slater-type Orbital
TF	Thomas-Fermi (model)
UFF	Universal Force Field
VitC	Vitamin C
α-TOH	α-Tocopherol

CHAPTER 1. INTRODUCTION

Free Radicals

Free radicals are any molecular species with one or more unpaired electrons in its valence shell.[1] The unpaired electrons render it more unstable and hence more reactive to other nearby species.[1] There are several endogenous sources of free radicals such as mitochondrial production of adenosine triphosphate (ATP), endoplasmic reticulum, and phagocytic cells.[2–5] External sources such as various medications, air pollution, and inhalation of cigarette smoke can also induce the formation of free radicals in biological systems.[1,2,4–6] To restabilize themselves, free radicals abstract an electron from another molecule which induces a chain reaction of single-electron abstractions from other molecules in the effort to regain stability.[2] Most free radicals are reactive oxygen species (ROS) or reactive nitrogen species (RNS) and constitute most other non-radical reactive species.[2] Examples of common ROS are hydroxyl radical (·OH), superoxide anion ($\cdot O_2^-$), and peroxide radical ($\cdot O_2^{2-}$), with the most reactive of the three being hydroxyl radical due to its extreme instability.[7] Examples of RNS include nitrogen dioxide radical ($\cdot NO_2$), peroxynitrite anion ($ONOO^-$), and nitroxyl anion (NO^-), which are generally derived from nitric oxide.[8] Excess concentrations of free radicals and other ROS/RNS results in oxidative stress which is detrimental to cell structures and deoxyribonucleic acid (DNA) and can denature proteins that are essential for enzymatic activity.[9] Oxidative stress is known to cause cancer,[10,11] neurological disorders,[12,13] cardiovascular disease,[14] and respiratory diseases,[15] so it is important to take measures to maintain heathy concentrations of free radicals in the body.[9,15] Our bodies have their own mechanisms for reducing excess concentrations of free radicals by producing chemicals that decrease free radical interactions. Antioxidants are defined as substances that inhibit oxidation or reactions promoted by oxygen, peroxides, or free radicals.[16] Since free

radicals require gaining another electron to become stable, antioxidants can terminate the chain reaction to prevent cellular structures from being damaged. While several natural antioxidants are produced endogenously, the most effective antioxidants are α-tocopherol (VitE), ascorbic acid (VitC), and β-carotene, which cannot be produced in the body and must be consumed through diet.[3,17,18] Glutathione, found in the cytosol of cells in concentrations of 1-10 mM,[19] is another common antioxidant but is endogenously produced by cells and is the most abundant low-molecular weight physiological thiol.[20]

Spin Traps

Accurate *in vitro* and *in vivo* detection of free radicals could be beneficial to monitoring oxidative stress in biological systems thus preventing disease development.[21,22] Electron paramagnetic resonance spectroscopy (EPR) is commonly used to precisely determine concentrations of oxygen-derived free radicals in various chemical and biological systems by employing spin traps.[23,24] Spin traps could be considered a sort of antioxidant that are used in EPR analysis since they can stabilize a free radical. Spin traps are defined as diamagnetic reagents that directly combine with transient radicals and form a more stable radical, called the spin adduct, composed of the original reagent and the radical where no atoms are lost in the process.[25] Without the formation of the spin adduct, the half-life of the free radical remains far too brief (10^{-7}-10^{-10} s) to be detected, where the formed spin adduct has a half-life far longer than those of hydroxyl or superoxide radicals.[2,23] While a spin trap could be an antioxidant, an antioxidant is not necessarily a spin trap, depending on its reaction pathway. An antioxidant can donate a proton to a radical, which in turn, stabilizes the radical but an adduct is not formed and the radical is now located on the antioxidant. Such is the case for VitE neutralizing a peroxyl radical. The spin trap, however, will "neutralize" the former radical while taking on a portion of

its spin density and forming the spin adduct. Nitrones, such as 5,5-dimethyl pyrroline-N-oxide (DMPO), are among the most commonly used spin traps in EPR analysis due to their ability to form stable, long-lasting spin adducts with multiple types of free radicals while maintaining their paramagnetism.[23]

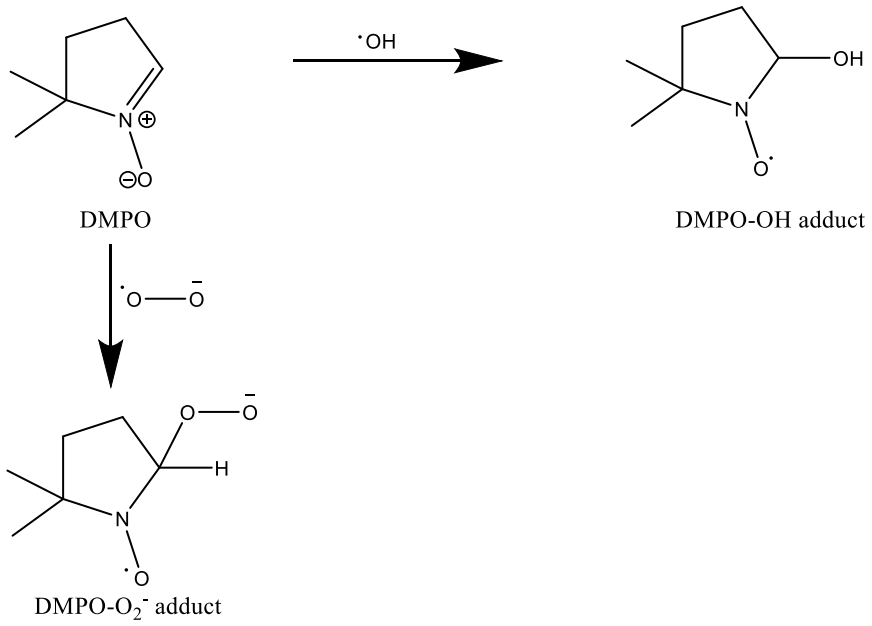

Figure 1: Formation of DMPO-OH and DMPO-O_2^- spin adducts

The DMPO spin adduct, like other nitrone spin traps, is resonance stabilized since the free radical can be delocalized to the oxygen atom. Another popular nitrone spin trap is 5-(Diethoxyphosphoryl)-5-methyl-1-pyrroline-N-oxide (DEPMPO) since it forms a spin adduct with hydroxyl radical that has a half-life of around 14 minutes, enabling detection by EPR instruments.[23]

Nitrone and nitroso compounds have been used to study free radicals in biological systems via immuno-spin trapping (IST).[26–28] Immuno-spin trapping is based on the reaction of a spin trap with a free radical to form a stable adduct followed by a method of detection. DMPO appears more than any other nitrone compound in most IST-related literature due to its high

sensitivity in EPR spectroscopy, good membrane permeability, and effectiveness in trapping free radicals.[28] For *in vivo* IST, the choice of spin trap is dependent upon not only its spin-trapping effectiveness but also its toxicity to the system in which it is employed. Khoo *et al.*[29] performed *in vivo* IST using DMPO in rats with diet-induced obesity to measure the presence of radicals in lipids in areas of high-fat density. The toxicity of DMPO, as well as other synthetic spin traps, is not well-documented and remains unknown up to this point since current literature is devoid of their pharmacodynamics and pharmacokinetics. In fact, some find that a spin trap that is known to be non-toxic and readily accepted by the body would be of interest in many fields of medicine. Perhaps chemicals such as antioxidants that are already produced in our bodies and other living systems pose a possible solution to this issue.

Melatonin, naturally produced from tryptophan in the brain, is a popular example of an endogenously produced chemical that has been extensively studied both experimentally and computationally for its antioxidant and spin trapping capabilities.[30–34] Melatonin can readily react with a multitude of ROS because of its hyperconjugation within its rings and its oxidation products are well known. An example of one of melatonin's main oxidation products is N(1)-acetyl-N(2)-formyl-5-methoxykynurenine (AFMK), which has been shown to mitigate X-ray-induced oxidative damage to DNA, proteins, and lipids in mice.[35] Melatonin reacts with singlet oxygen ($^1O_2$) to form AFMK:[36]

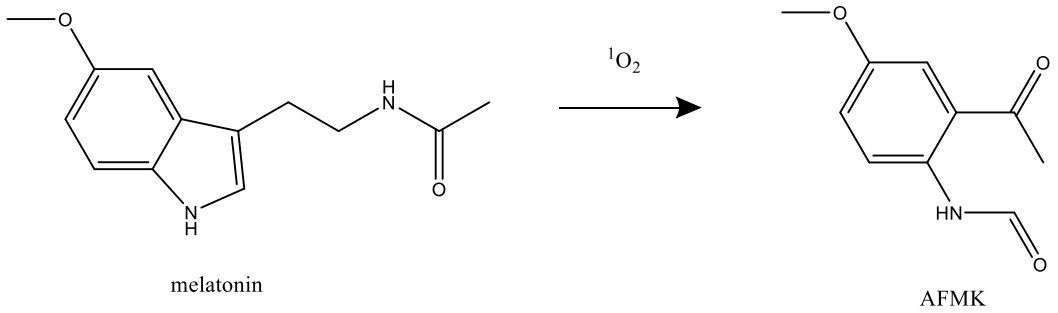

Figure 2: Melatonin reacting with $^1O_2$ to form AFMK

Lipoic and Dihydrolipoic Acid

Thiols, molecules that contain an -SH group, pose another potentially useful type of spin trap that differs from the typical nitrone or nitrosyl compounds commonly used in EPR spectroscopy. Specifically, α-lipoic acid (ALA) is a short chain fatty acid with two sulfur atoms that can be reduced to its dithiol form, dihydrolipoic acid (DHLA).

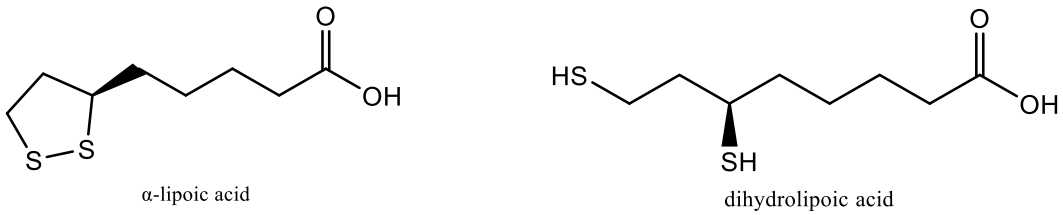

Figure 3: *(R)* enantiomeric structures of ALA and DHLA

ALA is an organic compound that is produced by animals, in which it is necessary for aerobic metabolism, and is primarily found in the heart and kidneys of humans where it functions as a cofactor in multienzyme energy production processes.[37–39] Since its discovery in 1937, ALA has been known to have many biochemical roles such as enhancing cellular glucose uptake,[40] serving as a cofactor for oxidative decarboxylations of α-keto acids,[41] managing and treating diabetic mellitus in patients with diabetic neuropathy,[42] and reducing the oxidized forms of other

important antioxidants including VitC, VitE, and glutathione (GSH).[37,40] ALA is an endogenously produced antioxidant and its ROS scavenging abilities have been studied by various groups and their effectiveness determined.[37,43] While racemic amounts of both the *R*- and *S*- enantiomers of ALA and DHLA exist, only the *R*- enantiomer is synthesized by organisms and is biologically active.[44] It has been shown that phenolic antioxidants (ArOH's) are able to deactivate galvinoxyl radical (GO·) and 2,2-diphenyl-1-picrylhydrazyl (DPPH·) through various mechanisms such as hydrogen atom transfer (HAT) and sequential proton loss electron transfer (SPLET).[44,45] Mikulski *et al.* [44] considered the close similarity between the O-H and S-H bonds and proposed that both the HAT and SPLET mechanisms can apply to ALA and DHLA for the trapping of ROS (Figure 4).

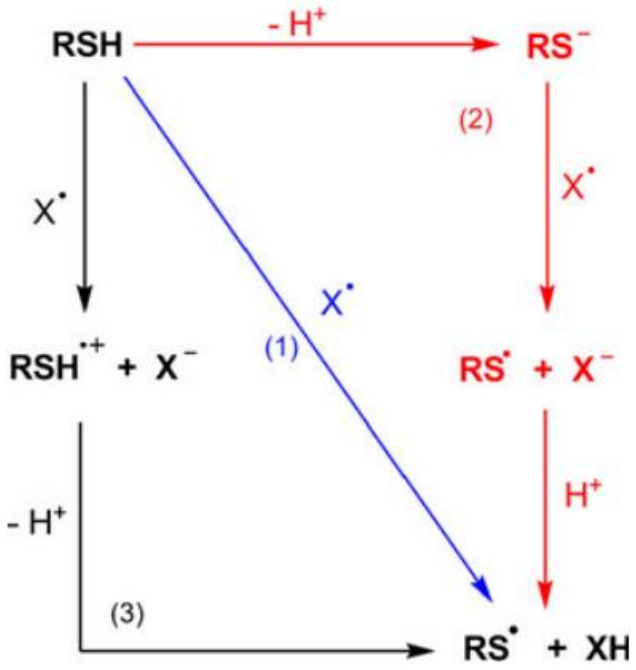

Figure 4: General antioxidant mechanisms of thiol compounds; HAT (blue), SPLET (black), SET-PT (red)[44]

The single electron transfer followed by proton transfer (SET-PT) mechanism differs only slightly from the SPLET mechanism in that the proton loss occurs before the interaction with the

free radical and the proton then stabilizes the now negatively charged X-ion.[44] Theoretical calculations by Castañ Eda-Arriaga *et al.*[46] revealed that the termination of ROS by DHLA, specifically with peroxyl radicals, most likely proceeds via the HAT mechanism and that DHLA is the main form of lipoic acid that has antioxidant properties. While ALA can react with strongly reactive free radicals to form a stable adduct, it has been observed that the reduced form, DHLA, is the main proponent in exhibiting antioxidant properties due to its two thiol groups.[44,46] Suzuki *et al.*[47] determined, through EPR analysis, that DHLA was significantly more effective than ALA at eliminating superoxide radical ($O_2^{-}\cdot$). Both ALA and DHLA were effective antioxidants in the presence of OH· due to its high reactivity. Shorter chain homologues of DHLA, such as 2,4-bisthiobutanoic acid and 4,6-bisthiohexanoic acid (Figure 5) were shown to have better antioxidant properties against $O_2^{-}\cdot$ compared to the longer chain homologues and the effectiveness against ROS varied in different environment polarities. DHLA performed better against ROO· in nonpolar environments and against $O_2^{-}\cdot$ in polar environments.[47,48]

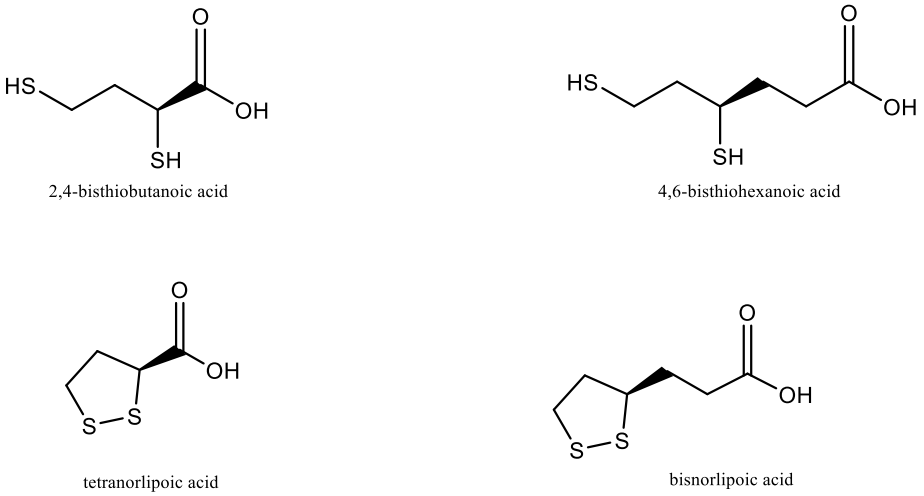

Figure 5: Homologues of ALA and DHLA

The role of ALA and DHLA in physiological systems is illustrated in Figure 6, which describes the peroxidation of unsaturated lipids. The lipid peroxyl radical, created after the lipid

is exposed to OH·, abstracts a proton from α-tocopherol (α-TOH) to form α-TO·. The peroxyl radical reacting with α-TO· is 1000-fold faster than it reacting with another unsaturated lipid, so the formation of α-TO· is far more likely and the antioxidant pathway will proceed. Alpha-tocopherol is regenerated by the presence of other antioxidants such as coenzyme Q_{10} (CoQ_{10}), VitC, and GSH. These antioxidants are oxidized after regenerating α-TOH but are then reduced back to their antioxidant states by DHLA, which is oxidized to ALA. Nicotinamide adenine dinucleotide phosphate (NADPH), an essential electron donor in all living organisms, reduces ALA back to DHLA, which is then ready to regenerate the other antioxidants. Although Figure 6 depicts the main task of the ALA/DHLA pair as an antioxidant regenerator in a biological system, it suggests that it may be possible for ALA and DHLA to follow a path similar to that of the lipid after its interaction with OH· and form a spin adduct with ROS. However, for the formation and existence of the spin adduct, this implies that a stable radical species involving either ALA or DHLA must exist. This species would most likely form during the 'Initiation' step in Figure 6, where OH· would be introduced to ALA or DHLA. However, an addition of the hydroxyl radical to some part of the molecule through some mechanism must generate a spin adduct. If a hydrogen abstraction should occur, another radical species may react to form a singlet-state adduct with ALA· or DHLA· and this would indicate a lack of spin trapping properties.

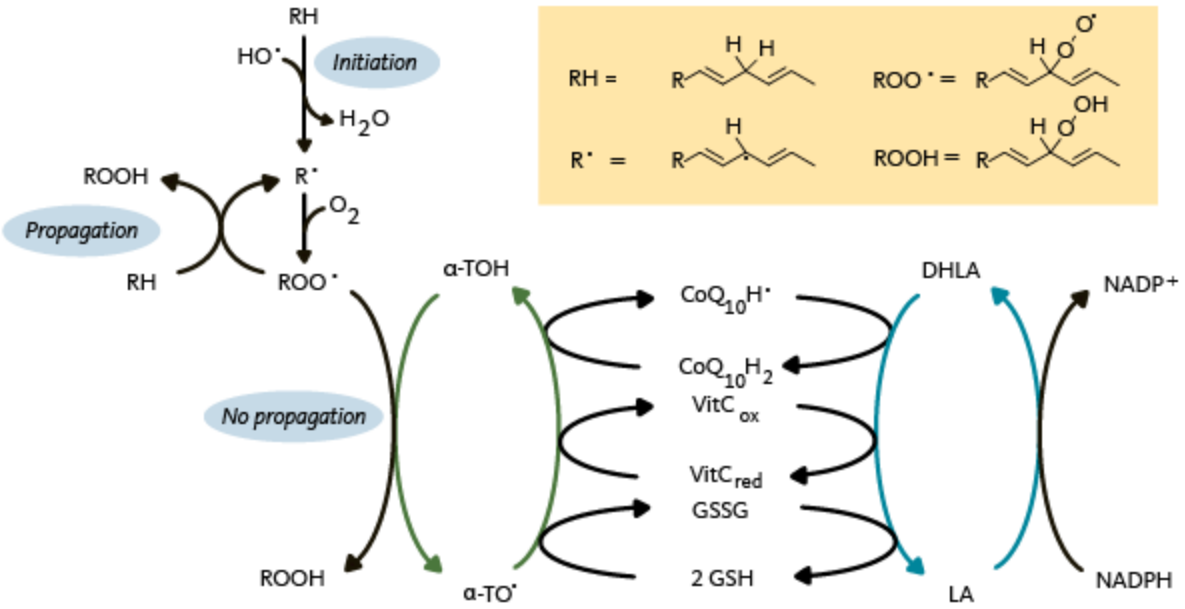

Figure 6: Role of ALA and DHLA in lipid peroxidation pathway[49]

Research Aims and Goals

The goal of this research is to investigate the spin trapping properties of both ALA and DHLA by way of computational analysis. This analysis is part of the search for naturally produced spin traps for use in *in vivo* EPR spectroscopy applications. Density Functional Theory geometry optimizations will provide sufficiently accurate results and could provide insight into any possible spin trap formation and trapping mechanisms that may be possible. Geometry optimizations and single-point energy calculations will allow for the determination of radical binding energies on ALA and DHLA which will help pinpoint the more likely candidate for adduct formation. Assuming a radical addition could generate a stable doublet-state anion in solution, binding energies and molecular orbital surface calculations may indicate the most likely site for radical addition. Spin density profiles for proposed adducts may illustrate quantitatively the relative extent of radical delocalization from the free radical to ALA or DHLA. Geometry

optimizations for ALA and DHLA radical adducts with other free radical ROS will paint a clearer picture for predicting which interactions are the most energetically favorable. Since EPR spectra can be computationally generated, doublet-state adducts formed with several different free radicals could be analyzed and the spin trapping properties of ALA and DHLA could be determined.

CHAPTER 2. QUANTUM MECHANICS

Introduction to Computational Chemistry

The inception of powerful processing units in today's computers has opened the door for extensive applications of quantum mechanics to analyze complex biological and chemical systems and are central to solving some of the most relevant issues in chemistry such as in the discovery of new pharmaceuticals.[50] While the past 40 years have offered protein crystallography and nuclear magnetic resonance (NMR) spectroscopy, enabling the 3D modelling of protein-ligand complexes to determine drug selectivity, computational methods have established ways to predict molecular interactions and *in silico* characterization of these complexes.[51] Computational methods have also offered valuable insight on the mechanism of various catalytic processes such transition metal-mediated C-C bond activation, reduction of atmospheric CO_2, and the splitting of water as a potentially revolutionary source of clean renewable energy.[52–54]

Many-body systems can be analyzed and approximated by applying theoretical approximation methods to calculate chemical properties such as possible geometrical conformations, relative energies, and reaction rates. Theoretical calculations of many-body systems could have hardly been roughly approximated before the introduction of electronic computers in the 1960s and 70s since an immense number of iterations are needed to obtain reasonably accurate approximations.[55] While today's computers have been and are still mostly used as analytical tools to feed other disciplines of chemistry, the increasing performance of modern-day computers has paved the way to a newer branch of chemistry, computational chemistry. In this discipline of chemistry, the computer is used as the main "experimental" tool to analyze chemical systems down to the atomic level. While developing new theoretical

methods allows for the analysis of a larger variety of systems, the primary focus of many computational chemists is to use methods that are currently available to analyze the problems at hand.[55] Fundamental chemical theory becomes increasingly useful as the processing power of modern computers becomes more capable.[56] While the Schrödinger equation cannot provide exact wavefunctions for molecules of any significant size, quantum mechanics can allow extremely accurate approximations of bond energies, transition states, and optimized molecular structures.

Common Methodologies of Computational Chemistry

Depending on the size of the molecule or chemical system, various computational methods can be applied to maximize accuracy without incurring substantial computation time. For large biological molecules such as cholesterol and proteins, a computational method called molecular mechanics (MM) can be applied to the system, which classically treats the atoms and bonds as a collection of "balls and springs."[57] The individual bonds are each assigned their own continuous interaction potentials which can be gathered from empirical data. Invoking classical mechanical treatment of quantum mechanical systems by using MM force-fields drastically decreases computation time by several orders of magnitude, depending on the size of the system.[58] Geometry optimizations using molecular mechanics can be performed in a matter of seconds on most computers due to the simplification of the molecule via classical interpretations.[57] Although MM calculations for large molecules take relatively little time, they can still yield very accurate results when the correct parameters are available. However, MM cannot generate geometries relating to the formation and breaking of bonds during a chemical reaction since parameters of only ground state molecules are considered.[59]

Ab initio methodology is another valuable tool in computation chemistry and utilizes the Schrödinger equation to calculate a wavefunction for the chemical system. The wavefunction is then used to derive the electron distribution around the target molecule or system and can allocate several properties such as polarity, vibrational modes, and optimized geometry along a potential energy surface (PES).[57,58,60] Popular *ab initio* methods include Hartree-Fock theory (HF),[61,62] second-order Møller-Plesset (MP2) perturbation theory,[62] and coupled cluster (CC).[60,63] Though several post-HF methods have been developed to overcome the shortcomings of the original, it still remains an iconic starting point in *ab initio* methods. While *ab initio* methods yield desirable results for relatively small molecules, calculations performed on larger molecules are not computationally economical and require the use of extremely powerful computers to keep computation time practical.[60]

Density Functional Theory (DFT) is another increasingly popular and useful computational tool that is also based on the Schrödinger equation, however, this method does not involve the computation of the wavefunction in order calculate the molecular electron density. The inclusion of interelectron repulsion in DFT methods has allowed these calculations to be much more accurate than HF especially when dealing with larger molecules and keeps computational costs low, making it arguably the most widely used quantum mechanical computational method today. [57,64,65] Two commonly used DFT hybrid functionals are Becke, 3-paramter, Lee-Yang-Parr (B3LYP) and Generalized Gradient Approximation (GGA), each with their own primary applications.[66–69]

Semi-empirical (SE) methods are like *ab initio* calculations in that they calculate a wavefunction using the Schrödinger equation, but the resultant complex integrals are not evaluated. Instead, best-fit experimental values (hence *empirical*) are plugged into the

mathematical procedure using a process called parametrization. This half-experimental, half-theoretical approach allows semi-empirical calculations to be orders of magnitude faster than *ab initio* methods while still maintaining reasonable accuracy for calculations such as geometry optimizations of large biomolecules.[57] For such large-scale molecules, the most popular semi-empirical methods approximate HF theory to streamline the evaluation of millions or billions of biomolecular interactions.[70] The most popular SE methods are based on the Neglect of Diatomic Differential Overlap (NDDO) approximation and include Austin Model 1 (AM1)[71] and Parametric Method (PM) series models (*e.g.* PM3[72], PM6[73]). AM1 showed potential by being able to better reproduce hydrogen bonds compared to the Modified Neglect of Diatomic Overlap (MNDO) approximation, which also stems from NDDO.[72] The PM3 method is an improvement upon AM1 by introducing automatically optimizable spectroscopic parameters,[72] while PM6 yields smaller errors in heats of formation for main-group elements, offering an extension of NDDO method to all transition metals and improved core-core repulsion potentials for lighter first- and second-row p-block elements.[70,73]

Schrödinger Equation

The time-dependent Schrödinger equation originates from classical mechanics but describes the state of a quantum mechanical system and how it changes with the evolution of time: [74,75]

$$\frac{-\hbar^2}{2m}\frac{\partial^2\Psi(x,t)}{\partial x^2} + V(x)\Psi(x,t) = -i\hbar\frac{\partial\Psi(x,t)}{\partial t} \quad (2\text{-}1)$$

where $\hbar$ is Plank's constant, h, divided by 2π, the reduced Planck constant, $\Psi(x,t)$ is the wavefunction of the system as a function of 1-dimensional position, x, and time, t, m is the total mass of the quantum system, V is the potential energy operator, and i is the imaginary operator

($i = \sqrt{-1}$). The term on the right side of Equation 2-1 is equivalent to the Hamiltonian operator. From the time-dependent equation, the time-independent Schrödinger equation can be derived by evaluating the time evolution of the wavefunction:

$$\widehat{H}\Psi = i\hbar\frac{\partial\Psi}{\partial t} \qquad \frac{-\hbar^2}{2m}\frac{\partial^2\Psi(x)}{\partial x^2} + V(x)\Psi(x) = E\Psi(x) \qquad (2\text{-}2)$$

where $\widehat{H}$ is the Hamiltonian operator. Note that the time-independent equation is only a function of position x. The Hamiltonian operating on the wavefunction produces an eigenvalue E which represents the total scalar energy of the wave state. Both the time-dependent and time-independent equations show that the total energy of the system is equal to the sum of the kinetic energy and potential energy. While Equations 2-1 and 2-2 represent space in one dimension, the equations can be expanded to three spatial dimensions in both scalar and polar coordinates.

$$\frac{-\hbar^2}{2m}\left[\frac{\partial^2\Psi}{\partial x^2} + \frac{\partial^2\Psi}{\partial y^2} + \frac{\partial^2\Psi}{\partial z^2}\right] + V(x,y,z)\Psi(x,y,z) = E\Psi(x,y,z) \qquad (2\text{-}3)$$

Using a Laplacian operator further simplifies the three-dimensional equation, making it far less laborious to write.

$$\nabla^2 f = \frac{\partial^2 f}{\partial x^2} + \frac{\partial^2 f}{\partial y^2} + \frac{\partial^2 f}{\partial z^2} \qquad (2\text{-}4)$$

$$\frac{-\hbar^2}{2m}\nabla^2\Psi + V(x,y,z)\Psi(x,y,z) = E\Psi(x,y,z) \qquad (2\text{-}5)$$

The equation can also be written using polar coordinates, which is preferred when describing a spherically symmetric quantum state.

$$\frac{-\hbar^2}{2m}\nabla^2\Psi + V(r,\theta,\Phi)\Psi(r,\theta,\Phi) = E\Psi(r,\theta,\Phi) \quad (2\text{-}6)$$

The Schrödinger equation cannot be solved exactly for systems larger than a hydrogen atom because anything larger, such as a helium atom, introduces a third body to the system and poses the issue of the Three-Body problem. This problem has no currently defined solution with the mathematics that are available but making reasonable assumptions about the system can yield accurate approximations when deriving the wavefunction of more complex systems. Applying these approximations is essential to obtaining experimentally accurate results in computational chemistry. However, there is a trade-off between accuracy and computational economy.

Hamiltonian Operator

In quantum mechanics, an operator carries out an operation on a defined function Ψ, which represents the wavefunction of a quantum state. The most well-known operator in quantum mechanics is the Hamiltonian operator which appears in the Schrödinger equation (Equation 2-6). Equation 2-2 defines the Hamiltonian operator $\hat{H}$ as the sum of the kinetic energy and potential energy operators of the quantum system. The resulting eigenvalue produced by the operation on the wavefunction corresponds to the total energy of the system.

$$\hat{H} = \hat{T} + \hat{V} \quad (2\text{-}7)$$

where $\hat{T}$ is the kinetic energy operator and $\hat{V}$ is the potential energy operator of a hydrogen atom,

$$\hat{T} = \frac{-\hbar^2}{2m}\left[\frac{\partial^2}{\partial x^2} + \frac{\partial^2}{\partial y^2} + \frac{\partial^2}{\partial z^2}\right] \quad (2\text{-}8)$$

$$\hat{V} = \frac{1}{4\pi\varepsilon_0}\frac{q_1 q_2}{r_{12}} = -\frac{1}{4\pi\varepsilon_0}\frac{e^2}{r} \tag{2-9}$$

where ε_0 is the permittivity of free space, q_1 and q_2 correspond to the charges of particle 1 and particle 2, *e* is the charge of a proton and r_{12} is the distance between the two interacting particles. The potential energy operator in Equation 2-9 depicts the Coulomb potential of a two-particle system. By inspection, the potential energy of the system increases as the distance between the particles decreases since it results in higher Coulomb attraction.

Since atoms contain both electrons and nuclei, the kinetic and potential energies of all components must be factored into the Hamiltonian. For example, the components of the total Hamiltonian shown in Equation 2-10. Equation 2-11 expands Equation 2-10 for a molecule.

$$\hat{H} = \hat{H}_{elec}^{kin} + \hat{H}_{nuc}^{kin} + \hat{H}_{elec-elec}^{pot} + \hat{H}_{elec-nuc}^{pot} + \hat{H}_{nuc-nuc}^{pot} \tag{2-10}$$

$$\hat{H} = -\sum_i \frac{\hbar^2}{2m_e}\nabla_{r_i}^2 - \sum_i \frac{\hbar^2}{2M_m}\nabla_{R_m}^2 + \sum_i \sum_{j>i} \frac{e^2}{4\pi\varepsilon_0 r_{ij}} - \sum_i \sum_j \frac{Z_M e^2}{4\pi\varepsilon_0 r_{iM}} + \sum_i \sum_{j>i} \frac{Z_M Z_N e^2}{4\pi\varepsilon_0 r_{MN}} \tag{2-11}$$

$\hat{H}_{elec}^{kin}$ and $\hat{H}_{nuc}^{kin}$ are the kinetic energy terms for the electrons and the nuclei, respectively. $\hat{H}_{elec-elec}^{pot}$ is the potential energy between the electrons, $\hat{H}_{elec-nuc}^{pot}$ is the potential energy between the electrons and nucleus, and $\hat{H}_{nuc-nuc}^{pot}$ is the potential energy between the nuclei, assuming a polyatomic system. The terms in Equation 2-11 are in respective order as those in Equation 2-10. The third term denotes interelectronic distance of *I* and *j* as radius r_{ij}, the fourth term denotes a distance between electron *i* and nucleus *M* by radius r_{iM}, and the fifth term denotes internuclear distance of radius r_{MN}.

Atomic Units

The inherent intricacy of the Hamiltonian suggests that it can be simplified to allow more facile calculation of the energy of the system.[74–76] By reducing the constants to atomic units (a.u.), the Hamiltonian becomes more suitable for quantitative analysis. Energy is measured in units of hartree (E_h) and one hartree is equivalent to the Coulombic repulsion force between 2 electrons that are separated by the distance of one Bohr radius, a_0. Reducing to atomic units gives us:[61]

$$\hbar = e = m_e = a_0 = 1\ a.u. \tag{2-12}$$

which simplifies Equation 2-11:

$$\widehat{H} = -\frac{1}{2}\sum_i \nabla_{r_i}^2 - \frac{1}{2}\sum_i \frac{1}{M_m}\nabla_{R_m}^2 + \sum_i \sum_{j>i} \frac{1}{r_{ij}} - \sum_i \sum_j \frac{Z_m}{r_{im}} + \sum_i \sum_{j>i} \frac{Z_m Z_n}{r_{mn}} \tag{2-13}$$

$$E_h = \frac{\hbar^2}{m_e {a_0}^2} = 4.3597447x10^{-18}\ J \tag{2-14}$$

$$a_0 = \frac{4\pi\varepsilon_0\hbar^2}{m_e e^2} = 5.2917721x10^{-11}\ m \tag{2-15}$$

Born-Oppenheimer Approximation

The Born-Oppenheimer approximation greatly simplifies the Hamiltonian by allowing for separate treatment of the wavefunctions for the nuclei and electrons.

$$\Psi_{total} = \Psi_{elec}\Psi_{nuc} \tag{2-16}$$

For example, for a two-electron and two-nuclei system:

$$\Psi(q_i, q_j, N_m, N_n) = \Psi(q_i, q_j; N_m, N_n)\Psi(N_m, N_n) \tag{2-17}$$

the wavefunction, which is originally a function of the positions of Electrons 1 and 2 (q_i, q_j) and nuclei *m* and *n* (N_m, N_n), is split into an electronic and nuclear component. Ψ_{elec} is the electronic component of the wavefunction and Ψ_{nuc} is the nuclear component. The electronic component is only a factor of the positions of the electrons which are only parametrically dependent on positions of the nuclei. In the case of a hydrogen atom, the Equipartition Theorem asserts the kinetic energies of the electron is equal to that of the nucleus so it can be assumed that because the velocity of the electron is far greater than that of the nucleus and the nucleus is therefore stationary in relation to the electron; the Born-Oppenheimer Approximation.

$$m_N \gg m_e; \quad T_N = T_e \tag{2-18}$$

By assuming a stationary nucleus, the nuclear kinetic energy component of the Hamiltonian can be neglected, thus simplifying the electronic Hamiltonian.[77] Equation 2-13 is reduced to Equation 2-19:

$$\hat{H} = -\frac{1}{2}\sum_i \nabla_{r_i}^2 + \sum_i \sum_{j>i} \frac{1}{r_{ij}} - \sum_i \sum_j \frac{Z_m}{r_{im}} + \sum_i \sum_{j>i} \frac{Z_m Z_n}{r_{mn}} \tag{2-19}$$

The eigenfunction of the electronic motion in the system is calculated using Equation 2-20:

$$\widehat{H}_{elec}\Psi_{elec} = E_{elec}\Psi_{elec} \tag{2-20}$$

and, using atomic units, $\widehat{H}_{elec}$ is defined as:

$$\widehat{H}_{elec} = -\frac{1}{2}\sum_{i}\nabla_{r_i}^2 + \sum_{i}\sum_{j>i}\frac{1}{r_{ij}} - \sum_{i}\sum_{j}\frac{Z_m}{r_{im}} \tag{2-21}$$

From Equation 2-19, the internuclear potential energy V_{nuc} is defined as:

$$V_{nuc} = \sum_{i}\sum_{j>i}\frac{Z_m Z_n}{r_{mn}} \tag{2-22}$$

Under the Born-Oppenheimer approximation, combining Equations 2-21 and 2-22 gives the total energy, *U*, of the system.

$$U = E_{elec} + V_{nuc} \tag{2-23}$$

The Hartree-Fock Self-Consistent Field Theory

The Hartree-Fock Self-Consistent Field Theory (HF-SCF) method provides an approximation for calculating the wavefunction of a quantum mechanical many-body system. As previously stated, the exact wavefunction of a hydrogen atom can be determined but anything larger requires approximations to overcome the many-body problem and additional interelectronic repulsion terms.[61] The Hartree-Fock procedure calculates the energy as a product of atomic orbitals while in accordance with the Pauli Exclusion principle, which states that two fermions cannot occupy the same quantum state. For example, starting with the helium atom, the

total wavefunction of the system is equal to the product of the wavefunctions for Electrons 1 and 2 located at point $\vec{r}_1$ and $\vec{r}_2$ respectively (Equation 2-24).

$$\Psi(\overrightarrow{r_1},\overrightarrow{r_2}) = \Psi(\overrightarrow{r_1})\Psi(\overrightarrow{r_2}) \tag{2-24}$$

Rather than an electron feeling the exact point charge of the other, it instead feels the mean field of the other electron: its effective potential V_r^{eff}. The potential that Electron 1 feels at point $\overrightarrow{r_1}$ from the mean field produced by Electron 2 is:

$$V_1^{eff}(\overrightarrow{r_1}) = \int \Psi^*(\overrightarrow{r_2})\frac{1}{r_{12}}\Psi(\overrightarrow{r_2})dr_2 \tag{2-25}$$

where $\frac{1}{r_{12}}$ is the interelectronic repulsion operator denoting the distance r_{12} between Electrons 1 and 2. This probability distribution can also be classically interpreted as the charge density of Electron 2.[78] The effective Hamiltonian of Electron 1 is defined in Eq. 2-27 as

$$\hat{H}_1^{eff} = \hat{T}_1 + V_1^{eff} \tag{2-26}$$

$$\hat{H}_1^{eff} = -\frac{1}{2}\nabla_1^2 - \frac{2}{r_1} + V^{eff} \tag{2-27}$$

where the first term is the electronic kinetic energy, the second term is the potential between the electron and nucleus, and the third is the effect of the second electron. The Hartree-Fock equation can be written as

$$\hat{H}_1^{eff}(\overrightarrow{r_1})\Psi(\overrightarrow{r_1}) = E_1\Psi(\overrightarrow{r_1}) \tag{2-28}$$

which gives the best orbital wavefunction for a helium atom.[78] In general, the Hartree product (Equation 2-29) suggests that the overall orbital wavefunction is equal to the product of the individual atomic orbital wavefunctions for an N-body system.

$$\Psi_{HP}(\vec{r}_1, \vec{r}_2, \dots, \vec{r}_N) = \phi_1(\vec{r}_1)\phi_2(\vec{r}_2) \dots \phi_N(\vec{r}_N) \tag{2-29}$$

The Hartree product is a simple and concise way of describing the orbital wavefunction but fails to satisfy the anti-symmetry principle, which states that electrons are described by wavefunctions that are anti-symmetric with respect to the interchange of the coordinates of an electron pair.[78–81] For a two-electron system, the coordinates of the electrons can be switched to give Equation 2-30:

$$\Psi_{HP}(\vec{r}_1, \vec{r}_2) = \phi_1(\vec{r}_2)\phi_2(\vec{r}_1) \tag{2-30}$$

such that Electron 1 is located at $\vec{r}_2$ and Electron 2 is located at $\vec{r}_1$. Applying the anti-symmetry principle, the original wavefunction can only be obtained by:

$$\phi_1(\vec{r}_2)\phi_2(\vec{r}_1) = -\phi_1(\vec{r}_1)\phi_2(\vec{r}_2) \tag{2-31}$$

which is not generally true for complete sets with N electrons.[80]

Slater Determinants

For multi-fermionic systems, Slater determinants provide wavefunctions that satisfy the anti-symmetry principle and, therefore, the Pauli exclusion principle. Upon interchange of two electrons, the wavefunction produced by the Slater determinant automatically changes signs for those electrons as a function of their spin and position. For a two-electron system, a linear combination of both sides of Equation 2-31 is taken:

$$\Psi(\vec{r}_1, \vec{r}_2) = c[\phi_1(\vec{r}_1)\phi_2(\vec{r}_2) - \phi_1(\vec{r}_2)\phi_2(\vec{r}_1)] \tag{2-32}$$

where *c* is a normalization constant. Equation 2-33 can be expressed as a Slater determinant (Equation 2-33).

$$\Psi(\vec{r}_1, \vec{r}_2) = \frac{1}{\sqrt{2}} \begin{vmatrix} \phi_1(\vec{r}_1) & \phi_2(\vec{r}_1) \\ \phi_1(\vec{r}_2) & \phi_2(\vec{r}_2) \end{vmatrix} \tag{2-33}$$

For a multi-electron case with N electrons, the Slater determinant takes the following generalized form:

$$\Psi(\vec{r}_1, \vec{r}_2, \dots, \vec{r}_N) = \frac{1}{\sqrt{N!}} \begin{vmatrix} \phi_1(\vec{r}_1) & \phi_2(\vec{r}_1) & \cdots & \phi_N(\vec{r}_1) \\ \phi_1(\vec{r}_2) & \phi_2(\vec{r}_2) & \cdots & \phi_N(\vec{r}_2) \\ \vdots & \vdots & \ddots & \vdots \\ \phi_1(\vec{r}_N) & \phi_2(\vec{r}_N) & \cdots & \phi_N(\vec{r}_N) \end{vmatrix} \tag{2-34}$$

where N is the number electrons modeled by the Slater determinant. Constructing determinants for small systems of 3 or 4 electrons is feasible but anything larger becomes tedious and time-consuming. An important consequence of this mathematical form is that it suggests all electrons represented within a wavefunction are indistinguishable, which satisfies the Pauli exclusion principle.

Variational Principle

Assuming a normalized wavefunction, the electronic energy of a system can be represented using Dirac notation:

$$E_{trial} = \frac{\langle \Psi_{trial} | \hat{H}_{elec} | \Psi_{trial} \rangle}{\langle \Psi_{trial} | \Psi_{trial} \rangle} \tag{2-36}$$

where $\hat{H}_{elec}$ was previously defined in Equation 2-21. For symmetric energy expressions such as Equation 2-27, the variational theorem states that the approximated energy of the system is always greater than that of the true energy:[82]

$$E_{trial} \geq E_o \tag{2-37}$$

where E_{trial} is the energy calculated using a trial wavefunction Ψ_{trial}. The calculated trial energy is always an upper bound to the true energy of the system. The denominator in Equation 2-36 is necessary only if Ψ_{trial} is not initially normalized. The trial function is dependent upon a set of variational parameters and determines the accuracy of the function in relation to the true wavefunction.[82]

The Hartree Procedure

The helium model is a special case regarding the construction of the Slater determinant since the wavefunction can be split into its spatial and spin parts, but this cannot be done for systems with more than two electrons. For simplicity, consider a closed-shell system with 2*N* electrons:

$$\begin{aligned}\hat{H} &= -\frac{1}{2}\sum_{j=1}^{2N}\nabla_j^2 - \sum_{j=1}^{2N}\frac{Z}{r_j} + \sum_{j=1}^{2N}\sum_{j>i}\frac{1}{r_{ij}} \\ &= \sum_{j=1}^{2N}\hat{h}_j + \sum_{j=1}^{2N}\sum_{j>i}\frac{1}{r_{ij}}\end{aligned} \tag{2-38}$$

where

$$\hat{h}_j = -\frac{1}{2}\nabla_j^2 - \frac{Z}{r_j} \tag{2-39}$$

and the atomic orbital wavefunction takes the form of a complete Slater determinant. For the sake of this example, the complete set will incorporate electron spin for each atomic order.

$$\Psi(\vec{r}_1, \vec{r}_2, \ldots, \vec{r}_{2N}) = \frac{1}{\sqrt{(2N)!}}\begin{vmatrix} \phi_1\alpha(\vec{r}_1) & \phi_1\beta(\vec{r}_1) & \cdots & \phi_N\alpha(\vec{r}_1) & \phi_N\beta(\vec{r}_1) \\ \phi_1\alpha(\vec{r}_2) & \phi_1\beta(\vec{r}_2) & \cdots & \phi_N\alpha(\vec{r}_2) & \phi_N\beta(\vec{r}_2) \\ \vdots & \vdots & \ddots & \vdots & \vdots \\ \phi_1\alpha(\vec{r}_{2N}) & \phi_1\beta(\vec{r}_{2N}) & \cdots & \phi_N\alpha(\vec{r}_{2N}) & \phi_N\beta(\vec{r}_{2N}) \end{vmatrix} \tag{2-40}$$

where α and β represent spin-up and spin-down orientations of electrons. Evaluating the energy of the system is done similarly to Equation 2-35 and the result becomes:

$$E = 2\sum_{j=1}^{N} I_j + \sum_{i=1}^{N}\sum_{j=1}^{N}(2J_{ij} - K_{ij}) \tag{2-41}$$

where:

$$I_j = \int \Psi_j^*(\vec{r}_1)\hat{h}_j(\vec{r}_1)\Psi_j d\vec{r}_1 \tag{2-42}$$

$$J_{ij} = \iint \Psi_i^*(\vec{r}_1)\,\Psi_j^*(\vec{r}_2)\frac{1}{r_{12}}\Psi_i(\vec{r}_1)\Psi_j(\vec{r}_2)d\vec{r}_1 d\vec{r}_2 \tag{2-43}$$

$$K_{ij} = \iint \Psi_i^*(\vec{r}_1)\,\Psi_j^*(\vec{r}_2)\frac{1}{r_{12}}\Psi_i(\vec{r}_2)\Psi_j(\vec{r}_1)d\vec{r}_1 d\vec{r}_2 \tag{2-44}$$

where J_{ij} is the coulomb integral and K_{ij} is the exchange integral. There are no orbitals involving integration over more than 2 electrons since Equation 2-40 only involves 1- and 2-electron operators.[78] Applying the Variational Principle to Equation 2-40 gives the Fock operator, $\hat{F}$, which allows for determining the spatial orbital wavefunctions, $\Psi_i(\vec{r}_1)$:

$$\hat{F}(\vec{r}_1)\Psi_i(\vec{r}_1) = \varepsilon_i\Psi_i(\vec{r}_1); \quad i = 1,2,\ldots,N \tag{2-45}$$

Energy, ε_i, is the Hartree-Fock orbital energy. The values of i do not progress to 2*N* since the spatial component of the orbital wavefunction does not have *up* and *down* states like the electron spin component. The Fock operator is given by:

$$\hat{F}(\vec{r}_1) = \hat{h}(\vec{r}_1) + \sum_{j}^{N}[2\hat{J}_j(\vec{r}_1) - \hat{K}_j(\vec{r}_1)] \tag{2-46}$$

where $\hat{J}$ is the Coulomb operator and $\hat{K}$ is the exchange operator.

$$\hat{J}_j(\vec{r}_1)\Psi_i(\vec{r}_1) = \Psi_i(\vec{r}_1)\int \Psi_j^*(\vec{r}_2)\frac{1}{r_{12}}\Psi_j d\vec{r}_2 \tag{2-47}$$

$$\hat{K}_j(\vec{r}_1)\Psi_i(\vec{r}_1) = \Psi_j(\vec{r}_1)\int \Psi_j^*(\vec{r}_2)\frac{1}{r_{12}}\Psi_i(\vec{r}_2) d\vec{r}_2 \tag{2-48}$$

Solving for the energy of the i^{th} molecular orbital of the system gives:

$$\varepsilon_i = \int \Psi_i^*(\vec{r}_1)\hat{F}(\vec{r}_1)\Psi_i(\vec{r}_1)d\vec{r}_1 \tag{2-49}$$

such that Equation 2-49 becomes:

$$\varepsilon_i = I_i + \sum_{j=1}^{N}(2J_{ij} - K_{ij}) \tag{2-50}$$

Comparing Equation 2-50 to Equation 2-41 gives the total energy E of the system:

$$E = \sum_{i=1}^{N}(I_i + \varepsilon_i) \tag{2-51}$$

which sums up the first iteration of approximating the total energy of the system by entering a trial wavefunction to solve the Fock operator, generating a new wavefunction. This is a self-consistent procedure that forms the basis of all Hartree-Fock computational calculations. The process continues until wavefunctions converge and there are no longer any remaining changes to the initial guess that are outside of the predetermined tolerance limits. Figure 7 shows a visual schematic of the HF-SCF procedure. However, it must be recognized that this theory treats electrons as if they do not "feel" repulsion from other individual electrons from any specific point but rather the overall mean field produced by the movement of other electrons, eliminating the need to solve a many-body problem. The use of Slater Determinant also improves this theory by introducing anti-symmetric wavefunctions.

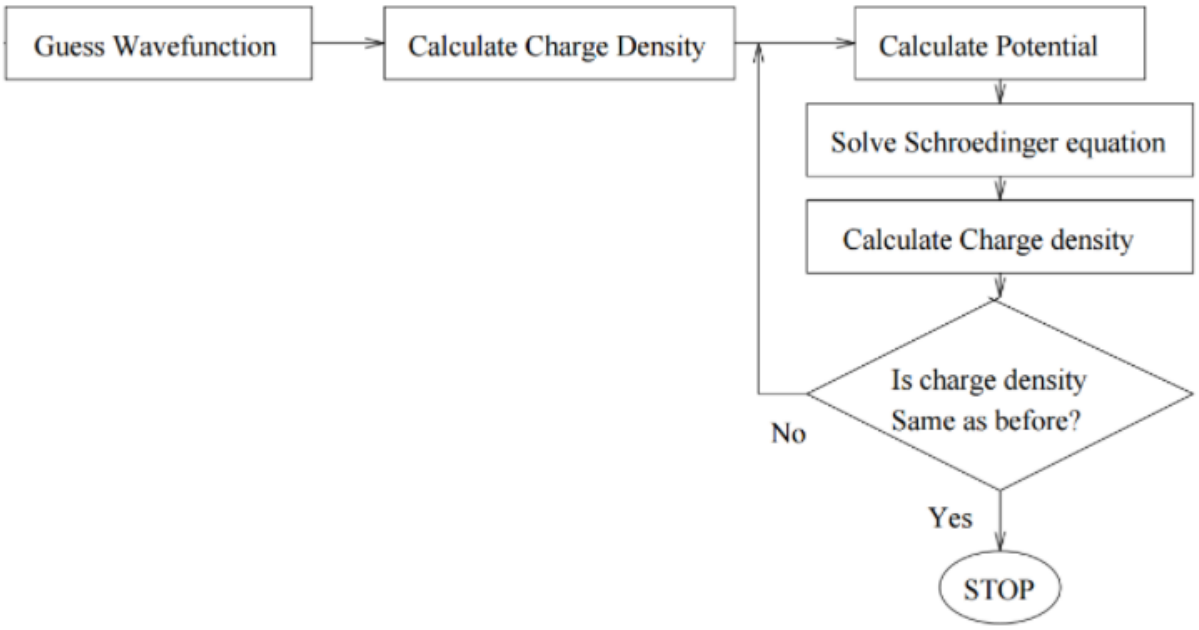

Figure 7: Flow chart of the Self-Consistent Hartree procedure[83]

Density Functional Theory

Modern Density Functional Theory (DFT) is an improvement upon Thomas-Fermi (TF) theory, whose creators, Llewellyn Thomas and Enrico Fermi, independently published atomic orbital calculations in 1927 without incorporating a wavefunction but rather by calculating the electron density of the system.[84–86] DFT is based on the 2 Hohenberg-Kohn theorems:[87,88]

1.) The ground-state properties of an atom or molecule are determined by electron density $\rho(r)$
2.) According to the variational theorem, a trial electron density must give an energy greater than or equal to the true energy

Electron density is defined as the quantity of electrons within a defined volume:

$$\rho(r) = \frac{\#\ of\ elecrons}{V} \tag{2-52}$$

but electron density can also be related to the wavefunction of the system by:

$$\rho(r) = \sum_{i=1}^{N} |\Psi_i|^2 \tag{2-53}$$

where N is the number of electrons and $|\Psi_i|^2$ is the probability density of an electron in the i^{th} state.

Unlike the wavefunction, the electron density of a system is experimentally observable. The total partitioned electronic energy of a system is written as Equation 2-54:

$$E_{tot} = E_T + E_V + E_J + E_{XC} \tag{2-54}$$

where E_T, E_V, and E_J represent the electronic kinetic energy, the energy of attraction between the electrons and nuclei, and the Coulombic repulsion between two electrons, respectively. These

first three terms were first introduced by TF theory, but this approximation had significant flaws in that it was not capable of calculating atomic orbital shell structure.[87] The electronic exchange energy term E_{XC}. was later independently introduced by Paul Dirac and Eugene Wigner in the 1930s.[89,90] The exchange energy term compensates for the oversimplification of electron repulsion introduced by E_J. which does not account for the correlation of the electrons with respect to their spin and motion. Hohenberg and Kohn showed that the atomic electronic energy can be calculated in terms of electron density $\rho(r)$. and all other components of the system are functionals, $E[\rho(r)]$, of electron density.[91,92] By incorporating electron density, Equation 2-54 can be rewritten as:

$$E_{tot}[n] = E_T[n] + E_V[n] + E_J[n] + E_{XC}[n] \quad (2\text{-}55)$$

where each energy term is now written as a functional of electron density. Equation 2-55 represents the Schrödinger equation of a "fictitious system of noninteracting electrons that generate the same density as the system of interest."[84,91] This fictitious system mitigates two huge problems in DFT:

1.) The exact energy functional is unknown
2.) An accurate *a priori* electron density is unknown

This method is considered the Kohn-Sham (KS) approach where the molecular energy can be expressed as the sum of terms including an unknown functional and an initial guess of $\rho(r)$ is used to calculate the initial guess of KS orbital and energy levels.[89] The KS approach is analogous to the variational approach in that an initial guess is made and tested with the wavefunction to obtain a new guess. The ground-state energy of the atomic or molecular system is represented by:[88,92]

$$E_0 = \langle T[\rho(r)]\rangle + \langle V_{Ne}[\rho(r)]\rangle + \langle V_{ee}[\rho(r)]\rangle \tag{2-56}$$

where the first term represents the kinetic energy of the system, the second represents the attraction between the nucleus and electrons, and the third represents the Coulombic repulsion term. Note that all three terms are functionals of electron density. Evaluating the second term using the potential energy operator $\hat{V}_{Ne}$ and applying the definition of an expectation value:

$$\hat{V}_{Ne} = \sum_{i=1}^{2N} v(r_i) \tag{2-57}$$

$$\langle V_{Ne}\rangle = \langle \Psi | \hat{V}_{Ne} | \Psi \rangle = \int \rho(r) v(r) dr \tag{2-58}$$

where $v(r_i)$ is the external potential caused by the attraction of electron *i* at distance *r* away from the nucleus. The ground-state energy equation can be rewritten as:

$$E_0 = \langle T[\rho(r)]\rangle + \int \rho(r) v(r) dr + \langle V_{ee}[\rho(r)]\rangle \tag{2-59}$$

while the first and third functionals cannot be evaluated exactly. The KS reference method instead incorporates the deviation of the real electronic kinetic and real potential energies from those of the reference.[92]

$$\Delta\langle T[\rho_0]\rangle = \langle T[\rho_0]\rangle_{real} - \langle T[\rho_0]\rangle_{ref} \tag{2-60}$$

$$\Delta\langle V_{ee}[\rho_0]\rangle = \langle V_{ee}[\rho_0]\rangle_{real} - \frac{1}{2}\iint \frac{\rho_0(r_1)\rho_0(r_2)}{r_{12}} dr_1 dr_2 \tag{2-61}$$

Equation 2-59 becomes:

$$E_0 = \langle T[\rho(r)]\rangle_{ref} + \int \rho(r)v(r)dr + \frac{1}{2}\iint \frac{\rho_0(r_1)\rho_0(r_2)}{r_{12}} dr_1 dr_2 + E_{XC}[\rho_0] \quad (2\text{-}62)$$

$$\langle T[\rho(r)]\rangle_{ref} = \langle \Psi_r \left| \sum_{i=1}^{2N} -\frac{1}{2}\nabla_i^2 \right| \Psi_r \rangle \quad (2\text{-}63)$$

where $E_{XC}[\rho_0]$ is the electron exchange-correlation energy functional and is equivalent to the sum of $\Delta\langle T[\rho_0]\rangle$ and $\Delta\langle V_{ee}[\rho_0]\rangle$. Taking half of the double integral prevents the inclusion of redundant repulsion energies (*e.g.* r_1/r_2 and r_2/r_1 cause the same repulsion).

Density Functional Theory is both feasible and applicable because electron density can be represented as the sum of the square of *N* orbital densities which define a single Slater determinant. As previously mentioned, finding the exact form of the electronic exchange-correlation energy E_{XC} is an established problem in DFT but the Schrödinger equation of a many-electron system can be solved self-consistently, analogous to HF-SCF method.

$$\hat{H}_{KS}\Psi_i(\vec{r}) = \varepsilon_i \Psi_i(\vec{r}) \quad (2\text{-}64)$$

$$\hat{H}_{KS} = -\frac{1}{2}\nabla^2 + v_{KS}(r) \quad (2\text{-}65)$$

$$v_{KS} = v_{ext}(r) + v_H(r) + v_{XC}(r) \quad (2\text{-}66)$$

where $\hat{H}_{KS}$ is the KS Hamiltonian represented by Equation 2-65. The KS potential (Equation 2-66) is defined as the sum of the external potential v_{ext}, the Hartree potential v_H, and the

electronic exchange-correlation potential v_{XC}. A self-consistent process would begin with a guess of the initial trial electron density which is then used to calculate the KS potential. A new electron density can be found using Equation 2-53 and Equation 2-64. This iterative process is repeated until the initial guess is equivalent to the new guess.[89,92] This calculation must be done computationally due to its complexity, but approximations are made to reduce the amount of time required for such a calculation to be performed.

DFT Exchange-Correlation Functionals

Approximations are made when using DFT for computational calculations since they reduce the amount of processing power required to obtain reasonably accurate results. The simplest approximation model of DFT is the Local Density Approximation (LDA), which takes the electronic exchange energy at each point in space to be the same for a homogenous electron gas with electron density $\rho(r)$ for that point. Local Density Approximation defines the electronic exchange energy functional as:

$$E_X^{LDA}[\rho(r)] = \int \rho(r)\varepsilon_X^{LDA}[\rho(r)]dr \tag{2-67}$$

where ε_{XC}^{LDA} is the exchange and correlation energy per electron in a homogeneous electron gas with electron density $\rho(r)$.[88] LDA can also be applied to spin-polarized systems by incorporating spin-up and spin-down elements:[93]

$$E_{XC}^{LSDA}[\rho_\alpha, \rho_\beta] = \int \rho(r)\varepsilon_{XC}^{LSDA}[\rho_\alpha, \rho_\beta]dr \tag{2-68}$$

where ρ_α and ρ_β represent the electron density of spin-up and spin-down electrons, respectively. LDA tends to underestimate exchange energy by roughly 10% and overestimates correlation energy. While this deviation from ideality from both energies balances itself to a degree, better

approximations can be made to consider atomic and molecular systems. An electron density gradient can be considered to correct this error to account for non-homogeneity.[90] The GGA model is used to incorporate these gradients:[94–97]

$$E_{XC}^{GGA}[\rho_\alpha, \rho_\beta] = \int \rho(r)\varepsilon_{XC}^{GGA}[\rho_\alpha, \rho_\beta, \nabla\rho_\alpha, \nabla\rho_\beta]d^3r \quad (2\text{-}69)$$

where $\nabla\rho_\alpha$ and $\nabla\rho_\beta$ are the electron density gradient functions for spin-up and spin-down electrons, respectively. The B88 DFT functional, named after its creator and publication year, is one of the first proposed LDA functionals and serves as the foundation of many modern DFT functionals:[97]

$$E_X = E_X^{LDA} - \beta\sum_\sigma \int \rho_\sigma^{4/3} \frac{x_\sigma^2}{1 + 6\beta x_\sigma sinh^{-1}} d^3r \quad (2\text{-}70)$$

where β is a parametric constant, σ denotes spin-up or spin-down electrons, and x_σ is a dimensionless ratio of the electronic density gradient function $\nabla\rho_0$ and the spherical density $\rho_\sigma^{4/3}$. The PW91 functional, developed by Perdew and Wang in 1991, is a popular GGA functional used in solid-state DFT band structure calculations and comprises a non-empirical structure.[95,98] Rather than incorporating parameters that match experimental data, the PW91 functional exactly calculates the *ab initio* quantum mechanical relations and is an analytical fit to the GGA functional but can also accept modifications to fit other exact paramters.[95,99] An advancement of exchange-correlation functionals are hybrid functions, which incorporates a portion of Hartree-Fock exact exchange energy while the rest of the exchange-correlation energy comes from *ab initio* or semi-empirical sources. Equation 2-71 describes the *adiabatic connection* model which demonstrates the "switching on" of interelectronic repulsion:

$$E_{XC} = \int_0^1 \langle \Psi(\lambda) | V_{XC} | \Psi(\lambda) \rangle \qquad (2\text{-}71)$$

where λ is the coupling parameter. There is no interelectronic interaction when $\lambda = 0$ and the exact system is represented when $\lambda = 1$.

The sum of the entire area under the curve, including the HF exchange energy area, is equal to E_{XC}. Equation 2-72 incorporates a factor *z*, which is an optimizable parameter that represents the fraction of the upper rectangle included under the curve. The exchange-correlation energy can also be defined as:[69,100]

$$E_{XC} = E_X^{HF} - z\left(\sum_{XC}^{DFT} - \sum_{X}^{HF}\right) \qquad (2\text{-}72)$$

Becke used this equivalence and set $z = 0.5$ when applying it to the G1 test set in his paper [67] The error in enthalpy of formation for this test set was only 6.4 kcal/mol and this approximation was termed the Half-and-Half method.[67,69] This led to Becke developing his 3-parameter DFT functional (B3PW91) based on the PW91 functional and was later improved by Lee, Yang, and Par to produce the Becke, 3-parameter, Lee-Yang-Par (B3LYP) functional: [67,68,93,101,102]

$$E_{XC}^{B3LYP} = (1-a)E_X^{LSDA} - aE_X^{HF} + b\nabla E_X^B + (1-c)E_C^{LSDA} + cE_C^{LYP} \qquad (2\text{-}73)$$

where *a, b,* and *c* are variable parameters that were experimentally determined to be 0.20, 0.72, and 0.81, respectively. The first term is the LSDA exchange energy, the second term is a percentage of HF exchange energy that replaces the LSDA exchange energy, the third term is the scaled GGA exchange correction, the fourth term is the LSDA correlation energy, and the fifth term is the percentage of generalized gradient of LSDA correlation energy. A report from 2007

shows that B3LYP was by far the most used DFT functional among several others over a period of 5 years.[102] While B3LYP can accurately calculate small molecular systems, it tends to degrade with the inclusion of metals and solid-state systems since it lacks a good description of a "free-electron-like" system.[103] A useful functional for studying solid-state or semi-conductor systems is PBE0, a hybrid version of the original PBE functional, however the performance of B3LYP is still comparable depending on the system.[103–105]

Basis Sets

A basis set is a set of functions that describes an electronic wavefunction generated via HF or DFT methods. Such functions used in chemistry-related *ab initio* calculations are Gaussian-type functions since they best represent atomic and molecular orbitals.[57] Atomic orbitals can be represented by either Slater-type (STO) or Gaussian-type orbitals (GTO). STO's are solutions to the Schrödinger equation of hydrogen-like atoms and they decay exponentially as the distance from the nucleus increases. These functions represent atomic orbitals and can be linearly combined to form molecular orbital functions. Taking the following form:

$$\chi_{n,l,m}(r,\theta,\phi) = N_{n,l,m,\xi} Y_{l,m}(\theta,\phi) r^{n-1} e^{-\xi r} \tag{2-74}$$

where $N_{n,l,m,\xi}$ represents a normalization constant; *n, l, and m,* the quantum numbers, and characterize the STO while $r, \theta,$ and ϕ are the spherical coordinates. $Y_{l,m}$ is a spherical harmonic.

The exact wavefunction for a hydrogen-like atom is known but this is not useful when factoring in intramolecular interactions from the surrounding atoms which alter the electron density around the atom being described. Therefore, the STO's do not accurately describe

electron correlation and calculating the 2-electron integrals is computationally expensive. S.F. Boys[103] stated that STO's can be approximated as linear combinations of GTO's and do not require the laborious evaluation of these complex 2-electron integrals.[103] This discovery led to the development of STO basis sets formed by the combination of primitive Gaussian functions which take the general form:

$$\chi_{a,b,c}(r,\theta,\phi) = N_{a,b,c,\alpha}\mathbf{x}^a\mathbf{y}^b\mathbf{z}^c e^{-\alpha r^2} \tag{2-75}$$

where **x**, **y**, and **z** are cartesian coordinates and $r = x^2 + y^2 + z^2$.

Minimal basis sets prescribe a certain number of Gaussian functions to a single STO in an atom. The number of GTOs used in a minimal basis set is denoted by the notation used these sets: STO-*n*G, where *n* is the number of GTOs used to approximate the single STO. For example, considering a carbon atom that has electron configuration [1s, 2s, 2p], 5 STOs would be required to describe the atomic orbitals since the 1s and 2s orbitals require 1 STO each, and the 2p orbital requires 3 STOs since it can be broken into a $2p_x$, $2p_y$, and $2p_z$ orbital. For an STO-3G basis set, 3 Gaussians will be combined for each STO used in the evaluation of each atomic orbital. A larger number of Gaussians used in a minimal basis set typically increases the accuracy of the calculation up to a point. Minimal basis sets are computationally cheap but are insufficient for obtaining research-level quantitative results since a single Slater function is used to describe an atomic orbital. Typical minimal basis sets that are used are STO-3G, -4G, -5G, and -6G while additional functions can be included to account for polarization. Polarization functions are typically denoted by an asterisk (*e.g.* STO-*nG**) which adds empty valence orbital functions to the basis set. For hydrogen, a polarized set would add a 2s function and 3 2p functions which allows for the electron containing orbitals to be more asymmetric about the

nucleus. Inclusion of a polarization function for an atom with valence *p* oribitals adds 5 *d* orbital functions and so on.

The most common type of basis sets suitable for accurate *ab initio* calculations are split-valence basis sets. Made famous by John Pople,[104] split-valence sets prescribe more than one basis function for each valence orbital. Pople basis set notation takes the form X-YZG, where X is the number of primitive Gaussians assigned to each core atomic orbital, Y is the number of Gaussians of one type assigned for each valence orbital, and Z is the number of Gaussians of another type assigned for each valence orbital. Since there are two different types of GTOs used for the valence orbital, this notation implies a doubly-split split-valence basis set. The importance of using GTOs is outlined by analyzing the zeta component of a typical 1s Gaussian orbital function:

$$f_{1s}(r) = N_{1s}e^{-\zeta r^2} \tag{2-76}$$

where N_{1s} a constant for the 1s orbital, r is the distance away from the nucleus, and ζ (zeta) is the orbital exponent. The orbital exponent determines the size of the orbital and, in turn, determines its diffuseness over the distance, r, from the nucleus. The orbital exponent for a 1s orbital ζ_{1s} is known exactly but unknown when in a molecule due to electron density distortions caused by other atoms in its surroundings. Using two types (double zeta) of 1s-type orbital in the set allows for variations in electron density of the atom due to bonding and other intramolecular interactions. By including a second 1s-type orbital with a different orbital exponent, one that makes the function broader and more diffuse, the representation of the electron density becomes closer to that of the true system. Figure 8 depicts two different 1s-type orbitals with different orbital exponents, where $\zeta = 3.0$ Å^{-2} for Function 1 and $\zeta = 1.0$ Å^{-2} for Function 2.[105]

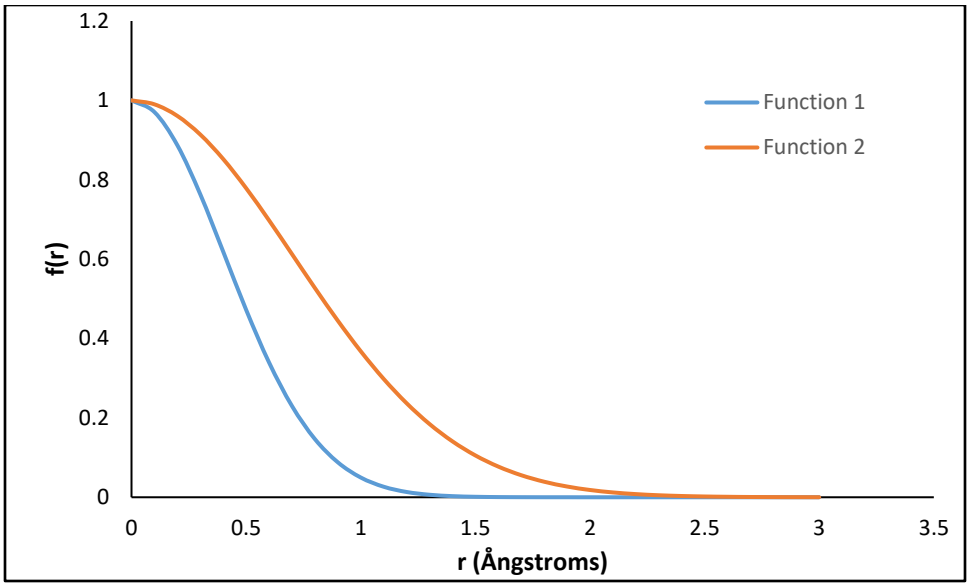

Figure 8: Representation of two 1s-type orbitals with different orbital exponents

Commonly used doubly split Pople basis sets include 3-21G, 3-21G*, 6-31G, and 6-31G*, where the asterisk denotes added polarization. Extended Pople basis sets can also include diffuse functions which are denoted by (+). The 6-31+G* represents a set that uses a linear combination of 6 GTOs to describe each core orbital, 3 GTOs of one type and 1 GTO of another type to describe the valence orbitals, a diffuse function, and polarization function. Diffuse functions have very small orbital exponents, so they decay slowly with distance *r* from the nucleus and are useful for calculating the energy of molecules with anions, weak bonds, and calculating NMR chemical shifts and dipole moments.[106–110] Higher order split-valence Pople basis sets exist (*e.g.* 6-311++G**) with even more diffuse functions and extensive polarization and offer extreme accuracy but are very computationally expensive.

Another widely used category of split-valence basis sets is the *correlation-consistent* category, proposed by Dunning and coworkers, and a systematic pathway for symmetric convergence of post-Hartree-Fock calculations and empirical extrapolation to an infinitely large

basis set.[111–115] Correlation-consistent basis sets add shells of functions upon the core atomic functions. Also referred to as Dunning basis sets, the notation takes the form *cc-pVNZ*, where *cc-p* is *correlation-consistent-polarized*, *V* indicates these are valence-only functions, and *NZ* indicates the amount splitting or number of valence functions added to the core functions. Common correlation-consistent basis sets include cc-pVDZ, cc-pVTZ, cc-pVQZ, cc-pV5Z, etc.; each set indicates increasing zeta splitting as *N* increases. For first and second row atoms, a cc-pVDZ basis set will add an s-type, a p-type, and a d-type function to the core function. Diffuse functions can also be added and are represented as *aug-cc-pVNZ*, where *aug* indicates the addition of diffuse functions. Heavier second row atoms (Na-Ar) can be better represented using additional d-type orbitals and these basis sets are written as *cc-pV(n+d)Z*, where *n+d* indicates the number of tight d-type functions added to the original basis set. These correlation-consistent basis sets allow extrapolation to an infinitely large basis set. This method requires data from typically three or more different calculations with different basis sets (*e.g.* -VDZ, -VTZ, and -VQZ) and is then fit to a power function:

$$E_X^{corr} = E_\infty^{corr} + AN^{-3} \tag{2-77}$$

where E_X^{corr} is the correlation energy obtained by the basis set with *N* splitting indicated by the Dunning set notation (D = 2, T = 3, etc.), E_∞^{corr} is the basis set limit of the correlation energy, and *A* is a fitting parameter.[116] In the case of a two-point data set obtained by using correlation-consistent basis sets with N values of X and Y, the basis set limit of the correlation energy, E_{XY}^{∞} produced by extrapolating said basis sets can be calculated using Equation 2-78.

$$E_{XY}^{\infty} = \frac{E_X^{corr}X^3 - E_Y^{corr}Y^3}{X^3 - Y^3} \tag{2-78}$$

Two-point Complete Basis Set (CBS) extrapolations are possible using this method when higher-order Dunning sets are used such as when X=5 and Y=6 but these basis sets are computationally expensive and will increase wall time significantly depending on the calculation hardware's capability. It may be easier to use a three-point CBS extrapolation that utilizes lower-order sets such as double- and triple-zeta sets, but these lower-order sets contain little information about the asymptotic convergence of the dynamical correlation energy and results in larger absolute error, on the scale of mHa, in the energy.[116]

Solvation Models

While gas-phase *in vacuo* calculations yield good thermodynamic data, it may be necessary to observe the interactions between the molecule of interest and a solvent. The way that the solvent is portrayed or treated in a calculation is called the solvent model and knowing which model to choose for a calculation is an important criterion for obtaining useful data. This is particularly useful in novel drug synthesis as the drug must be able to function as intended while solvated with water. The two main solvent models used in computational chemistry are *implicit* and *explicit* solvent models.

Implicit solvent models represent the solvent as a continuous isotropic medium (continuum) and are often used to observe biomolecular solute-solvent interactions such as protein folding or the behavior of drugs passing through a biological membrane.[117–120] The solvent properties are calculated as the mean behavior of several solvent molecules and have specific dielectric properties. The solute is placed in a cavity within the continuum and is subjected to approximated intermolecular forces.[121] The charge distribution of the solute polarizes the solvent medium at the solute-solvent interface. The Hamiltonian of the total

implicitly represented system can be represented by the sum of energy operators which are functions of the solute molecule coordinates:

$$\hat{H}^{total}(r_m) = \hat{H}^{molecule}(r_m) + \hat{V}^{molecule+solvent}(r_m) \tag{2-79}$$

where $\hat{H}^{molecule}(r_m)$ is the Hamiltonian for the solute molecule and $\hat{V}^{molecule+solvent}(r_m)$ is the potential energy operator of the energy potential between the solute molecule and solvent medium.[121] A continuous function of the solute geometry determines the effects that the first solvent shell has on the solute molecule, which includes charge transfer, approximated hydrogen bonding, and dispersion interactions. This serves as the basis for the *accessible surface area* (ASA) method which defines the Gibbs energy of the solvent as the sum of the products of the solute's ASA and solvation parameter:

$$\Delta G_{solv} = \sum_i \sigma_i ASA_i \tag{2-80}$$

where σ_i is the solvation parameter and is a contribution of free energy from the solvent per unit area. The free energy of solvation can also be represented by the sum of thermodynamic portions of the system:

$$\Delta G_{solv} = \Delta G_{cavity} + \Delta G_{disp} + \Delta G_{elec} + \Delta G_{hb} \tag{2-81}$$

where ΔG_{cavity} is the energy required to form the solute cavity in the medium, ΔG_{disp} is the energy of dispersion in the first solvent shell, ΔG_{elec} is the electrostatic energy or polarization induced by the molecule, ΔG_{hb} is the hydrogen bonding component. For calculating the electrostatic contribution to the total free energy of solvation, the Poisson-Boltzmann equation is

used and particularly useful in this continuum model for analyzing solvents that contain ions:[122–125]

$$\vec{\nabla} * \left[\varepsilon(\vec{r})\vec{\nabla}\Psi(\vec{r})\right] = -\rho^f(\vec{r}) - \sum_i c_i^{\infty} z_i q \lambda(\vec{r}) \exp\left(\frac{-z_i q \Psi(\vec{r})}{kT}\right) \quad (2\text{-}81)$$

where $\varepsilon(\vec{r})$ is the solvent dielectric constant, $\Psi(\vec{r})$ is the electrostatic potential, $\rho^f(\vec{r})$ is the charge density of the solute, c_i^{∞} is the concentration of ion *i* at infinite distance from the solute, z_i is the ion's valence number, q is the charge of a proton, $\lambda(\vec{r})$ is a factor of ion accessibility to the solute, *k* is Boltzmann's constant, and *T* is temperature. The Poisson-Boltzmann equation (PBE) can be computationally expensive without applying approximations and is not suitable for molecular dynamics calculations, but it can be linearized if the electrostatic potential is not too large, which reduces computational cost.[126] The Generalized-Born (GB) model is based on the linearized approximation of the PBE and treats the solute as a collection of spheres with an interior dielectric constant different from that of the solvent continuum. The GB model of the electrostatic energy is represented by:

$$\Delta\Delta G_{solv}^{el} = \frac{1}{2}\sum \frac{q_i q_j}{f_{ij}}\left(\frac{\exp\left(-k f_{ij}\right)}{\varepsilon_{out}} - \frac{1}{\varepsilon_{in}}\right) \quad (2\text{-}83)$$

$$f_{ij} = \sqrt{r_{ij}^2 + B_i B_j \exp\left(-\frac{r^2}{4B_i B_j}\right)} \quad (2\text{-}84)$$

$$B_i = -\frac{q_i^2}{2\varepsilon_{in}\Delta\Delta G_i} \quad (2\text{-}85)$$

where q_i and q_j are the charges of the solute spheres *i* and *j*, ε_{in} is the dielectric constant of the solute, ε_{out} is the dielectric constant of continuum that extends to $r = \infty$, r_{ij} is the distance

between sphere i and j, and B_i and B_j are the effective Born radii of the i^{th} and j^{th} spheres. The effective Born radius can be thought as the distance from the center or "nucleus" of the sphere to the molecular surface and proper estimation of this radius is crucial to the accuracy of GB model calculations. The averaged continuum model makes for fast approximations that are accurate for observing solvated biomolecules such as pharmaceuticals and proteins but the short-range physics of solvation such as hydrogen bonding cannot be accurately represented.

The explicit solvent model treats the solvent as individual explicit solvent molecules surrounding the solute, which produces a more intuitively realistic picture for observing the physics of solute-solvent interactions. Explicit solvation is commonly used in molecular mechanics, molecular dynamics,[127] and Monte Carlo calculations,[128] and is typically evaluated quantum mechanically. Zheng and coworkers[129] compared PB and GB implicit models and explicit models for calculating the solvation free energy in organic solvents and found that the implicit models gave poor agreement with explicit models and even worse agreement with experimental values. They determined that the main source of error was from not being able to correctly predict the nonpolar free energy contribution to the total solvation free energy:

$$\Delta G_{solv} = \Delta G_{polar} + \Delta G_{apolar} \tag{2-86}$$

implicit models crudely approximate ΔG_{solv} by uncoupling polar electrostatic and nonpolar interactions.[129]

Explicit solvation interactions can be evaluated quantum mechanically using HF, DFT, MP2, etc., but can also be calculated using MM forcefield models such as Simple Point Charge (SPC). Forcefields simplify the structure of the solvent molecules by treating them as point charges but retaining their dispersion and repulsion parameters. The treatment of these point

charges is entirely dependent on the type of model used as there are several different parameters that can be modified according to the forcefield, such as temperature-dependent maximum density, critical point, dielectric constant, bond angles, and bond lengths.[130]

Conformer Analysis

Searching for stable low-energy conformers is useful for generating a good starting structure before performing a geometry optimization or calculating vibrational frequencies of the molecule. A conformational search utilizes MM or MD to identify a likely molecular conformation, an arrangement of atoms in a molecule introduced by the rotation of a sigma bond, that exhibits the actual behavior of the molecule at a minimum along the potential energy surface (PES).[131] During a conformer search, several conformers are tried and tested and are either higher or lower in energy relative to the base molecule. For example, butane has higher and lower energy conformations based upon the central sigma bond. Rotation about this bond introduces the lower energy "staggered" and higher energy "eclipsed" conformations, dependent upon the relative locations of the methyl groups. There are various methods for conformational analysis:[131]

1. *Systematic*/*Grid Search*: The dihedral angles are systematically varied while keeping the bond lengths and angles fixed. This method generates a possibly large number of conformers but does not identify those with the lowest energies.
2. *Structure-based*: This manipulates smaller fragments of the molecule and considers each fragment to be independent of one another.
3. *Random*: The base molecule is modified through random movement of the Cartesian space in which it lies, and each new generated structure is added to a library. This iterative process of random change and measurement persists until either the desired

structure is obtained, all structures are sampled, or a desired number of steps are performed.

4. *Distance Geometry*: Many independent structures are generated in the conformational space within the specified constraints. Each structure is evaluated for its energy using force fields.[132] Since each molecule can be described with minimum and maximum distances between each pair of atoms, a matrix is generated, and conformers are made using these upper- and lower-bound conditions.
5. *Monte Carlo*: Random changes to the dihedral angles and coordinates of atoms generate new conformers, which are added to the list if the energy is lower than that of the starting structure. However, if the newly generated structure is higher than the base structure in energy, it is accepted by analyzing its algorithmic probability, applying the energy to a probability distribution function (*e.g.* Boltzmann distribution).
6. *Genetic algorithm*: A random pool size of *n* conformers is generated and all structures are energy minimized. At least 2 lowest-energy conformers are selected before a genetic operation is performed. A "roulette wheel" decision is performed on the selection of the conformers. A fitness function assigns a "fitness level" or probability to each conformer. The probability of a specific sample being selected is dependent upon its energy and can be envisioned similarly to placing a bet on a casino roulette wheel, where certain bets bear higher or lower probability of a payout. A mutation is performed on the selected conformers and the energies of the resulting "children" structures are minimized. This new generation comprises the lowest energy conformers and the iterative process is repeated until the desired number of conformers is obtained.[133] This method has been

shown to outperform Monte Carlo conformational analyses for longer unbranched alkanes (18-38 carbons).[134]

Force fields are used to estimate intramolecular and intermolecular forces in MM and MD calculations without being computationally costly. A force field can be described as a set of parameters that calculate the potential energy of an atom of molecule in the simulation.[135] In comparison to QM methods such as DFT and Coupled Cluster theory,[136] force field calculations do not describe the intramolecular interactions and electron polarization as accurately.[135] Several different force fields exist and are implemented depending on the molecular system being described. One of the earliest force fields developed for molecular mechanics calculations as the MM2 force field, initially created for precisely analyzing and modeling hydrocarbons and small organic molecules.[137] Additions to the MM2 force field included improved treatment of aliphatic hydrocarbons (MM3)[138] and calculations of vibrational frequencies and rotational barriers for alkanes a cycloalkanes (MM4).[139] The Assisted Model Building and Energy Refinement (AMBER) is a collection of various force fields used to describe proteins and other large biomolecules.[140] The Merck Molecular Force Field (MMFF) is a family of force fields that were developed to model a wide range of organic molecules, with the first of them published being MMFF94. This force field parametrizes several properties of the molecule against several crystallographically determined structures.[141] Universal Force Field (UFF), like MMFF, was developed to serve as a universal force field (hence the name) for a wide variety of molecules but while also including parameters for the rest of the periodic table, including actinides. However, its overall generality introduces inaccuracies (mHa scale) in molecules other than hydrocarbons and those that contain heteroatoms.[142]

This chapter has outlined the fundamental concepts of quantum mechanics and computational methods necessary for undertaking the bulk of this research. While these fundamentals will be not be further expanded upon in detail, they are still prevalent in the background while utilizing various basis sets, theories (HF, MP2, or DFT), functionals, force fields, conformer searches, and *ab initio* or semi-empirical (PM6) calculations involving geometry optimizations.

CHAPTER 3. RESULTS AND DISCUSSION

Computational Details

All *ab initio* calculations were performed using NWChem,[143] developed and maintained by the Environment Molecular Sciences Laboratory located at the Pacific Northwest National Laboratory. Semi-empirical calculations were performed using the Molecular Orbital PACkage (MOPAC) PM6 parameterization method.[73] Initial solvent configurations for explicit solvation calculations were generated by an open-source program, PACKMOL, which was developed by the Institute of Chemistry and Institute of Mathematics at the University of Campinas, and by the Institute of Mathematics and Statistics at the University of São Paulo.[144] Force field optimizations and conformational analyses were performed using Avogadro, an open-source molecular modeling and visualization program.[145,146] All geometries of DHLA, ALA, and their hydroxyl radical adducts were optimized using DFT/B3LYP level of theory with 6-31G* and cc-pVDZ basis sets. Complete basis set (CBS) energies were calculated through extrapolation using fully reoptimized geometries obtained by cc-pVDZ, cc-pVTZ, and cc-pVQZ DFT and HF optimizations, and were compared to energies obtained using DFT/B3LYP/6-31G* level of theory. The WebMO quantum chemistry package was used for the molecular editor and graphic visualizations software when running and queueing *ab initio* and semi-empirical calculations.[147]

Energies and Geometries of ALA and DHLA

It should be noted that all *ab initio* (NWChem) geometry optimizations were performed in the gas-phase. Before submitting a job into WebMO, the structure of interest was derived from a 50-children genetic algorithm conformational analysis, performed in Avogadro, using a UFF force field. Analyzing and understanding the initial optimized geometry of the parent molecules, DHLA and ALA, gives a better understanding of the effects that free radicals have on them after the formation of a spin adduct. The bond lengths and angles of interest for DHLA and ALA are listed in Table 1. The labeling scheme for both molecules is in Figure 9.

Table 1: Calculated bond lengths and angles for DHLA and ALA, optimized at DFT/B3LYP/cc-pVDZ

DHLA		ALA	
Set of atoms	Bond length (Å) or angle (deg.)	Set of atoms	Bond length (Å) or angle (deg.)
C1-S2	1.855	S1-S2	2.124
C3-S1	1.880	C1-S2	1.839
S1-H1	1.359	C3-S1	1.885
S2-H2	1.359		
S1-C3-C2	111.481	S1-C3-C2	111.710
S2-C1-C2	112.692	S2-C1-C2	106.370
S1-C3-C4	113.110	S1-C3-C4	112.837
C2-C3-C4	113.299	C2-C3-C4	112.362
C1-C2-C3	118.524	C1-C2-C3	112.581

Note: All other bond lengths and angles not listed are found in Appendix A1

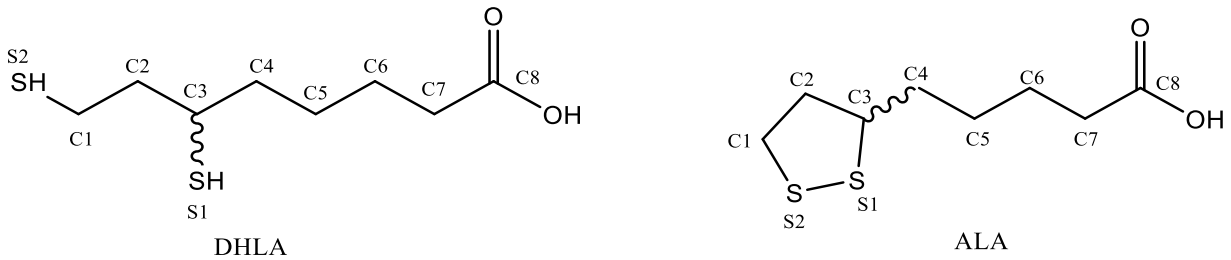

Figure 9**:** Labeling scheme for DHLA and ALA

The S2-C1 bond (1.855 Å) is just longer than the S2-C1 bond in ALA (1.839 Å) since S2 can rotate freely along C1-C2 and C2-C3. The same reasoning can be used to describe the differences in bond angles, especially within the 3-carbon chain of the ring: C1-C2-C3. The distance between S1 and S2 in DHLA was not listed in Table 1 since they are not bonded like they are in ALA and their distance is not relevant to this study.

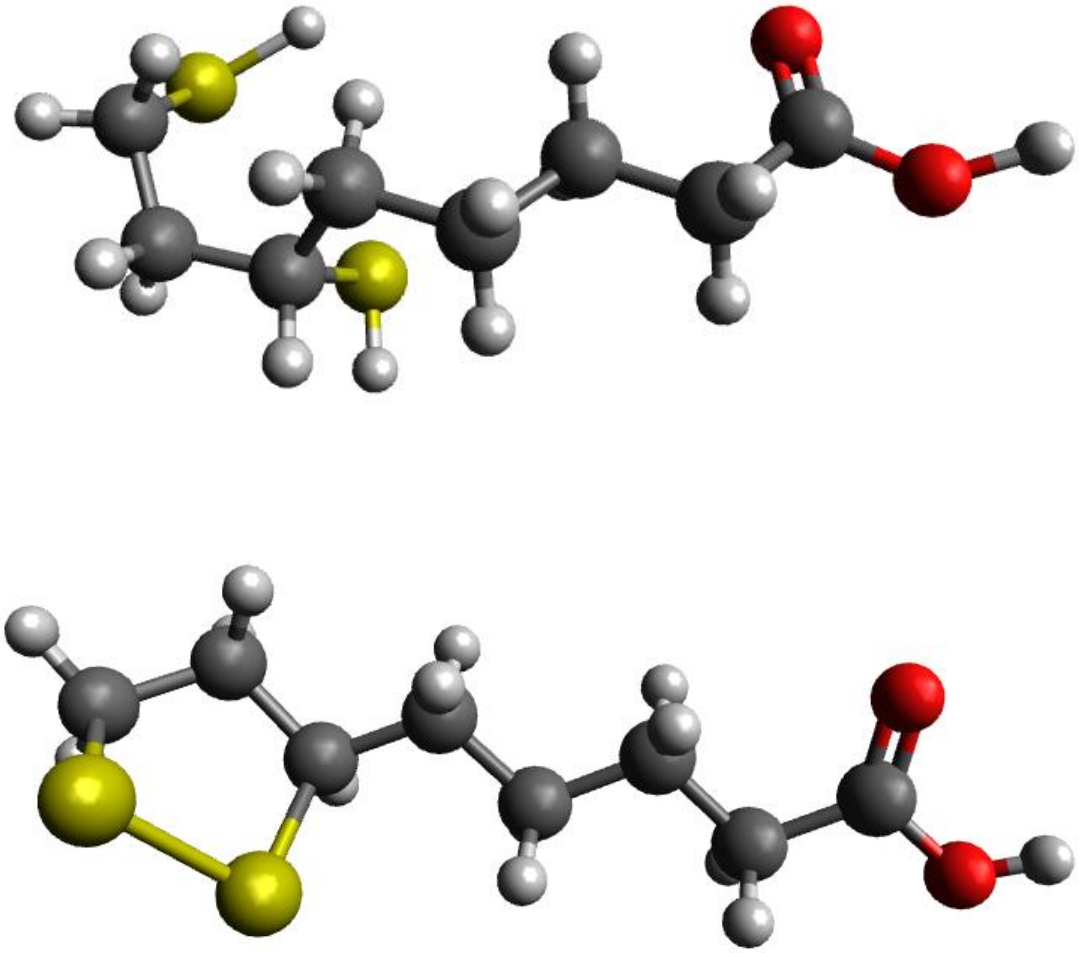

Figure 10: Avogadro 3-D representations of DHLA and ALA

Table 2: Geometry-optimized energies of ALA and DHLA under HF and DFT/B3LYP with various Pople and Dunning basis sets

ALA	HF/MP2/6-31G* (E_h)	-1255.85496		
	DFT/B3LYP/6-31G* (E_h)	-1260.12244		
	DFT/B3LYP/cc-pVDZ (E_h)	-1260.19892		
	DFT/B3LYP/cc-pVTZ (E_h)	-1260.38501	ECBS limit (E_h)	-1260.45256
	DFT/B3LYP/cc-pVQZ (E_h)	-1260.43457		
	HF/cc-pVDZ (E_h)	-1255.94339		
	HF/cc-pVTZ (E_h)	-1256.10822	ECBS limit (E_h)	-1256.160861
	HF/cc-pVQZ (E_h)	-1256.14812		
DHLA	HF/MP2/6-31G* (E_h)	-1257.00987		
	DFT/B3LYP/6-31G* (E_h)	-1261.32224		
	DFT/B3LYP/cc-pVDZ (E_h)	-1261.39606		
	DFT/B3LYP/cc-pVTZ (E_h)	-1261.58990	ECBS limit (E_h)	-1261.65587
	DFT/B3LYP/cc-pVQZ (E_h)	-1261.63912		
	HF/cc-pVDZ (E_h)	-1257.11099		
	HF/cc-pVTZ (E_h)	-1257.27377	ECBS limit (E_h)	-1257.32671
	HF/cc-pVQZ (E_h)	-1257.31371		

Note: Complete basis set energies (E_{CBS}) were calculated using the exponential function[116,148]

Table 3: Gas-phase energies of optimized structures of DHLA-OH adducts and their binding energies at DFT/B3LYP/cc-pVDZ

Adduct	**Energy (E_h)**	**Binding Energy (E_h)**	**Binding energy (kcal/mol)[a]**
DHLA-OH(S1)	-1337.1582	-0.79146	-496.64115
DHLA-OH(S2)	-1337.15944	-0.79270	-497.41925
DHLA-OH(S1) (Habs)[b]	-1336.61381	-0.24707	-155.03642
DHLA-OH(S2) (Habs)	-1336.60453	-0.23779	-149.21322
DHLA-OH(C1)	-1337.1829	-0.81616	-512.14040
DHLA-OH(C2)	-1337.17566	-0.80892	-507.59730
DHLA-OH(C3)	-1337.18401	-0.81727	-512.83692
DHLA-OH(C1) (Habs)	-1329.35737	7.00937	4398.37967
DHLA-OH(C2) (Habs)	-1329.35018	7.01656	4402.89140
DHLA-OH(C3) (Habs)	-1336.63018	-0.26344	-165.30860

Table 4: Gas-phase energies of optimized structures of ALA-OH adducts and their binding energies at DFT/B3LYP/cc-pVDZ

Adduct	Energy (E_h)	Binding Energy (E_h)	Binding energy (kcal/mol)
ALA-OH(S1)	-1335.96142	-0.79182	-496.86705
ALA-OH(S2)	-1335.96590	-0.7963	-499.67825
ALA-OH(C1)	-1336.00778	-0.83818	-525.95795
ALA-OH(C2)	-1335.96656	-0.79696	-500.0924
ALA-OH(C3)	-1336.01069	-0.84109	-527.783975
ALA-OH(C1) (Habs)	-1328.18541	6.984181	4382.573578
ALA-OH(C2) (Habs)	-1335.41673	-0.24713	-155.074075
ALA-OH(C3) (Habs)	-1328.19190	6.9777	4378.50675

Notes: Adducts are named [parent]-[radical](binding site)

'Habs' refers to a reaction where the hydrogen atom is abstracted and replaced by ·OH

$$\text{Binding energy } (\Delta E) = E_{\text{product(s)}} - E_{\text{reactants}} = [E_{\text{adduct}} + E_{side\ product}] - [E_{\text{parent}} + 2 * E_{\text{radical}}]$$

$$\textit{Example: } \Delta E_{ALA-OH(S1)} = [-1335.96142 - 76.42184] - [-1260.19892 - 2 * 75.69626] = -0.79182$$

$$E_{\text{water}} = -76.42184\ E_h;\ E_{\cdot OH} = -75.69626\ E_h$$

Table 2 shows the calculated energies of the geometry-optimized structures of ALA and DHLA under HF and DFT with various basis sets. The energies calculated for ALA in Table 2 are comparable to those found by Mikulski *et al.*, who used MP2 with both Dunning and Pople basis sets [-DZ, -TZ, -QZ, 6-31G(3df,2p), 6-31+G(3df,2p), 6-31++G(3df,2p), and 6-311++G(3df,2p)],[44] and this suggests that these data obtained using correlation-consistent basis sets are in acceptable agreement with literature data. The DHLA energies are about 1 E_h lower in energy than those for ALA because of the presence of 2 additional hydrogens from the dithiol. The energies derived from DFT optimizations are roughly 4 E_h lower than those calculated under

HF. Tables 3 and 4 contain the optimized geometry energies of DHLA-OH and ALA-OH, which are the spin adducts formed after a reaction with ·OH. Each adduct is labeled such that it is easy to determine to which atom ·OH is directly bonded. For example, DHLA-OH(S1) has ·OH bonded to sulfur S1 as shown in Figure 9. The term "Habs" refers to reaction in a which a hydrogen is abstracted the residual radical is quenched by ·OH, forming a singlet state adduct. Adducts that do not involve a hydrogen abstraction are also considered but their optimized structures suggest that ·OH addition is not favorable so a doublet state not likely to be obtained.

Determining Primary Binding Sites

The binding energies for DHLA-OH are mostly negative, which indicates thermodynamically favored adduct formations, aside from the "DHLA-OH(C1) Habs" and "DHLA-OH(C2) Habs" isomers which exhibit largely endergonic reactions. Surprisingly, the most negative binding energies belong to the formations of DHLA-OH(C1, C2, and C3) adducts in absence of a hydrogen abstraction but, as previously state, these addition products are not expected. Previous computational literature on DHLA and ALA indicate that the more likely binding sites for ·OH is at the sulfurs since the HOMO are located on the sulfur atoms and their transition state calculations support this.[44,46] Although kinetics calculations were not performed as a part of this research, kinetics data from literature strongly suggests that DHLA is the dominant radical-quenching species.[39,44,46–48] Literature also suggests that the sulfur atoms are the most likely binding sites for adduct formation, but this still raises a questions of whether a hydrogen will be abstracted in the process. These considerations suggest that a radical hydrogen abstraction from DHLA by free ·OH is likely to occur before a second ·OH bonds to the abstraction site, forming the spin adduct. The HOMO surfaces for DHLA and ALA were generated and are shown in Figure 11.

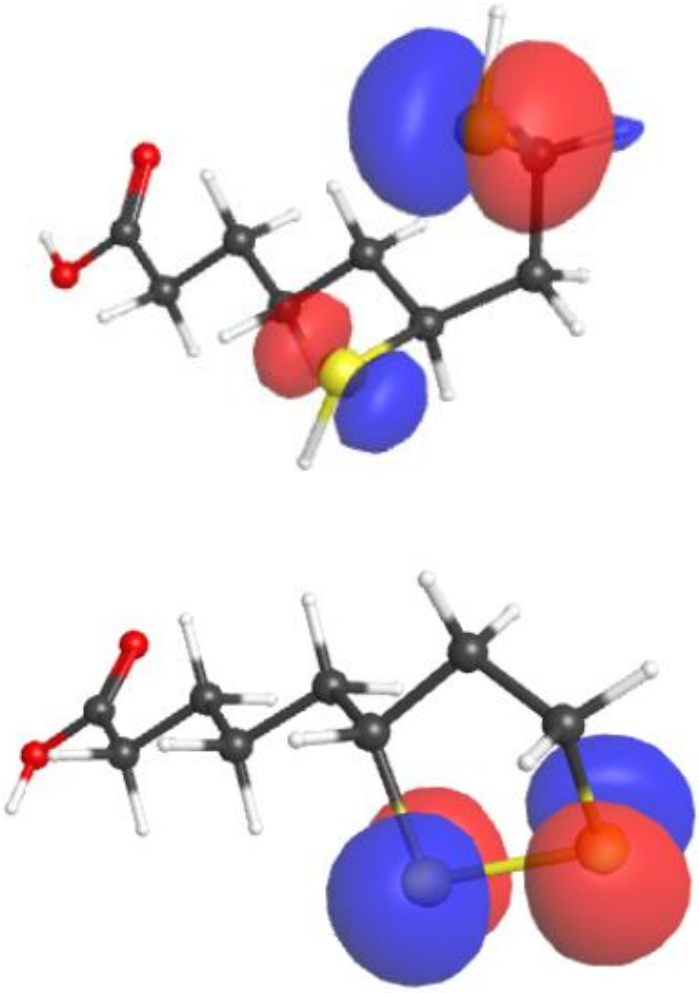

Figure 11**:** HOMO in DHLA (top) and ALA (bottom)

Proposing a Mechanism

Since a hydrogen abstraction with DHLA may be suggested based on the results of found in this study, the energies of several single radical hydrogen-abstracted isomers are analyzed and listed in Table 5. This hydrogen transfer study was adapted from a publication by Castañ *et al.*[46] and an illustrated representation of it is found in Figure 12.

Table 5: Gas-phase energies of single hydrogen abstractions from DHLA calculated at DFT/B3LYP/cc-pVDZ

Radical structure	**Energy (E_h)**	**Abstraction energy (E_h)**	**Abstraction energy (kcal/mol)**
HTC1	-1260.74288	-0.07240	-45.43100
HTC2	-1260.73912	-0.06864	-43.07160
HTC3	-1260.74548	-0.07500	-47.06250
HTC4	-1260.73481	-0.06433	-40.36707
HTC5	-1260.73066	-0.06018	-37.76295
HTC6	-1260.73073	-0.06025	-37.80687
HTC7	-1260.66396	0.00652	4.09130
HTS1	-1260.754835	-0.084355	-52.93276
HTS2	-1260.76049	-0.090017	-56.48566

$$\text{Abstraction energy} = E_{\text{product(s)}} - E_{\text{reactants}} = [E_{\text{DHLA}\bullet} + E_{\text{water}}] - [E_{\text{parent}} + E_{\text{radical}}]$$

Table 5 indicates that the most energetically favorable hydrogen abstractions in DHLA occur at the sulfur atoms, with sulfur S2 having a slightly thermodynamic preference of about 3.5 kcal/mol over sulfur S1. This further suggests that a hydrogen abstraction from sulfur S1 or S2 is thermodynamically favored over an abstraction occurring at any of the carbons. An abstraction from carbon C7 (HTC7) yielded a net positive ΔE which is likely due to its proximity to the -COOH moiety. The protonated form (-COOH instead of -COO^-) was studied in the gas-phase, however the deprotonated form would be the dominant in aqueous media since the pKa of -COOH ~5 and the pH of most physiological systems have a pH of 7.4. The protonated form

would be tested in lipid/nonpolar media since deprotonation of the carboxylic acid moiety is less likely to occur. When calculating abstraction energies, it is necessary to consider the solvent medium within which the molecule exists so that the proper form is considered to best simulate a real environment and choice of solvent affects energy calculations. The trend of thermodynamic stability between all samples in Table 5 follows the same trend found in the literature, however these values were calculated in both water and lipid continuums.[46] These energies are roughly 15-19 kcal/mol higher in water than they are *in vacuo*. The differences in abstraction energy from the sulfur atoms and the other carbon atoms suggests that a S-H abstraction is far more likely than a C-H abstraction.

Another common theoretical calculation done with DHLA and ALA is the single-electron transfer mechanism (SET), but this was not performed in this study due to time constraints because Castañ *et al.* states that SET is an endergonic process in both polar and nonpolar media. On the other hand, SET in ALA is exergonic in aqueous media but endergonic in lipid media. A nonpolar medium (*e.g.* lipid) prevents SET from being a favorable mechanism since anionic products are not stabilized in a nonpolar solvent. A similar hydrogen abstraction study was also performed by Galano and Alvarez-Idaboy for glutathione (GSH) and it was found also found that the thiol group held the greatest potential for a HT mechanism.[149] In agreement with the literature, it can be concluded that the sulfurs in DHLA are the primary reaction site for any radical scavenging activity.

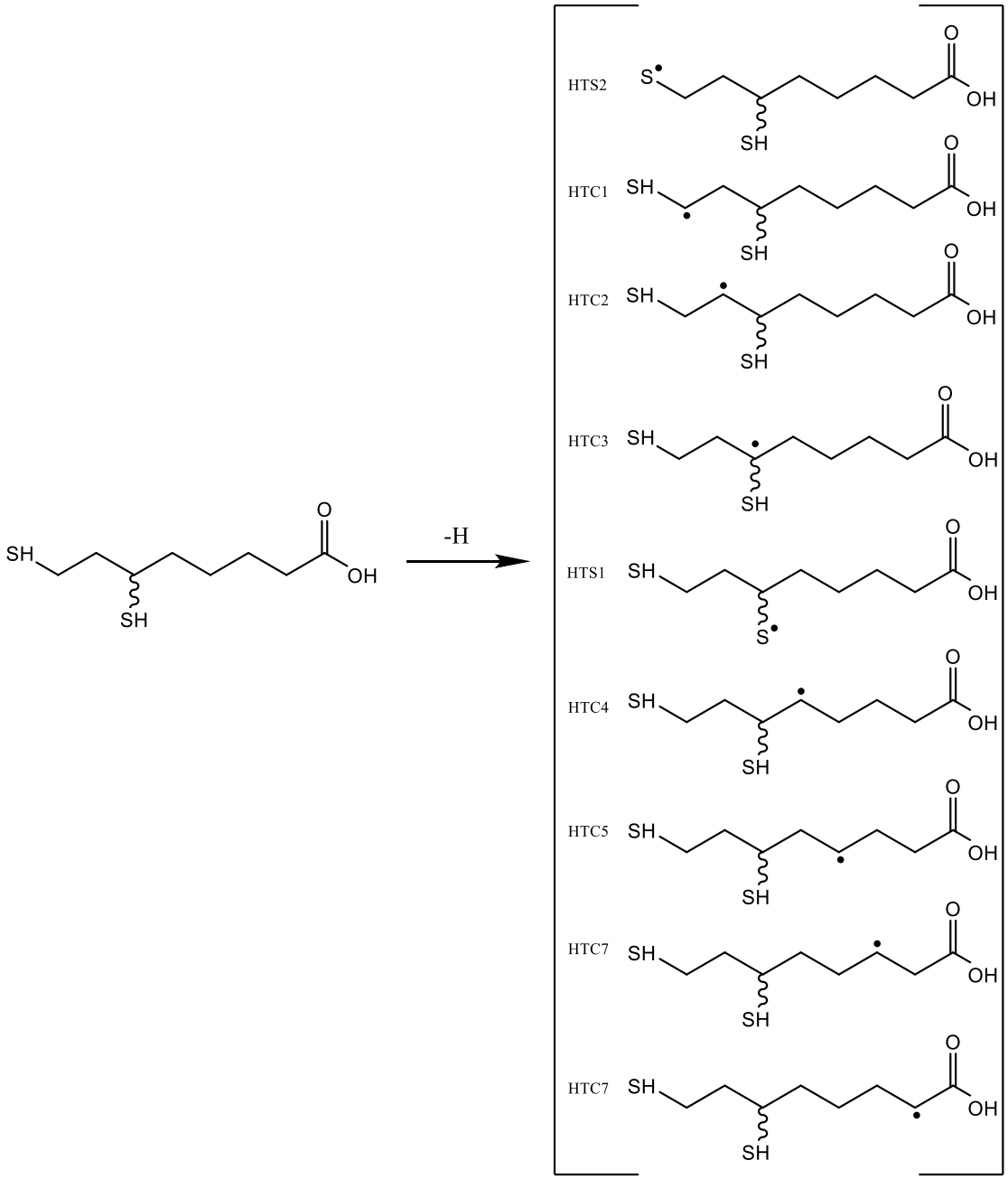

Figure 12**:** Visual representation of hydrogen abstraction study

Radical Delocalization in Doublet and Triplet States

Spin density calculations for the DHLA-OH adduct were performed to determine the extent to which radical delocalization occurs upon addition of hydroxyl radical to one of the sulfur atoms. Spin density is defined as the difference in electron densities of spin-up and spin-down electrons and is represented by Equation 3-1:

$$\rho_e = \rho_\alpha - \rho_\beta \tag{3-1}$$

where ρ_e is the total spin density, ρ_α is the density of spin-up electrons, and ρ_β is the density of spin-down electrons. The DHLA-OH(S1) (Habs) and DHLA-OH(S2) (Habs) anion adducts, where ·OH is bound to sulfur S1 or S2 after a hydrogen abstraction, were used as the model for calculations. Spin density files were generated using the NWChem dplot task. Since the dplot command enables Gaussian '.cube' files to be generated, the spin density surface can be visualized in Avogadro. Figure 13 shows the spin density surfaces over DHLA-OH(S1) for both the doublet-multiplicity anion and triplet-multiplicity versions.

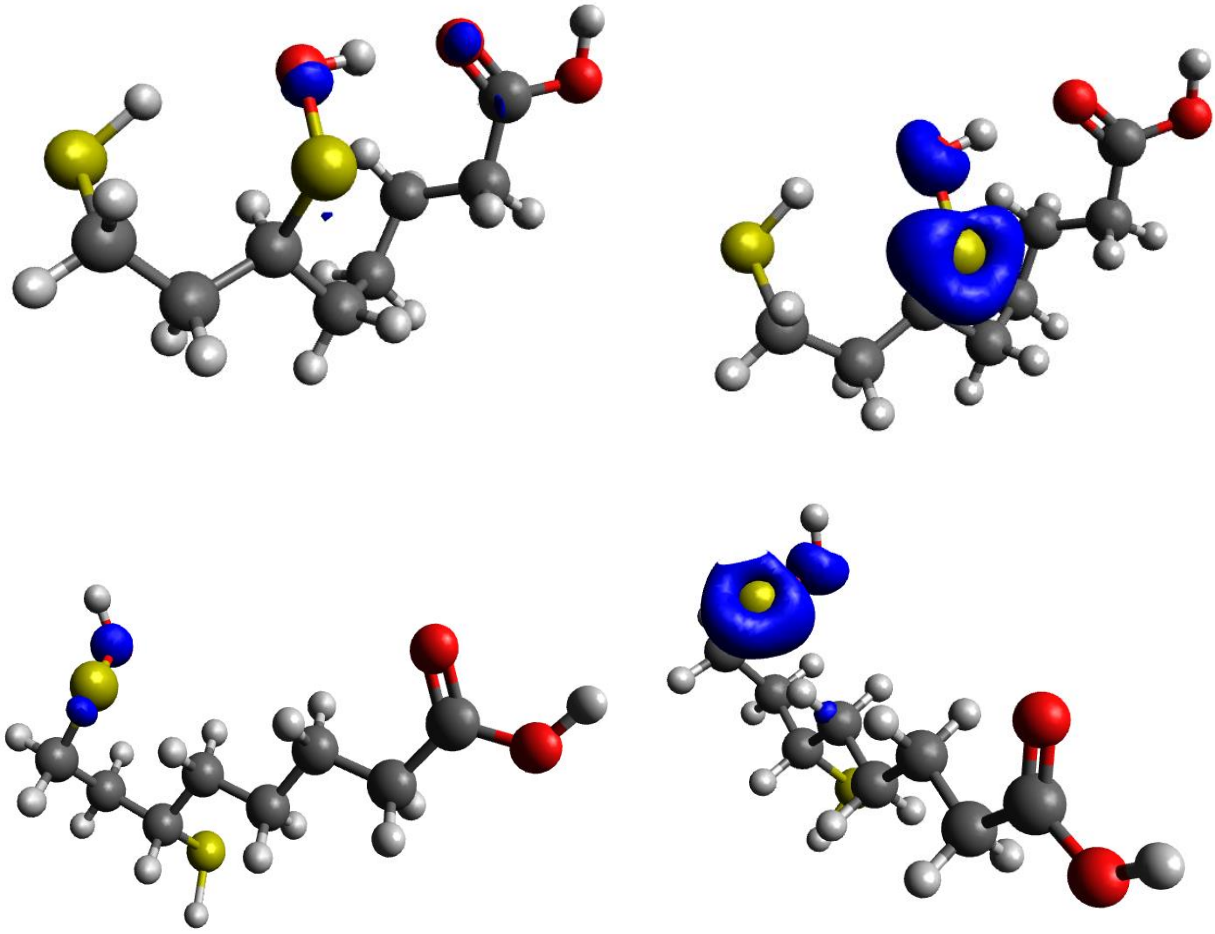

Figure 13**:** Spin density surfaces (blue) generated for DHLA-OH(S1) doublet anion (top left), DHLA-OH(S1) triplet (top right), DHLA-OH(S2) doublet anion (bottom left), and DHLA-OH(S2) triplet (bottom right)

*All surfaces were generated in Avogadro and were assigned an iso-value of 0.02

Since the iso-value is set to 0.02 in Avogadro for all four images in Figure 13, it could be said that the spin density surfaces can be directly compared. The doublet anion versions of DHLA-OH (both S1 and S2) are notably different when comparing which atoms the spin density surfaces cover. For DHLA-OH(S1), the doublet anion conformer shows most of the surface covering the hydroxyl oxygen and the carbonyl oxygen. There seems to also be a very small portion of spin density over sulfur S1, which indicates that a delocalization of the radical to the sulfur is possible but not necessarily probable. This sharing of spin density between the ·OH oxygen and C=O oxygen may suggest that a transition state involving hydrogen bonding between the -COOH moiety and hydrogen on the hydroxyl radical is possible, assuming the overall adduction mechanism involves the formation of a stable anionic doublet state. Strangely, there is also some shared spin density on the C=O carbon, which is likely due to the tight carbonyl double bond. As touched on previously, this state would be unlikely to form in a nonpolar medium since anionic structures are not stabilized in this medium, so an aqueous environment would be necessary for this to be considered. As for the triplet state, it would be more appropriate to model the addition of a diradical such as triplet oxygen ($^3O_2$) paired with an abstraction to the other sulfur. These possibilities were not considered at the time of spin density data acquisition so it will necessary to expand on this in future work. It would be beneficial to analyze the effect on spin densities observed when other biologically relevant ROS are bound to DHLA to in hopes that it would paint a better picture for understanding the degree of delocalization. While testing both the doublet anionic and triplet states of the adduct is good practice, a proper mechanism must be established to accurately represent the spin density.

Optimizations of Various Radical Adducts

To observe the effects that the adduct formation of various free radicals have on binding energies, geometry optimizations were calculated at DFT/B3LYP/cc-pVDZ for DHLA, with the ROS bound to sulfur S1. The molecular energies and binding energies for the spin adducts are listed in Table 6. Calculating binding energy requires geometrically optimizing and calculating energies of the new radicals (Table 7) and energies of their products after abstracting a hydrogen (Table 8). The graphic representations of geometry optimized structures of each DHLA spin adduct is shown in Figure 14. A ChemDraw diagram listing all tested adducts is included in Figure 15.

Table 6: Gas-phase molecular and binding energies of DHLA-rad(S1) adducts at DFT/B3LYP/cc-pVDZ

Spin adduct (S1 site)	**Energy (Eh)**	**Binding energy (Eh)**	**Binding energy (kcal/mol)**
DHLA-·OH	-1336.61381	-0.24707	-155.03642
DHLA-·CH_3	-1300.713649	-0.15499	-97.25622
DHLA-·OOH	-1411.72953	-0.051315	-32.20016
DHLA-·OCH_3	-1375.911849	-0.207962	-130.49615
DHLA-·$OOCH_3$	-1451.047558	-0.057647	-36.17349
DHLA-·$OOCH_2CH_3$	-1490.373611	-0.058613	-36.77965
DHLA-·$OOCCl_3$	-2829.897813	-0.078652	-49.35413

Table 7: Optimized energies and dipole moments of various free radicals

Radical	Energy (E_h) HF/6-31G*	Energy (E_h) DFT/6-31G*	Energy (E_h) DFT/cc-pVDZ	Dipole moment (Debye) (DFT/cc-pVDZ)
·OH	-75.21347	-75.68641	-75.69626	1.685
$\cdot CH_3$	-39.55472	-39.83829	-39.83987	0
·OOH	-150.16478	-150.89915	-150.91764	2.219
$\cdot OCH_3$	-114.41623	-115.01028	-115.01614	2.146
$\cdot OOCH_3$	-189.19641	-190.21394	-190.22914	2.643
$\cdot OOCH_2CH_3$	-228.23679	-229.53501	-229.55222	2.663
$\cdot OOCCl_3$	-1565.86305	-1568.96762	-1569.06181	1.076

Table 8: Energies of other coproducts as a result of a hydrogen abstraction at DFT/B3LYP/cc-pVDZ

Coproducts	Energy (Eh)
H_2O	-76.42184
CH_4	-40.517141
H_2O_2	-151.553139
CH_3OH	-115.724461
$HOOCH_3$	-190.864429
$HOOCH_2CH_3$	-230.185512
$HOOCCl_3$	-1569.700523

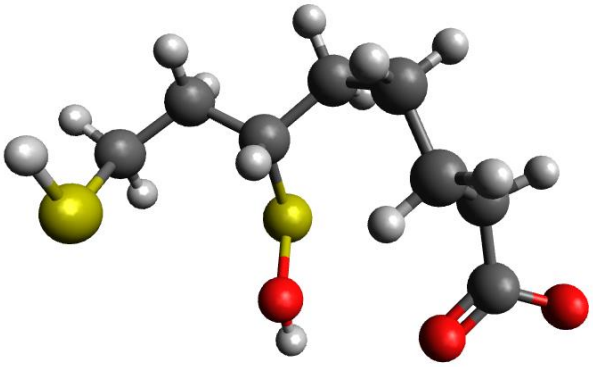

DHLA-OH

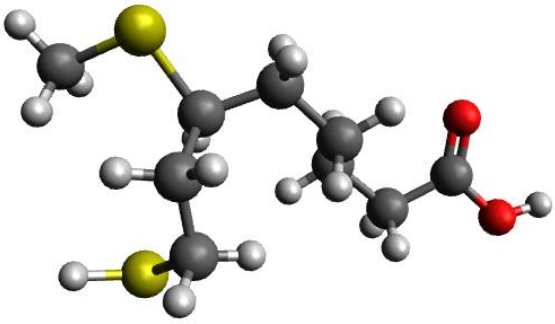

DHLA-CH_3

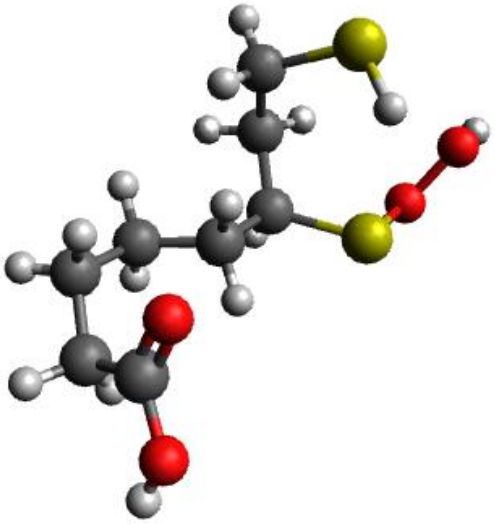

DHLA-OOH

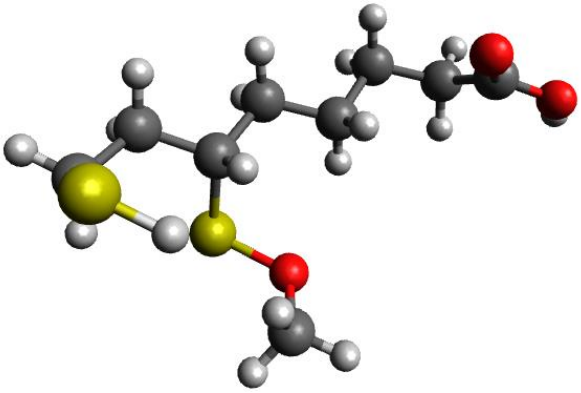

DHLA-OCH_3

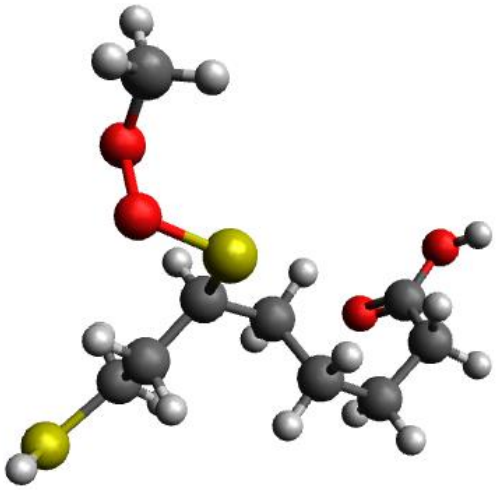

DHLA-$OOCH_3$

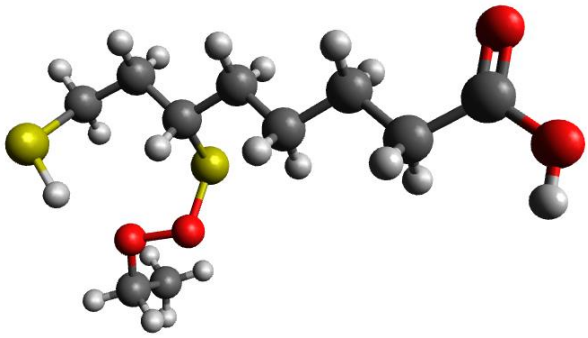

DHLA-$OOCH_2CH_3$

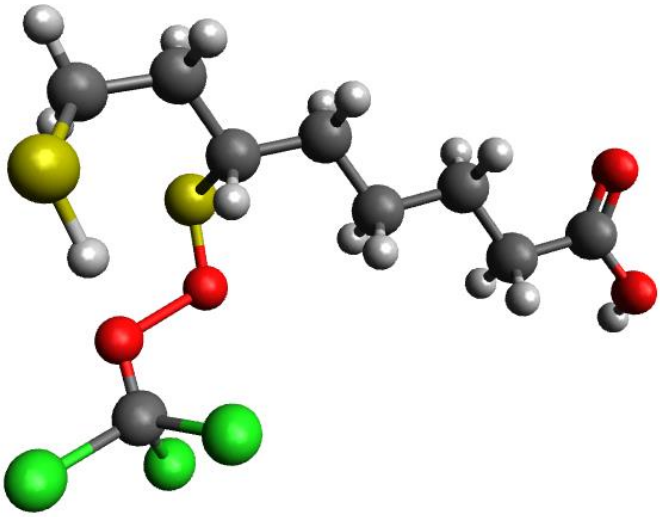

DHLA-$OOCCl_3$

Figure 14**:** 3-D representations of geometry optimized spin adducts of DHLA with different radicals

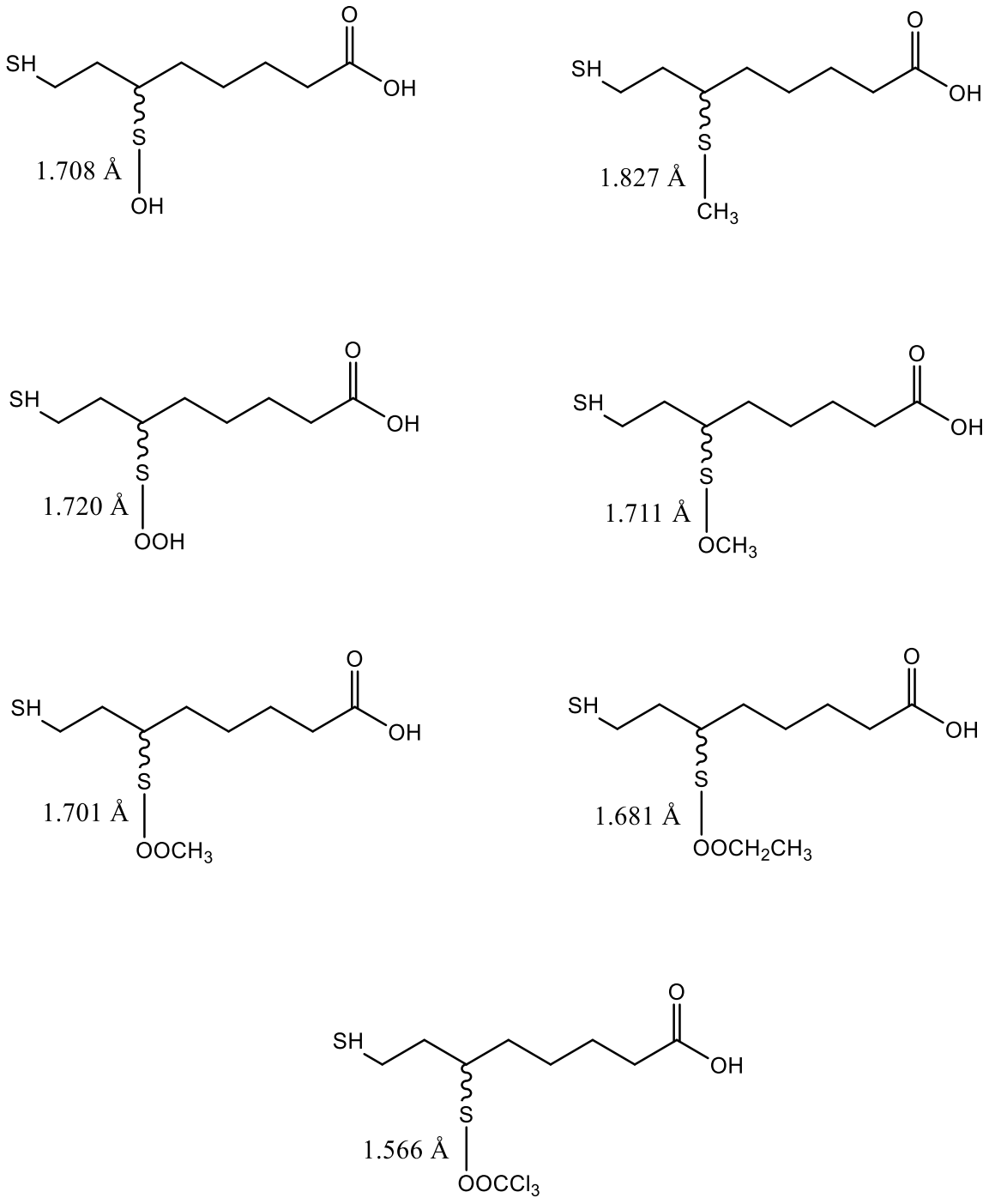

Figure 15**:** ChemDraw structures of tested DHLA-radical adducts and their corresponding bond S1-radical bond distances labeled

Geometry optimizations at DFT/B3LYP/cc-pVDZ of the different DHLA radical adducts show the following species ranked in decreasing thermodynamic favorability: -OH > -OCH_3 > -CH_3 > -$OOCCl_3$ > -$OOCH_2CH_3$ ~ -$OOCH_3$ > -OOH. As expected, the addition of ·OH to sulfur S1 yields the largest binding energy and is the most thermodynamically favored due to its high reactivity, followed by methoxy radical, ·OCH_3. Thermodynamic favorability significantly decreases as the number of oxygens within the radical increases, with an 81.2 kcal/mol increase in binding energy between ·OCH_3 and ·$OOCCl_3$. The reasoning for this is that the partial negative charge of the inside oxygen in ·$OOCCl_3$ pulls electron density from the reaction site on the other oxygen, reducing the reactivity of the overall radical. In ·OCH_3, the carbon is not electronegative enough to significantly delocalize the oxygen's valence electrons, so its reactivity is more like that of ·OH. In ·$OOCCl_3$, the central carbon acts as a sort of insulator to halt delocalization by the strong electron withdrawing trichloride group, making it more reactive than ·$OOCH_2CH_3$, ·$OOCH_3$, and ·OOH, which all have another oxygen bonded to the reaction site. Electron density surfaces should be mapped to properly visualize electron densities over each radical. The choice of radicals was based on the choices found in a similar study by Galano *et al.*[149] Methyl radical was used as a reference to measure the effect of adding an adjacent electronegative atom (·OCH_3), ·$OOCH_3$ was selected to illustrate the effect of adding another oxygen (·OCH_3 vs. ·$OOCH_3$), ·$OOCH_2CH_3$ was used to show the effect of an additional carbon (·$OOCH_3$ vs. ·$OOCH_2CH_3$), and ·$OOCCl_3$ showed the effect on binding energy when a strongly electron-withdrawing group was present (trichloride). Hydroperoxyl radical (·OOH) was included in this list since it is among the most common ROS present in physiological systems, along with hydroxyl radical.[3] The bond length between the sulfur S1 and the adducted radical

was determined at DFT/cc-VDZ for all previously mentioned radicals. These bond lengths are shows in Table 9.

Table 9: Bond lengths between sulfur S1 in DHLA and various free radicals after adduct formation; C3-S1-rad. bond angles are included

Bond	Bond length (Å)	Bond angle (deg.) (C3-S1-rad.)
S1-OH·	1.708	101.279
S1-CH_3·	1.827	100.827
S1-OOH·	1.720	99.684
S1-OCH_3·	1.711	102.214
S1-$OOCH_3$·	1.701	99.650
S1-$OOCH_2CH_3$·	1.681	101.715
S1-$OOCCl_3$·	1.566	104.211

The differences in S1-rad. bond lengths vary slightly, with the longest bond length belonging to S1-CH_3· (1.827 Å) and shortest being S1-$OOCCl_3$· (1.566 Å). As expected, the shortest bond length species corresponds to the largest C3-S1-rad. bond angle. Aside from the S1-CH_3· bond, the rest of the S1-rad. follow the same trend, where longer bond lengths correspond to smaller bond angles. As the distance between the sulfur and the bound radical decreases, electronic repulsion and steric hinderance increases, causing the bond to slightly open and achieve stability. Comparing the DHLA adducts of $OOCH_3$· and $OOCH_2CH_3$·, the additional -CH_2- introduces more hinderance between the radical and DHLA and results in a 2 degree increase in bond angle. However, the opposite is observed when comparing adducts with -OH· and -OOH·, where the presence of an additional oxygen corresponds to the smaller bond angle.

Explicit Solvation Study

Most outside literature mentioned in this work has utilized a continuum, or implicit, solvent model to observe solvent effects on antioxidant properties of variety of molecules.[44,149–151] As previously stated, continuum solvents provide the benefit of reduced computational power requirements and cleaner input structures. Continuum models are useful for solvating large biomolecules and studying the long-range chemistry interactions between the solute and the "solvent." However, this does not accurately represent a "real" chemical system and the short-range physics between the target molecule and solvent cannot be properly observed. ALA and DHLA were explicitly solvated and their interactions with water molecules was observed. Initial molecular configurations were generated using PACKMOL before semi-empirical PM6 geometry optimizations were performed to calculate the total energy of the system. The energies of ALA, DHLA, and DHLA-OH(S2) were compared against different quantities of water solvent molecules and the results are listed in Table 10 for ALA, Table 11 for DHLA, and Table 12 for DHLA-OH. Graphs were also constructed, plotting molecular energy against the number of solvent water molecules in the system for ALA, DHLA, and DHLA-OH(S2) and are shown in Figure 16. The PM6 heat of formation of water was calculated to be 56.30636 kcal/mol.

Table 10: Energy of the explicit solvent system and ALA against the number of water molecules using PM6

No. H2O	System Energy (kcal/mol)	Molecular Energy (kcal/mol)
0	-116.17344	-116.17344
1	-175.71132	-121.40496
2	-237.77244	-129.15972
3	-298.80915	-135.89007
4	-364.29907	-147.07363
5	-425.59754	-154.06574
6	-484.20536	-158.3672
7	-544.54049	-164.39597
8	-608.61466	-174.16378
9	-665.72565	-176.96841
10	-732.29992	-189.23632
20	-1362.67072	-276.54352

$\text{Molecular energy} = \left[\text{E}_{\text{system}}\right] - [\text{No. of } \text{H}_2\text{O}] * [\text{E}_{\text{parent}}]$; where E_{parent} is the PM6 heat of formation of the target molecule

Table 11: Energy of the system and DHLA against the number of water molecules using PM6

No. H2O	System Energy (kcal/mol)	Molecular Energy (kcal/mol)
0	-121.85158	-121.85158
1	-179.31407	-125.00771
2	-240.02213	-131.40941
3	-298.00399	-135.08491
4	-365.66981	-148.44437
5	-424.26419	-152.73239
6	-492.50411	-166.66595
7	-551.36009	-171.21557
8	-606.91593	-172.46505
9	-677.16348	-188.40624
10	-730.90424	-187.84064
20	-1367.74118	-281.61398

Table 12: Energy of the system and DHLA-OH(S2) against the number of water molecules using PM6

No. H2O	System energy (kcal/mol)	Molecular energy (kcal/mol)
0	-175.15459	-175.15459
1	-234.4486	-180.14224
2	-296.3106	-187.69788
3	-359.02006	-196.10098
4	-419.59229	-202.36685
5	-479.05848	-207.52668
6	-545.98102	-220.14286
7	-608.86094	-228.71642
8	-668.65395	-234.20307
9	-733.60052	-244.84328
10	-790.87578	-247.81218
20	-1426.19665	-340.06945

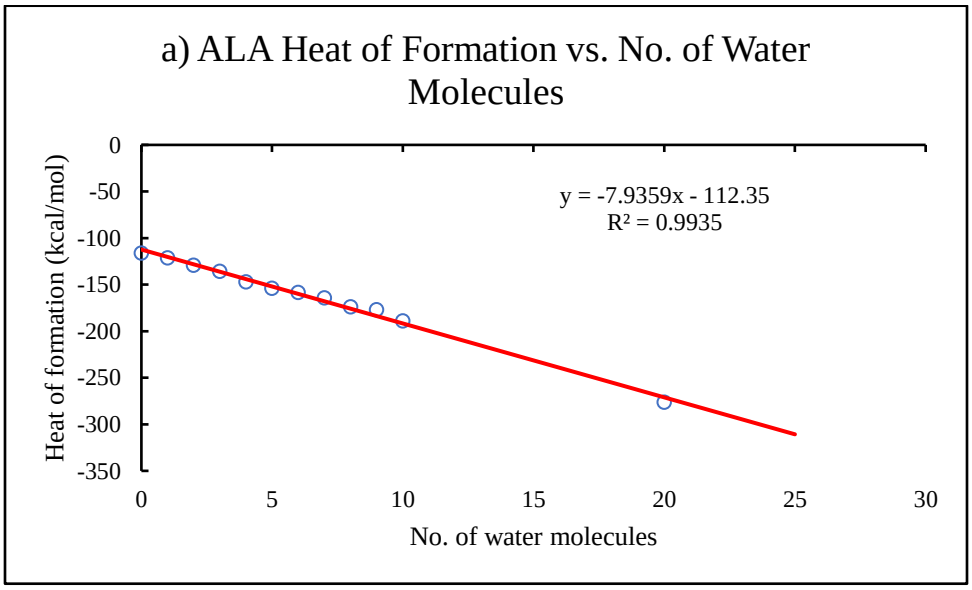

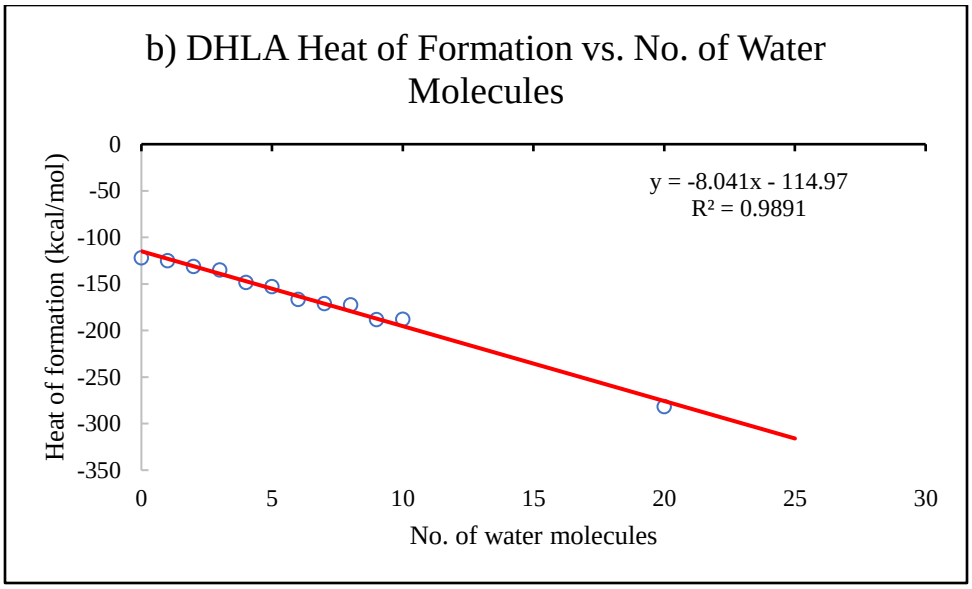

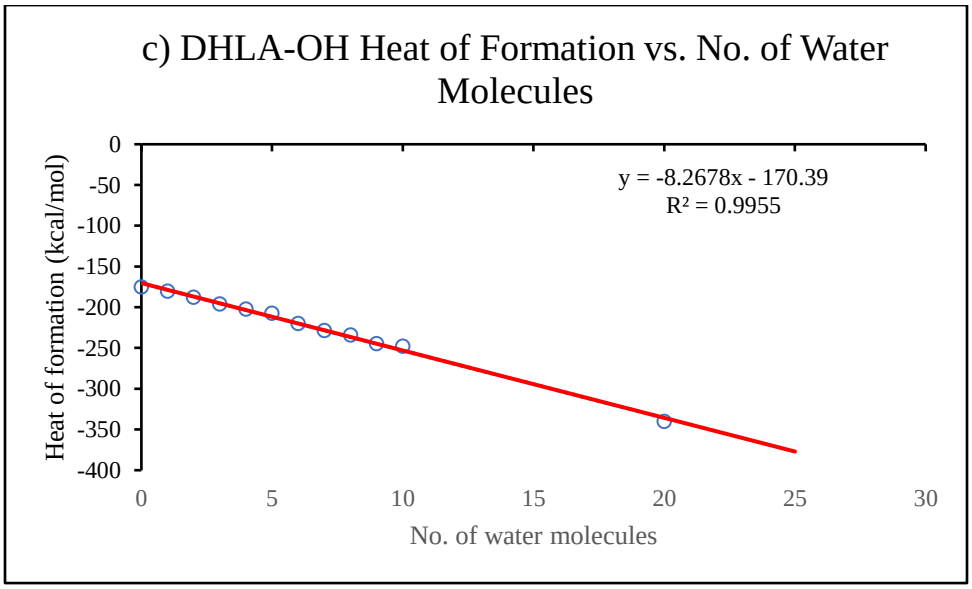

Figure 16**:** Molecular energy of (a) ALA, (b) DHLA, and (c) DHLA-OH(S2)

Figures 16a, 16b, and 16c depict a linear decrease in energy with the number of solvent water molecules but linear trends were not expected for this. When observing the final geometry optimized systems, water molecules tended to group near the acid group or near the sulfurs in all

three cases shown above. It is hypothesized that there were simply not enough water molecules added to the system to consider it a "solvated" solute and it was expected for these trends to slowly approach an asymptotic heat of formation after 5-7 water molecules were added. One study by Rognoni *et al.* analyzed computationally derived power spectra of solvent cages made of explicit water molecules and found that it may be necessary to have over 20 water molecules to solvate a solute.[152] However, based on searches for relevant literature, the optimization of explicit solvent models is not a hugely popular topic and further investigation must be done. It is also possible that the semi-empirical method employed was not sufficient for generating accurate energies of the explicitly solvated ALA and DHLA, so it may be beneficial to test other levels of theory.

CHAPTER 4. CONCLUSIONS AND FUTURE WORK

All calculations performed in this work, other than the explicit solvation study, were done in the gas phase, so future work on ALA, DHLA, and their adducts should include aqueous and nonaqueous solvent mediums to better emulate a physiological system. The initial goal of this research was to determine whether ALA or DHLA would make for an effective spin trap, but the data shows that they do the opposite and DHLA simply quenches ROS due to its well-established antioxidant properties. The quenching of ROS by DHLA results in a singlet-state adduct, which is not EPR-active and, therefore, cannot be considered a spin trap. Establishing a spin trapping mechanism of DHLA has proved itself to be beyond the scope of this work, but it was learned that DHLA shows far better antioxidant properties than ALA in both aqueous and non-aqueous media and that the most likely binding sites for transient radicals are the sulfur atoms, indicated by the HOMO and spin density surfaces. This helps narrow down the search for a viable transition state which can be computationally determined through saddle point optimizations. Saddle point calculations were attempted but were ultimately unsuccessful due to time and resource limitations. It is drawn from the data that a hydrogen transfer prior to the addition of a radical species is the most likely route for radical quenching. A transition state may be expected to involve an intramolecular hydrogen transfer between either the two sulfurs or between the radical-bound sulfur and -COOH moiety, but this hypothesis requires its own study to confirm. The ability of the DHLA-radical adduct to cyclize due to its network of single bonds may offer insight into choosing proper starting geometries for transition state calculations. The doublet anion DHLA-OH(S2) spin density calculation indicates that cyclization and hydrogen transfer may be possible since there is shared spin density at the bound radical and -COOH. The fact that the carboxylic acid group is most likely deprotonated at physiological pH holds greater

weight for considering the doublet anion adduct. Generating additional spin density plots with other radical species would provide insight into the credibility of the DHLA-OH calculations and looking at electron density surfaces for each individual radical species would help explain the binding energy trends observed. While qualitatively analyzing spin density surfaces on the spin adducts paints a general picture, being able to quantify the results would also prove useful for comparing systems that share similar spin density surface qualities. This should be done by computationally generating EPR spectra and analyzing partial charge distribution on each atom. This would allow for a quantitative comparison of spin density clouds on each sulfur, which may suggest the likelihood of one adduct forming over the other.

HF and HF/MP2 analysis of the adduct energies should be performed since most of the energies calculated in this research were done under DFT. While DFT is useful for fast and sufficiently accurate calculations, HF/MP2 data are more prevalent in today's literature and serves as the standard for most quantum mechanical calculations and applying it to this work would allow for a more direct comparison of values to those found in the literature. Establishing a mechanism may also require implementing molecular mechanics and kinetics calculations. There are sufficient kinetics data in literature indicating the rates of radical stabilization by DHLA in various solvent media. These data also reveal that the radical scavenging activity of DHLA is far higher than that of many other well-known radical scavengers such as melatonin, caffeine, canolol, dopamine, and glutathione.

While DHLA forms a singlet state upon the quenching of ROS, it is possible that making modifications to the structure of DHLA may allow the generation of EPR-active spin adducts. Modifying the length of the carbon chain could increase or decrease the energy required for intramolecular proton transfer between -COOH and the sulfur(s). Of course, this is mere

speculation but an example of another path that could be taken in future work. It must, however, be determined whether the modified structures of ALA and DHLA remain non-toxic in physiological systems to make such modifications justifiable in the future.

Lastly, successful explicit solvation calculations of ALA and DHLA should be pursued since they could possibly reveal the physical solute/solvent interactions and give a better idea of their behavior in physiological systems and would contribute to the research of other antioxidant mechanisms. Further investigation into explicit solvation in this study was halted early on and focus was diverted toward quantum mechanical gas-phase calculations when it was noticed that solvation energy trends were linear. Using a solvent shell consisting of at least 20-30 water molecules may be a good starting point for whoever continues work with ALA and DHLA. Utilizing PACKMOL proved to be an efficient method for generating starting structures and should be used in the continuation of this project.

While these data conclude that ALA and DHLA do not possess spin trapping capabilities, the search for naturally produced compounds with sufficient spin trapping ability should continue to be pursued in hopes of developing methods for safe *in vivo* analysis of free radical presence in physiological systems. While synthetic spin traps such as DMPO, DEPMPO, and PBN are commonly used in EPR spectroscopy, their toxicity to living systems is not well-documented. Computational research of endogenous antioxidants for potential use as spin traps is a small niche that offers plenty of opportunity to expand upon and generate new curiosity for computational chemists and biochemists alike.

REFERENCES

1. Pham-Huy, L. A.; He, H.; Pham-Huy, C. Free Radicals, Antioxidants in Disease and Health. *International Journal of Biomedical Science*. Master Publishing Group June 2008, pp 89–96.

2. Phaniendra, A.; Jestadi, D. B.; Periyasamy, L. Free Radicals: Properties, Sources, Targets, and Their Implication in Various Diseases. *Indian Journal of Clinical Biochemistry*. Springer India January 1, 2015, pp 11–26. DOI: 10.1007/s12291-014-0446-0.

3. Lobo, V.; Patil, A.; Phatak, A.; Chandra, N. Free Radicals, Antioxidants and Functional Foods: Impact on Human Health. *Pharmacognosy Reviews*. Wolters Kluwer -- Medknow Publications July 2010, pp 118–126. DOI: 10.4103/0973-7847.70902.

4. Uttara, B.; Singh, A.; Zamboni, P.; Mahajan, R. Oxidative Stress and Neurodegenerative Diseases: A Review of Upstream and Downstream Antioxidant Therapeutic Options. *Current Neuropharmacology* **2009**, *7* (1), 65–74. DOI: 10.2174/157015909787602823.

5. Kumar, S. Free Radicals and Antioxidants: Human and Food System. *Pelagia Research Library Advances in Applied Science Research* **2011**, *2* (1), 129–135.

6. Aseervatham, G. S. B.; Sivasudha, T.; Jeyadevi, R.; Arul Ananth, D. Environmental Factors and Unhealthy Lifestyle Influence Oxidative Stress in Humans--an Overview. *Environmental Science and Pollution Research International*. Environ Sci Pollut Res Int 2013, pp 4356–4369. DOI: 10.1007/s11356-013-1748-0.

7. Aprioku, J. S. Pharmacology of Free Radicals and the Impact of Reactive Oxygen Species on the Testis. *Journal of Reproduction and Infertility*. Avicenna Research Institute October 2013, pp 158–172.

8. Martínez, M. C.; Andriantsitohaina, R. Reactive Nitrogen Species: Molecular Mechanisms and Potential Significance in Health and Disease. *Antioxidants and Redox Signaling*. Mary Ann Liebert Inc. March 1, 2009, pp 669–702. DOI: 10.1089/ars.2007.1993.

9. Pizzino, G.; Irrera, N.; Cucinotta, M.; Pallio, G.; Mannino, F.; Arcoraci, V.; Squadrito, F.; Altavilla, D.; Bitto, A. Oxidative Stress: Harms and Benefits for Human Health. *Oxidative Medicine and Cellular Longevity*. Hindawi Limited 2017. DOI: 10.1155/2017/8416763.

10. Reuter, S.; Gupta, S. C.; Chaturvedi, M. M.; Aggarwal, B. B. Oxidative Stress, Inflammation, and Cancer: How Are They Linked? *Free Radical Biology and Medicine*. NIH Public Access December 1, 2010, pp 1603–1616. DOI: 10.1016/j.freeradbiomed.2010.09.006.

11. Valko, M.; Leibfritz, D.; Moncol, J.; Cronin, M. T. D.; Mazur, M.; Telser, J. Free Radicals and Antioxidants in Normal Physiological Functions and Human Disease. *International Journal of Biochemistry and Cell Biology*. Int J Biochem Cell Biol 2007, pp 44–84. DOI: 10.1016/j.biocel.2006.07.001.

12. Khan, F.; Kumar Garg, V.; Kumar Singh, A.; Tinku, T. Role of Free Radicals and Certain Antioxidants in the Management of Huntington's Disease: A Review. *Journal of Analytical & Pharmaceutical Research* **2018**, *7* (4). DOI: 10.15406/JAPLR.2018.07.00256.

13. Halliwell, B. Role of Free Radicals in the Neurodegenerative Diseases: Therapeutic Implications for Antioxidant Treatment. *Drugs and Aging*. Adis International Ltd 2001, pp 685–716. DOI: 10.2165/00002512-200118090-00004.

14. Senoner, T.; Dichtl, W. Oxidative Stress in Cardiovascular Diseases: Still a Therapeutic Target? *Nutrients*. MDPI AG September 1, 2019. DOI: 10.3390/nu11092090.

15. Santus, P.; Corsico, A.; Solidoro, P.; Braido, F.; di Marco, F.; Scichilone, N. Oxidative Stress and Respiratory System: Pharmacological and Clinical Reappraisal of N-Acetylcysteine. *COPD: Journal of Chronic Obstructive Pulmonary Disease*. Informa Healthcare December 1, 2014, pp 705–717. DOI: 10.3109/15412555.2014.898040.

16. Antioxidant | Definition of Antioxidant by Merriam-Webster https://www.merriam-webster.com/dictionary/antioxidant (accessed 2021 -09 -20).

17. Saljoughian, M. Natural Powerful Antioxidants https://www.uspharmacist.com/article/natural-powerful-antioxidants (accessed 2021 -06 -12).

18. Bouayed, J.; Bohn, T. Exogenous Antioxidants - Double-Edged Swords in Cellular Redox State: Health Beneficial Effects at Physiologic Doses Versus Deleterious Effects at High Doses. *Oxidative Medicine and Cellular Longevity*. Hindawi Limited 2010, pp 228–237. DOI: 10.4161/oxim.3.4.12858.

19. Meister, A. Glutathione Metabolism and Its Selective Modification. *Journal of Biological Chemistry* **1988**, *263* (33), 17205–17208. DOI: 10.1016/S0021-9258(19)77815-6.

20. Forman, H. J.; Zhang, H.; Rinna, A. Glutathione: Overview of Its Protective Roles, Measurement, and Biosynthesis. *Molecular Aspects of Medicine* **2009**, *30* (1–2), 1. DOI: 10.1016/J.MAM.2008.08.006.

21. Katerji, M.; Filippova, M.; Duerksen-Hughes, P. Approaches and Methods to Measure Oxidative Stress in Clinical Samples: Research Applications in the Cancer Field. *Oxidative Medicine and Cellular Longevity*. Hindawi Limited 2019. DOI: 10.1155/2019/1279250.

22. Mrakic-Sposta, S.; Gussoni, M.; Montorsi, M.; Porcelli, S.; Vezzoli, A. A Quantitative Method to Monitor Reactive Oxygen Species Production by Electron Paramagnetic Resonance in Physiological and Pathological Conditions. *Oxidative Medicine and Cellular Longevity* **2014**, *2014*. DOI: 10.1155/2014/306179.

23. Nawab, A.; Nichols, A.; Klug, R.; Shapiro, J. I.; Sodhi, K. Spin Trapping: A Review for the Study of Obesity Related Oxidative Stress and Na+/K+-ATPase. *Journal of Clinical & Cellular Immunology* **2017**, *08* (03). DOI: 10.4172/2155-9899.1000505.

24. Kempe, S.; Metz, H.; Mäder, K. Application of Electron Paramagnetic Resonance (EPR) Spectroscopy and Imaging in Drug Delivery Research - Chances and Challenges. *European Journal of Pharmaceutics and Biopharmaceutics* **2010**, *74* (1), 55–66. DOI: 10.1016/j.ejpb.2009.08.007.

25. *The IUPAC Compendium of Chemical Terminology*; International Union of Pure and Applied Chemistry (IUPAC), 2019. DOI: 10.1351/goldbook.

26. Hawkins, C. L.; Morgan, P. E.; Davies, M. J. Quantification of Protein Modification by Oxidants. *Free Radical Biology and Medicine* **2009**, *46* (8), 965–988. DOI: 10.1016/J.FREERADBIOMED.2009.01.007.

27. Gomez-Mejiba, S. E.; Zili, Z.; Della-Vedova, M. C.; Muñoz, M. D.; Chatterjee, S.; Towner, R. A.; Hensley, K.; Floyd, R. A.; Mason, R. P.; Ramirez, D. C. Immuno-Spin Trapping From Biochemistry to Medicine: Advances, Challenges, and Pitfalls: Focus on Protein-Centered Radicals. *Biochimica et Biophysica Acta* **2014**, *1840* (2), 722. DOI: 10.1016/J.BBAGEN.2013.04.039.

28. Davies, M. J.; Gilbert, B. C.; Haywood, R. M. Radical-Induced Damage to Proteins: E.S.R. Spin-Trapping Studies. *Free Radical Research Communications* **1991**, *15* (2), 111–127. DOI: 10.3109/10715769109049131.

29. Khoo, N. K. H.; Cantu-Medellin, N.; Croix, C. st.; Kelley, E. E. In Vivo Immuno-Spin Trapping: Imaging the Footprints of Oxidative Stress. *Current Protocols in Cytometry / Editorial Board, J. Paul Robinson, managing editor ... [et al.]* **2015**, *74* (1), 12.42.1. DOI: 10.1002/0471142956.CY1242S74.

30. Yoshida, M.; Fukuda, A.; Hara, M.; Terada, A.; Kitanaka, Y.; S, O. Melatonin Prevents the Increase in Hydroxyl Radical-Spin Trap Adduct Formation Caused by the Addition of Cisplatin in Vitro. *Life Sciences* **2003**, *72* (15), 1773–1780. DOI: 10.1016/S0024-3205(02)02480-3.

31. Galano, A.; Tan, D. X.; Reiter, R. J. Melatonin as a Natural Ally against Oxidative Stress: A Physicochemical Examination. *Journal of Pineal Research* **2011**, *51* (1), 1–16. DOI: 10.1111/J.1600-079X.2011.00916.X.

32. Hardeland, R.; Pandi-Perumal, S. Melatonin, a Potent Agent in Antioxidative Defense: Actions as a Natural Food Constituent, Gastrointestinal Factor, Drug and Prodrug. *Nutrition & Metabolism 2005 2:1* **2005**, *2* (1), 1–15. DOI: 10.1186/1743-7075-2-22.

33. Matuszak, Z.; Reszka, K. J.; Chignell, C. F. Reaction of Melatonin and Related Indoles With Hydroxyl Radicals: EPR and Spin Trapping Investigations. *Free Radical Biology and Medicine* **1997**, *23* (3), 367–372. DOI: 10.1016/S0891-5849(96)00614-4.

34. Reiter, R.; Tan, D.; Poeggeler, B.; Menendez-Palaez, A.; Chen, L.; Saarela, S. Melatonin as a Free Radical Scavenger: Implications for Aging and Age-Related Diseases. *Annals of the New York Academy of Sciences* **1994**, *719* (1), 1–12. DOI: 10.1111/J.1749-6632.1994.TB56817.X.

35. Manda, K.; Ueno, M.; Anzai, K. AFMK, a Melatonin Metabolite, Attenuates X-Ray-Induced Oxidative Damage to DNA, Proteins and Lipids in Mice. *Journal of Pineal Research* **2007**, *42* (4), 386–393. DOI: 10.1111/J.1600-079X.2007.00432.X.

36. Tan, D.; Manchester, L.; Reiter, R.; Plummer, B.; Limson, J.; Weintraub, S.; Qi, W. Melatonin Directly Scavenges Hydrogen Peroxide: A Potentially New Metabolic Pathway of Melatonin Biotransformation. *Free Radical Biology and Medicine* **2000**, *29* (11), 1177–1185. DOI: 10.1016/S0891-5849(00)00435-4.

37. Li, Y.; Zhao, Y.; Yu, W.; Jiang, S. Scavenging Ability on ROS of Alpha-Lipoic Acid (ALA). **2018**, *8146* (April), 3–8. DOI: 10.1016/S0308-8146(03)00279-6.

38. Yi, X.; Maeda, N. Endogenous Production of Lipoic Acid Is Essential for Mouse Development. *Molecular and Cellular Biology* **2005**, *25* (18), 8387–8392. DOI: 10.1128/mcb.25.18.8387-8392.2005.

39. Higdon, J.; Drake, V.; Delage, B.; Hagen, T. M. Lipoic Acid | Linus Pauling Institute | Oregon State University https://lpi.oregonstate.edu/mic/dietary-factors/lipoic-acid#references.

40. Tutelyan, V. A.; Makhova, A. A.; Pogozheva, A. V.; Shikh, E. V.; Elizarova, E. V.; Khotimchenko, S. A. Lipoic Acid: Physiological Role and Prospects for Clinical Application. *Voprosy Pitaniia*. Nutritec 2019, pp 6–11. DOI: 10.24411/0042-8833-2019-10035.

41. Lipoic Acid - an overview | ScienceDirect Topics https://www.sciencedirect.com/topics/agricultural-and-biological-sciences/lipoic-acid (accessed 2021 -06 -14).

42. Golbidi, S.; Badran, M.; Laher, I. Diabetes and Alpha Lipoic Acid. **2011**. DOI: 10.3389/fphar.2011.00069.

43. Perricone, N.; Nagy, K.; Horváth, F.; Dajkó, G.; Uray, I.; Zs.-Nagy, I. Alpha Lipoic Acid (ALA) Protects Proteins against the Hydroxyl Free Radical-Induced Alterations: Rationale for Its Geriatric Topical Application. *Archives of Gerontology and Geriatrics* **1999**, *29* (1), 45–56. DOI: 10.1016/S0167-4943(99)00022-9.

44. Mikulski, D.; Molski, M. Quantum-Chemical Investigation of the Structure and the Antioxidant Properties of α -Lipoic Acid and Its Metabolites. *Journal of Molecular Modeling* **2012**, 2907–2916. DOI: 10.1007/s00894-011-1306-y.

45. Shang, Y. J.; Qian, Y. P.; Liu, X. da; Dai, F.; Shang, X. L.; Jia, W. Q.; Liu, Q.; Fang, J. G.; Zhou, B. Radical-Scavenging Activity and Mechanism of Resveratrol-Oriented Analogues: Influence of the Solvent, Radical, and Substitution. *Journal of Organic Chemistry* **2009**, *74* (14), 5025–5031. DOI: 10.1021/jo9007095.

46. Castañ Eda-Arriaga, R.; Raul Alvarez-Idaboy, J. Lipoic Acid and Dihydrolipoic Acid. A Comprehensive Theoretical Study of Their Antioxidant Activity Supported by Available Experimental Kinetic Data. **2014**. DOI: 10.1021/ci500213p.

47. Suzuki, Y. J.; Tsuchiya, M.; Packer, L. Thioctic Acid and Dihydrolipoic Acid Are Novel Antioxidants Which Interact with Reactive Oxygen Species. *Free Radical Research* **1991**, *15* (5), 255–263. DOI: 10.3109/10715769109105221.

48. Suzuki, Y. J.; Tsuchiya, M.; Packer, L. Antioxidant Activities of Dihydrolipoic Acid and Its Structural Homologues. *Free Radical Research* **1993**, *18* (2), 115–122. DOI: 10.3109/10715769309147348.

49. Lipoic Acid | Linus Pauling Institute | Oregon State University https://lpi.oregonstate.edu/mic/dietary-factors/lipoic-acid#unbound-lipoic-acid (accessed 2021 -09 -19).

50. Sliwoski, G.; Kothiwale, S.; Meiler, J.; Lowe, E. W. Computational Methods in Drug Discovery. **2014**. DOI: 10.1124/pr.112.007336.

51. Cavasotto, C. N.; Aucar, M. G.; Adler, N. S. Computational Chemistry in Drug Lead Discovery and Design. *International Journal of Quantum Chemistry* **2019**, *119* (2), e25678. DOI: 10.1002/qua.25678.

52. Ying, F.; Zhang, Y.; Xiang, C.; Song, Z.; Xie, H.; Bao, W. Key Mechanistic Features in Palladium-Catalyzed Methylcyclopropanation of Norbornenes with Vinyl Bromides: Insights from DFT Calculations. *Frontiers in Chemistry* **2019**, *7* (MAR), 169. DOI: 10.3389/fchem.2019.00169.

53. Vogiatzis, K. D.; Polynski, M. v.; Kirkland, J. K.; Townsend, J.; Hashemi, A.; Liu, C.; Pidko, E. A. Computational Approach to Molecular Catalysis by 3d Transition Metals: Challenges and Opportunities. *Chemical Reviews*. American Chemical Society February 27, 2019, pp 2453–2523. DOI: 10.1021/acs.chemrev.8b00361.

54. Song, F.; Busch, M. M.; Lassalle-Kaiser, B.; Hsu, C. S.; Petkucheva, E.; Bensimon, M.; Chen, H. M.; Corminboeuf, C.; Hu, X. An Unconventional Iron Nickel Catalyst for the Oxygen Evolution Reaction. *ACS Central Science* **2019**, *5* (3), 558–568. DOI: 10.1021/acscentsci.9b00053.

55. Jensen, F. *Introduction to Computational Chemistry Computational Chemistry*; John Wiley & Sons, Inc, 2017; Vol. 132.

56. Century, N. R. C. (US) C. on C. for the C. S. in the 21st. Chemical Theory and Computer Modeling: From Computational Chemistry to Process Systems Engineering. **2003**.

57. Lewars, E. G. *Computational Chemistry: Introduction to the Theory and Applications of Molecular and Quantum Mechanics*; 2011. DOI: 10.1007/978-90-481-3862-3.

58. Vanommeslaeghe, K.; Guvench, O.; MacKerell, A. D. Molecular Mechanics. *Current Pharmaceutical Design* **2014**, *20* (20), 3281–3292. DOI: 10.2174/13816128113199990600.

59. Craik, D. Guidebook on Molecular Modeling in Drug Design. By N. C. Cohen. *Molecules* **1997**, *2* (12). DOI: 10.3390/21000154.

60. Friesner, R. A. Ab Initio Quantum Chemistry: Methodology and Applications. *Proceedings of the National Academy of Sciences of the United States of America*. National Academy of Sciences May 10, 2005, pp 6648–6653. DOI: 10.1073/pnas.0408036102.

61. Hartree, D. R. The Wave Mechanics of an Atom with a Non-Coulomb Central Field Part I Theory and Methods. *Mathematical Proceedings of the Cambridge Philosophical Society* **1928**, *24* (1), 89–110. DOI: 10.1017/S0305004100011919.

62. Møller, Chr.; Plesset, M. S. Note on an Approximation Treatment for Many-Electron Systems. *Physical Review* **1934**, *46* (7), 618. DOI: 10.1103/PhysRev.46.618.

63. Čížek, J. On the Correlation Problem in Atomic and Molecular Systems. Calculation of Wavefunction Components in Ursell-Type Expansion Using Quantum-Field Theoretical Methods. *The Journal of Chemical Physics* **2004**, *45* (11), 4256. DOI: 10.1063/1.1727484.

64. Baseden, K. A.; Tye, J. W. Introduction to Density Functional Theory: Calculations by Hand on the Helium Atom. **2014**. DOI: 10.1021/ed5004788.

65. van Mourik, T.; Bühl, M.; Gaigeot, M. P. Density Functional Theory across Chemistry, Physics and Biology. *Philosophical Transactions of the Royal Society A: Mathematical, Physical and Engineering Sciences* **2014**, *372* (2011). DOI: 10.1098/rsta.2012.0488.

66. Orio, M.; Dimitrios, A. E.; Ae, A. P.; Neese, F. Density Functional Theory. DOI: 10.1007/s11120-009-9404-8.

67. Becke, A. D. Density-Functional Thermochemistry. III. The Role of Exact Exchange. *The Journal of Chemical Physics* **1993**, *98* (7), 5648–5652. DOI: 10.1063/1.464913.

68. Lee, C.; Yang, W.; Parr, R. G. Development of the Colle-Salvetti Correlation-Energy Formula into a Functional of the Electron Density. *Physical Review B* **1988**, *37* (2), 785–789. DOI: 10.1103/PhysRevB.37.785.

69. Perdew, J. P.; Ernzerhof, M.; Burke, K. *Rationale for Mixing Exact Exchange With Density Functional Approximations*; 1996; Vol. 105.

70. Christensen, A. S.; Kubař, T.; Cui, Q.; Elstner, M. Semiempirical Quantum Mechanical Methods for Noncovalent Interactions for Chemical and Biochemical Applications. *Chemical Reviews* **2016**, *116* (9), 5301–5337. DOI: 10.1021/ACS.CHEMREV.5B00584.

71. Dewar, M. J. S.; Zoebisch, E. G.; Healy, E. F.; Stewart, J. J. P. Development and Use of Quantum Mechanical Molecular Models. 76. AM1: A New General Purpose Quantum Mechanical Molecular Model. *Journal of the American Chemical Society* **2002**, *107* (13), 3902–3909. DOI: 10.1021/JA00299A024.

72. Stewart, J. J. P. Optimization of Parameters for Semiempirical Methods II. Applications. *Journal of Computational Chemistry* **1989**, *10* (2), 221–264. DOI: 10.1002/JCC.540100209.

73. Stewart, J. J. P. Optimization of Parameters for Semiempirical Methods V: Modification of NDDO Approximations and Application to 70 Elements. *Journal of Molecular Modeling 2007 13:12* **2007**, *13* (12), 1173–1213. DOI: 10.1007/S00894-007-0233-4.

74. Schrödinger, E. Quantisierung Als Eigenwertproblem. *Annalen der Physik* **1926**, *384* (4), 361–376. DOI: 10.1002/andp.19263840404.

75. Schrödinger, E. An Undulatory Theory of the Mechanics of Atoms and Molecules. *Physical Review* **1926**, *28* (6), 1049–1070. DOI: 10.1103/PhysRev.28.1049.

76. Hartree, D. R. The Wave Mechanics of an Atom with a Non-Coulomb Central Field. Part I. Theory and Methods. *Mathematical Proceedings of the Cambridge Philosophical Society* **1928**, *24* (1), 89–110. DOI: 10.1017/S0305004100011919.

77. Born, M.; Oppenheimer, R. Zur Quantentheorie Der Molekeln. *Annalen der Physik* **1927**, *389* (20), 457–484. DOI: 10.1002/andp.19273892002.

78. McQuarrie, D. A. *Quantum Chemistry*, 2nd ed.; University Science Books: Sausalito, CA, 2008.

79. Minkin, V. I. Glossary of Terms Used in Theoretical Organic Chemistry (IUPAC Recommendations 1999). *Pure and Applied Chemistry* **1999**, *71* (10), 1919–1981. DOI: 10.1351/pac199971101919.

80. Sherrill, C. D. *An Introduction to Hartree-Fock Molecular Orbital Theory*; 2000.

81. Heilbron, J. L. The Origins of the Exclusion Principle. *Historical Studies in the Physical Sciences* **1983**, *13* (2), 261–310. DOI: 10.2307/27757517.

82. McQuarrie, D. A. The Variational Method Provides an Upper Bound to the Ground-State Energy of a System. In *Quantum Chemistry*; University Science Books, 2008; pp 381–382.

83. 8.3: Hartree-Fock Equations are Solved by the Self-Consistent Field Method - Chemistry LibreTexts https://chem.libretexts.org/Courses/BethuneCookman_University/BCU%3A_CH_332_Physical_Chemistry_II/Text/8%3A_Multielectron_Atoms/8.03%3A_Hartree-Fock_Equations_are_Solved_by_the_Self-Consistent_Field_Method (accessed 2021 -10 -19).

84. Baseden, K. A.; Tye, J. W. Introduction to Density Functional Theory: Calculations by Hand on the Helium Atom. *Journal of Chemical Education* **2014**, *91* (12), 2116–2123. DOI: 10.1021/ed5004788.

85. Thomas, L. H. The Calculation of Atomic Fields. *Mathematical Proceedings of the Cambridge Philosophical Society* **1927**, *23* (5), 542–548. DOI: 10.1017/S0305004100011683.

86. Fermi, E. Statistical Method to Determine Some Properties of Atoms. *Rendiconti Lincei* **1927**, *6*, 602–607.

87. Gill, P. M. W. Density Functional Theory (DFT), Hartree-Fock (HF), and the Self-Consistent Field. In *Encyclopedia of Computational Chemistry*; 2002; pp 678–689. DOI: 10.1002/0470845015.cda011.

88. Hohenberg, P.; Kohn, W. Inhomogeneous Electron Gas. *Physical Review* **1964**, *136* (3B), B864. DOI: 10.1103/PhysRev.136.B864.

89. Kohn, W.; Sham, L. J. Self-Consistent Equations Including Exchange and Correlation Effects. *Physical Review* **1965**, *140* (4A), A1133. DOI: 10.1103/PhysRev.140.A1133.

90. Becke, A. D. Perspective: Fifty Years of Density-Functional Theory in Chemical Physics. *Journal of Chemical Physics* **2014**, *140* (18), 18–301. DOI: 10.1063/1.4869598.

91. Kohn, W.; Sham, L. J. Self-Consistent Equations Including Exchange and Correlation Effects. *Physical Review* **1965**, *140* (4A), A1133. DOI: 10.1103/PhysRev.140.A1133.

92. Kohn, W.; Becke, A. D.; Parr, R. G. Density Functional Theory of Electronic Structure. *Journal of Physical Chemistry* **1996**, *100* (31), 12974–12980. DOI: 10.1021/jp960669l.

93. Vosko, S. H.; Wilk, L.; Nusair, M. Accurate Spin-Dependent Electron Liquid Correlation Energies for Local Spin Density Calculations: A Critical Analysis. *Canadian Journal of Physics* **1980**, *58* (8), 1200–1211. DOI: 10.1139/p80-159.

94. Perdew, J. P. Accurate Density Functional for the Energy: Real-Space Cutoff of the Gradient Expansion for the Exchange Hole. *Physical Review Letters* **1985**, *55* (16), 1665–1668. DOI: 10.1103/PhysRevLett.55.1665.

95. Perdew, J. P.; Chevary, J. A.; Vosko, S. H.; Jackson, K. A.; Pederson, M. R.; Singh, D. J.; Fiolhais, C. Atoms, Molecules, Solids, and Surfaces: Applications of the Generalized Gradient Approximation for Exchange and Correlation. *Physical Review B* **1992**, *46* (11), 6671–6687. DOI: 10.1103/PhysRevB.46.6671.

96. Langreth, D. C.; Mehl, M. J. Beyond the Local-Density Approximation in Calculations of Ground-State Electronic Properties. *Physical Review B* **1983**, *28* (4), 1809–1834. DOI: 10.1103/PhysRevB.28.1809.

97. Becke, A. D. *Density-Functional Exchange-Energy Approximation with Correct Asymptotic Behavior*; 1988; Vol. 38.

98. Odashima, M. M.; Capelle, K. Non-Empirical Hyper-Generalized-Gradient Functionals Constructed from the Lieb-Oxford Bound. *Physical Review A - Atomic, Molecular, and Optical Physics*. March 25, 2009.

99. Burke, K.; Perdew, J. P.; Wang, Y. Derivation of a Generalized Gradient Approximation: The PW91 Density Functional. In *Electronic Density Functional Theory*; Springer US, 1998; pp 81–111. DOI: 10.1007/978-1-4899-0316-7_7.

100. Nakata, A.; Imamura, Y.; Otsuka, T.; Nakai, H. Time-Dependent Density Functional Theory Calculations for Core-Excited States: Assessment of Standard Exchange-Correlation Functionals and Development of a Novel Hybrid Functional. *Journal of Chemical Physics* **2006**, *124* (9). DOI: 10.1063/1.2173987.

101. Stephens, P. J.; Devlin, F. J.; Chabalowski, C. F.; Frisch, M. J. Ab Initio Calculation of Vibrational Absorption and Circular Dichroism Spectra Using Density Functional Force Fields. *Journal of Physical Chemistry*® **1994**, *98* (45), 11623–11627. DOI: 10.1021/j100096a001.

102. Sousa, S. F.; Fernandes, P. A.; Ramos, M. J. General Performance of Density Functionals. *Journal of Physical Chemistry A* **2007**, *111* (42), 10439–10452. DOI: 10.1021/jp0734474.

103. Boys, S. F. Electronic Wave Functions - I. A General Method of Calculation for the Stationary States of Any Molecular System. *Proceedings of the Royal Society of London. Series A. Mathematical and Physical Sciences* **1950**, *200* (1063). DOI: 10.1098/rspa.1950.0036.

104. Ditchfield, R.; Hehre, W. J.; Pople, J. A. Self-Consistent Molecular-Orbital Methods. IX. An Extended Gaussian-Type Basis for Molecular-Orbital Studies of Organic Molecules. *The Journal of Chemical Physics* **1971**, *54* (2). DOI: 10.1063/1.1674902.

105. Standard, J. M. *Chemistry 460 Spring 2013 Dr. Basis Set Notation*; 2013.

106. Hunt, P. A. Quantum Chemical Modeling of Hydrogen Bonding in Ionic Liquids. *Topics in Current Chemistry*. Springer Verlag June 1, 2017. DOI: 10.1007/s41061-017-0142-7.

107. Papajak, E.; Truhlar, D. G. Efficient Diffuse Basis Sets for Density Functional Theory. *Journal of Chemical Theory and Computation* **2010**, *6* (3). DOI: 10.1021/ct900566x.

108. Lynch, B. J.; Zhao, Y.; Truhlar, D. G. *The Effectiveness of Diffuse Basis Functions for Calculating Relative Energies by Density Functional Theory*.

109. Treitel, N.; Shenhar, R.; Aprahamian, I.; Sheradsky, T.; Rabinovitz, M. Calculations of PAH Anions: When Are Diffuse Functions Necessary? DOI: 10.1039/b315069k.

110. Papajak, E.; Zheng, J.; Xu, X.; Leverentz, H. R.; Truhlar, D. G. Perspectives on Basis Sets Beautiful: Seasonal Plantings of Diffuse Basis Functions. *Journal of Chemical Theory and Computation*. 2011. DOI: 10.1021/ct200106a.

111. Wilson, A. K.; van Mourik, T.; Dunning, T. H. Gaussian Basis Sets for Use in Correlated Molecular Calculations. VI. Sextuple Zeta Correlation Consistent Basis Sets for Boron through Neon. *Journal of Molecular Structure: THEOCHEM* **1996**, *388* (1–3). DOI: 10.1016/s0166-1280(96)80048-0.

112. Peterson, K. A.; Woon, D. E.; Dunning, T. H. Benchmark Calculations with Correlated Molecular Wave Functions. IV. The Classical Barrier Height of the H+H2→H2+H Reaction. *The Journal of Chemical Physics* **1994**, *100* (10). DOI: 10.1063/1.466884.

113. Woon, D. E.; Dunning, T. H. Gaussian Basis Sets for Use in Correlated Molecular Calculations. III. The Atoms Aluminum through Argon. *The Journal of Chemical Physics* **1993**, *98* (2). DOI: 10.1063/1.464303.

114. Kendall, R. A.; Dunning, T. H.; Harrison, R. J. Electron Affinities of the First-Row Atoms Revisited. Systematic Basis Sets and Wave Functions. *The Journal of Chemical Physics* **1992**, *96* (9). DOI: 10.1063/1.462569.

115. Dunning, T. H. Gaussian Basis Sets for Use in Correlated Molecular Calculations. I. The Atoms Boron through Neon and Hydrogen. *The Journal of Chemical Physics* **1989**, *90* (2). DOI: 10.1063/1.456153.

116. Halkier, A.; Helgaker, T.; Jørgensen, P.; Klopper, W.; Koch, H.; Olsen, J.; Wilson, A. K. *Basis-Set Convergence in Correlated Calculations on Ne, N2, and H2O*; 1998; Vol. 286. DOI: 10.1016/S0009-2614(98)00111-0.

117. Chen, J.; Brooks, C. L.; Khandogin, J. Recent Advances in Implicit Solvent-Based Methods for Biomolecular Simulations. *Current Opinion in Structural Biology*. Elsevier Ltd 2008, pp 140–148. DOI: 10.1016/j.sbi.2008.01.003.

118. Shao, Q.; Zhu, W. How Well Can Implicit Solvent Simulations Explore Folding Pathways? A Quantitative Analysis of α-Helix Bundle Proteins. *Journal of Chemical Theory and Computation* **2017**, *13* (12), 6177–6190. DOI: 10.1021/acs.jctc.7b00726.

119. Brannigan, G.; Lin, L. C. L.; Brown, F. L. H. Implicit Solvent Simulation Models for Biomembranes. *European Biophysics Journal* **2006**, *35* (2), 104–124. DOI: 10.1007/s00249-005-0013-y.

120. Im, W.; Feig, M.; Brooks, C. L. An Implicit Membrane Generalized Born Theory for the Study of Structure, Stability, and Interactions of Membrane Proteins. *Biophysical Journal* **2003**, *85* (5), 2900–2918. DOI: 10.1016/S0006-3495(03)74712-2.

121. Cramer, C. J.; Truhlar, D. G. Implicit Solvation Models: Equilibria, Structure, Spectra, and Dynamics. *Chemical Reviews* **1999**, *99* (8), 2161–2200. DOI: 10.1021/cr960149m.

122. Cai, Q.; Wang, J.; Hsieh, M. J.; Ye, X.; Luo, R. Poisson-Boltzmann Implicit Solvation Models. In *Annual Reports in Computational Chemistry*; Elsevier Ltd, 2012; Vol. 8, pp 149–162. DOI: 10.1016/B978-0-444-59440-2.00006-5.

123. Im, W.; Beglov, D.; Roux, B. Continuum Solvation Model: Computation of Electrostatic Forces from Numerical Solutions to the Poisson-Boltzmann Equation. *Computer Physics Communications* **1998**, *111* (1–3), 59–75. DOI: 10.1016/s0010-4655(98)00016-2.

124. Zhou, S.; Cheng, L. T.; Dzubiella, J.; Li, B.; McCammon, J. A. Variational Implicit Solvation with Poisson-Boltzmann Theory. *Journal of Chemical Theory and Computation* **2014**, *10* (4), 1454–1467. DOI: 10.1021/ct401058w.

125. Tjong, H.; Zhou, H. X. The Dependence of Electrostatic Solvation Energy on Dielectric Constants in Poisson-Boltzmann Calculations. *Journal of Chemical Physics* **2006**, *125* (20), 206101. DOI: 10.1063/1.2393243.

126. Fogolari, F.; Zuccato, P.; Esposito, G.; Viglino, P. Biomolecular Electrostatics with the Linearized Poisson-Boltzmann Equation. *Biophysical Journal* **1999**, *76* (1 I), 1–16. DOI: 10.1016/S0006-3495(99)77173-0.

127. Boereboom, J. M.; Fleurat-Lessard, P.; Bulo, R. E. Explicit Solvation Matters: Performance of QM/MM Solvation Models in Nucleophilic Addition. *Journal of Chemical Theory and Computation* **2018**, *14* (4), 1841–1852. DOI: 10.1021/acs.jctc.7b01206.

128. Cho, H. M.; Lester, W. A. Explicit Solvent Model for Quantum Monte Carlo. *Journal of Physical Chemistry Letters* **2010**, *1* (23), 3376–3379. DOI: 10.1021/jz101336e.

129. Zhang, J.; Zhang, H.; Wu, T.; Wang, Q.; van der Spoel, D. Comparison of Implicit and Explicit Solvent Models for the Calculation of Solvation Free Energy in Organic Solvents. *Journal of Chemical Theory and Computation* **2017**, *13* (3), 1034–1043. DOI: 10.1021/acs.jctc.7b00169.

130. Guillot, B. A Reappraisal of What We Have Learnt during Three Decades of Computer Simulations on Water. In *Journal of Molecular Liquids*; Elsevier, 2002; Vol. 101, pp 219–260. DOI: 10.1016/S0167-7322(02)00094-6.

131. Roy, K.; Kar, S.; Das, R. N. *Understanding the Basics of QSAR for Applications in Pharmaceutical Sciences and Risk Assessment*; 2015. DOI: 10.1016/C2014-0-00286-9.

132. Spellmeyer, D. C.; Wong, A. K.; Bower, M. J.; Blaney, J. M. Conformational Analysis Using Distance Geometry Methods. *Journal of Molecular Graphics and Modelling* **1997**, *15* (1), 18–36. DOI: 10.1016/S1093-3263(97)00014-4.

133. Lipowski, A.; Lipowska, D. Roulette-Wheel Selection via Stochastic Acceptance. *Physica A: Statistical Mechanics and its Applications* **2012**, *391* (6), 2193–2196. DOI: 10.1016/J.PHYSA.2011.12.004.

134. Nair, N.; Goodman, J. M. Genetic Algorithms in Conformational Analysis. *American Chemical Society* **1998**, *38*, 317–320.

135. Fang, L.; Makkonen, E.; Todorović, M.; Rinke, P.; Chen, X. Efficient Amino Acid Conformer Search with Bayesian Optimization. *Journal of Chemical Theory and Computation* **2021**, *17* (3), 1955–1966. DOI: 10.1021/ACS.JCTC.0C00648.

136. Coester, F.; Kümmel, H. Short-Range Correlations in Nuclear Wave Functions. *Nuclear Physics* **1960**, *17* (C), 477–485. DOI: 10.1016/0029-5582(60)90140-1.

137. Allinger, N. L. Conformational Analysis. 130. MM2. A Hydrocarbon Force Field Utilizing V1 and V2 Torsional Terms. *Journal of the American Chemical Society* **2002**, *99* (25), 8127–8134. DOI: 10.1021/JA00467A001.

138. Allinger, N. L.; Yuh, Y. H.; Lii, J. H. Molecular Mechanics. The MM3 Force Field for Hydrocarbons. 1. *Journal of the American Chemical Society* **2002**, *111* (23), 8551–8566. DOI: 10.1021/JA00205A001.

139. Allinger', N. L.; Chen, K.; Lii, J.-H. An Improved Force Field (MM4) for Saturated Hydrocarbons. DOI: 10.1002/(SICI)1096-987X(199604)17:5/6.

140. Ponder, J. W.; Case, D. A. Force Fields for Protein Simulations. *Advances in Protein Chemistry* **2003**, *66*, 27–85.

141. Halgren, T. A. Basis, Form, Scope, Parameterization, and Performance of MMFF94. *Journal of Computational Chemistry* **1996**, *17*, 490–519. DOI: 10.1002/(SICI)1096-987X(199604)17:5/6.

142. Lewis-Atwell, T.; Townsend, P. A.; Grayson, M. N. Comparisons of Different Force Fields in Conformational Analysis and Searching of Organic Molecules: A Review. *Tetrahedron* **2021**, *79*, 131865. DOI: 10.1016/J.TET.2020.131865.

143. Valiev, M.; Bylaska, E. J.; Govind, N.; Kowalski, K.; Straatsma, T. P.; van Dam, H. J. J.; Wang, D.; Nieplocha, J.; Apra, E.; Windus, T. L.; de Jong, W. A. NWChem: A Comprehensive and Scalable Open-Source Solution for Large Scale Molecular Simulations. *Computer Physics Communications* **2010**, *181* (9), 1477–1489. DOI: 10.1016/j.cpc.2010.04.018.

144. Martinez, L.; Andrade, R.; Birgin, E. G.; Martinez, J. M. Packmol: A Package for Building Initial Configurations for Molecular Dynamics Simulations. *Journal of Computational Chemistry* **2009**, *30* (13), 2157–2164. DOI: 10.1002/jcc.21224.

145. Hanwell, M.; Curtis, D.; Lonie, D.; Vandermeersch, T.; Zurek, E.; Hutchinson, G. Avogadro: An Advanced Semantic Chemical Editor, Visualization, and Analysis Platform. *Journal of Cheminformatics* **2012**, *4*. DOI: 10.1186/1758-2946-4-17.

146. Avogadro: An Open-Source Molecular Builder and Visualization Tool.

147. Polik, W. F.; Schmidt, J. R. WebMO: Web-Based Computational Chemistry Calculations in Education and Research. *Wiley Interdisciplinary Reviews: Computational Molecular Science* **2021**, e1554. DOI: 10.1002/WCMS.1554.

148. Vasilyev, V. Online Complete Basis Set Limit Extrapolation Calculator. *Computational and Theoretical Chemistry* **2017**, *1115*, 1–3. DOI: 10.1016/J.COMPTC.2017.06.001.

149. Galano, A.; Alvarez-Idaboy, J. R. Glutathione: Mechanism and Kinetics of Its Non-Enzymatic Defense Action against Free Radicals. *RSC Advances* **2011**, *1* (9), 1763–1771. DOI: 10.1039/C1RA00474C.

150. Castañ Eda-Arriaga, R.; Raul Alvarez-Idaboy, J. Lipoic Acid and Dihydrolipoic Acid. A Comprehensive Theoretical Study of Their Antioxidant Activity Supported by Available Experimental Kinetic Data. *Journal of Chemical Information and Modeling* **2014**, *54*, 1642–1652. DOI: 10.1021/ci500213p.

151. Aguilera-Venegas, B.; Speisky, H. Identification of the Transition State for Fast Reactions: The Trapping of Hydroxyl and Methyl Radicals by DMPO - A DFT Approach. *Journal of Molecular Graphics and Modelling* **2014**, *52*, 57–70. DOI: 10.1016/j.jmgm.2014.06.006.

152. Rognoni, A.; Conte, R.; Ceotto, M. How Many Water Molecules Are Needed to Solvate One? *Chemical Science* **2021**, *12* (6), 2060–2064. DOI: 10.1039/D0SC05785A.

APPENDICES

Appendix A: ALA and DHLA

AA1: DHLA

geometry
zmatrix
C
C 1 B1
C 2 B2 1 A1
C 3 B3 2 A2 1 D1
C 4 B4 3 A3 2 D2
C 5 B5 4 A4 3 D3
C 6 B6 5 A5 4 D4
C 7 B7 6 A6 5 D5
O 8 B8 7 A7 6 D6
H 9 B9 8 A8 7 D7
O 8 B10 7 A9 6 D8
H 7 B11 6 A10 5 D9
H 7 B12 6 A11 5 D10
H 6 B13 5 A12 4 D11
H 6 B14 5 A13 4 D12
H 5 B15 4 A14 3 D13
H 5 B16 4 A15 3 D14
H 4 B17 3 A16 2 D15
H 4 B18 3 A17 2 D16
S 3 B19 2 A18 1 D17
H 20 B20 3 A19 2 D18
H 3 B21 2 A20 1 D19
H 2 B22 1 A21 3 D20
H 2 B23 1 A22 3 D21
S 1 B24 2 A23 3 D22
H 25 B25 1 A24 2 D23
H 1 B26 2 A25 3 D24
H 1 B27 2 A26 3 D25
variables
B1 1.535842765
B2 1.543888921
A1 114.5141161
B3 1.542826627
A2 110.2271436
D1 60.70137409
B4 1.537927827
A3 112.9211509
D2 -179.3341932
B5 1.534145039

A4 110.8459887
D3 60.75882362
B6 1.536330043
A5 111.1043359
D4 -179.3471996
B7 1.506693068
A6 113.0995356
D5 -179.2945423
B8 1.348746084
A7 119.0206298
D6 -179.5466289
B9 0.967938531
A8 121.4931233
D7 179.5430309
B10 1.223360127
A9 121.2292950
D8 0.159808454
B11 1.111302839
A10 109.1534477
D9 60.41800900
B12 1.112036420
A11 109.2787184
D10 -58.37027055
B13 1.112813551
A12 109.4735180
D11 59.77341761
B14 1.112671110
A13 108.8903976
D12 -59.21727433
B15 1.110648009
A14 110.0193700
D13 -59.13861529
B16 1.112271999
A15 109.2621036
D14 -178.4138838
B17 1.112524157
A16 108.7823658
D15 60.77261441
B18 1.111494939
A17 109.0763596
D16 -57.20539857
B19 1.833669000
A18 110.4804353
D17 -61.37553157
B20 1.408078833
A19 93.61785439

D18 -110.7907257
B21 1.111196202
A20 108.9632393
D19 178.5897956
B22 1.111664068
A21 107.9806840
D20 -121.8214367
B23 1.111786850
A22 108.1041918
D21 121.6243320
B24 1.823650460
A23 112.0271123
D22 60.65151608
B25 1.408486067
A24 93.64939884
D23 -127.1839729
B26 1.110141432
A25 110.0749639
D24 -61.65087766
B27 1.109687343
A26 109.8620467
D25 -179.1406717
end

AA2: ALA

geometry
zmatrix
C
C 1 B1
C 2 B2 1 A1
C 3 B3 2 A2 1 D1
C 4 B4 3 A3 2 D2
C 5 B5 4 A4 3 D3
C 6 B6 5 A5 4 D4
C 7 B7 6 A6 5 D5
O 8 B8 7 A7 6 D6
O 8 B9 7 A8 6 D7
H 10 B10 8 A9 7 D8
H 7 B11 6 A10 5 D9
H 7 B12 6 A11 5 D10
H 6 B13 5 A12 4 D11
H 6 B14 5 A13 4 D12
H 5 B15 4 A14 3 D13
H 5 B16 4 A15 3 D14
H 4 B17 3 A16 2 D15

H 4 B18 3 A17 2 D16
S 3 B19 2 A18 1 D17
S 1 B20 2 A19 3 D18
H 3 B21 2 A20 1 D19
H 2 B22 1 A21 21 D20
H 2 B23 1 A22 21 D21
H 1 B24 2 A23 3 D22
H 1 B25 2 A24 3 D23
variables
B1 1.513839159
B2 1.522495320
A1 107.4571364
B3 1.539246894
A2 110.0740930
D1 -177.6238911
B4 1.537080675
A3 112.7180322
D2 179.1020951
B5 1.533829521
A4 110.8474469
D3 176.7940334
B6 1.535320162
A5 111.1762357
D4 176.6835552
B7 1.510571415
A6 113.0738839
D5 179.3023298
B8 1.222250384
A7 120.9841081
D6 -1.306352150
B9 1.348719393
A8 119.9131233
D7 178.6575293
B10 0.967885840
A9 121.5290903
D8 -0.645697637
B11 1.111122405
A10 109.5770974
D9 58.36214989
B12 1.111680710
A11 108.8391356
D10 -60.43173255
B13 1.112616286
A12 109.3650806
D11 56.57344432
B14 1.113221451

A13 108.9615700
D12 -62.31145006
B15 1.112297173
A14 109.7266080
D13 56.21325395
B16 1.110979748
A15 109.3135086
D14 -63.04847100
B17 1.112881845
A16 109.8498468
D15 57.40649948
B18 1.113040431
A17 108.1718062
D16 -60.74749065
B19 1.824780809
A18 106.5939485
D17 -55.98834846
B20 1.816887999
A19 108.4085585
D18 53.37811007
B21 1.113149586
A20 110.0709710
D19 61.99906205
B22 1.113246603
A21 109.0455529
D20 -65.26991699
B23 1.111115656
A22 110.4122934
D21 175.4204252
B24 1.111084605
A23 110.4500761
D22 -66.08044922
B25 1.110395425
A24 108.8672092
D23 173.2794620
End

Appendix B: DHLA-OH Adducts

AB1: DHLA-OH(S1)

geometry
zmatrix
C
H 1 B1
C 1 B2 2 A1
S 3 B3 1 A2 2 D1
H 4 B4 3 A3 1 D2
H 3 B5 4 A4 5 D3
H 3 B6 4 A5 5 D4
H 1 B7 2 A6 3 D5
C 1 B8 2 A7 3 D6
H 9 B9 1 A8 2 D7
C 9 B10 10 A9 1 D8
H 11 B11 9 A10 10 D9
C 11 B12 12 A11 9 D10
H 13 B13 11 A12 12 D11
C 13 B14 14 A13 11 D12
H 15 B15 13 A14 14 D13
C 15 B16 16 A15 13 D14
H 17 B17 15 A16 16 D15
C 17 B18 18 A17 15 D16
O 19 B19 17 A18 18 D17
H 20 B20 19 A19 17 D18
O 19 B21 17 A20 18 D19
H 17 B22 18 A21 15 D20
H 15 B23 16 A22 13 D21
H 13 B24 14 A23 11 D22
H 11 B25 12 A24 9 D23
S 9 B26 10 A25 1 D24
O 27 B27 9 A26 10 D25
H 28 B28 27 A27 9 D26
H 27 B29 9 A28 10 D27
variables
B1 1.112373139
B2 1.535023778
A1 107.8483724
B3 1.823195272
A2 112.0065574
D1 -61.17166164
B4 1.408667455
A3 93.38352655
D2 -136.8705640
B5 1.109110004

A4 109.8155666
D3 -14.72748089
B6 1.110449909
A5 108.2123345
D4 102.4101420
B7 1.111408566
A6 107.9757329
D5 116.5171214
B8 1.544193641
A7 108.6163085
D6 -125.4051556
B9 1.112117800
A8 109.8608542
D7 59.93848829
B10 1.545946312
A9 107.1303016
D8 119.8144563
B11 1.111996853
A10 109.6926642
D9 -62.15059547
B12 1.541030824
A11 108.8561184
D10 -124.0596392
B13 1.111966726
A12 109.8581913
D11 59.21061772
B14 1.532331883
A13 110.3702029
D12 123.7062864
B15 1.111306438
A14 109.9821777
D13 -59.42578406
B16 1.537792574
A15 110.4534405
D14 -121.8140498
B17 1.111099005
A16 109.4649040
D15 60.31919013
B18 1.504566383
A17 108.8078668
D16 124.6072343
B19 1.350025926
A18 118.8192572
D17 59.48039343
B20 0.967447673
A19 121.5391807

D18 178.8645394
B21 1.223121825
A20 121.2808216
D19 -121.3568469
B22 1.112198723
A21 108.6162872
D20 -118.7689300
B23 1.113120838
A22 108.9836500
D21 119.0372300
B24 1.108769588
A23 108.3762780
D22 -119.8908030
B25 1.113082656
A24 108.3169482
D23 117.7603711
B26 1.832195132
A25 108.4179655
D24 -123.4336987
B27 1.713052247
A26 178.2427859
D25 4.580523088
B28 0.992989929
A27 103.2814963
D26 -91.51346545
B29 1.406473604
A28 89.91524363
D27 39.82012167
End

AB2: DHLA-OH(S2)

geometry
zmatrix
C
H 1 B1
H 1 B2 2 A1
C 1 B3 2 A2 3 D1
S 4 B4 1 A3 2 D2
O 5 B5 4 A4 1 D3
H 6 B6 5 A5 4 D4
H 5 B7 4 A6 1 D5
H 4 B8 5 A7 6 D6
H 4 B9 5 A8 6 D7
C 1 B10 2 A9 3 D8

H 11 B11 1 A10 2 D9
S 11 B12 12 A11 1 D10
H 13 B13 11 A12 12 D11
C 11 B14 12 A13 1 D12
H 15 B15 11 A14 12 D13
H 15 B16 16 A15 11 D14
C 15 B17 16 A16 11 D15
H 18 B18 15 A17 16 D16
H 18 B19 19 A18 15 D17
C 18 B20 19 A19 15 D18
H 21 B21 18 A20 19 D19
H 21 B22 22 A21 18 D20
C 21 B23 22 A22 18 D21
H 24 B24 21 A23 22 D22
H 24 B25 25 A24 21 D23
C 24 B26 25 A25 21 D24
O 27 B27 24 A26 25 D25
H 28 B28 27 A27 24 D26
O 27 B29 24 A28 25 D27
variables
B1 1.111390570
B2 1.112150170
A1 107.6912923
B3 1.536302379
A2 109.4722175
D1 -113.2170982
B4 1.815865083
A3 118.2493163
D2 -53.69327338
B5 1.714661774
A4 178.3548323
D3 -109.3350773
B6 0.993795251
A5 102.9856550
D4 -96.20213303
B7 1.402703105
A6 89.75044698
D5 -90.19964412
B8 1.108623471
A7 108.7415480
D6 19.67852595
B9 1.109155535
A8 104.2909293
D7 130.0825435
B10 1.547104715
A9 110.2376872

D8 115.9982290
B11 1.112472472
A10 109.6276178
D9 57.58798140
B12 1.835969771
A11 108.9220837
D10 -120.6698097
B13 1.407732219
A12 93.75833316
D11 2.119749618
B14 1.550608268
A13 109.9657944
D12 119.1498569
B15 1.111915464
A14 109.1970481
D13 -60.67658169
B16 1.113307235
A15 108.0935993
D14 117.1061053
B17 1.539622356
A16 108.6263462
D15 -126.2728367
B18 1.110851025
A17 109.8229159
D16 59.54934333
B19 1.110204936
A18 108.8240810
D17 -120.2311299
B20 1.539031839
A19 110.3715049
D18 121.8620123
B21 1.112569548
A20 109.6366606
D19 -60.84096302
B22 1.113169349
A21 108.7254855
D20 118.8173411
B23 1.536440367
A22 109.5838893
D21 -122.7566131
B24 1.110678171
A23 109.2946724
D22 60.68518795
B25 1.111735580
A24 108.7674866
D23 -119.0978308

B26 1.507996684
A25 108.5108852
D24 123.8592682
B27 1.349801467
A26 119.0763640
D25 58.90137626
B28 0.968073344
A27 121.5193155
D26 179.5991439
B29 1.223568551
A28 121.2228386
D27 -121.5296799
End

AB3: DHLA-OH(S1) (Habs)

geometry
zmatrix
C
H 1 B1
H 1 B2 2 A1
C 1 B3 2 A2 3 D1
S 4 B4 1 A3 2 D2
H 5 B5 4 A4 1 D3
H 4 B6 5 A5 6 D4
H 4 B7 5 A6 6 D5
C 1 B8 2 A7 3 D6
H 9 B9 1 A8 2 D7
S 9 B10 10 A9 1 D8
O 11 B11 9 A10 10 D9
H 12 B12 11 A11 9 D10
C 9 B13 10 A12 1 D11
H 14 B14 9 A13 10 D12
H 14 B15 15 A14 9 D13
C 14 B16 15 A15 9 D14
H 17 B17 14 A16 15 D15
H 17 B18 18 A17 14 D16
C 17 B19 18 A18 14 D17
H 20 B20 17 A19 18 D18
H 20 B21 21 A20 17 D19
C 20 B22 21 A21 17 D20
H 23 B23 20 A22 21 D21
H 23 B24 24 A23 20 D22
C 23 B25 24 A24 20 D23
O 26 B26 23 A25 24 D24

H 27 B27 26 A26 23 D25
O 26 B28 23 A27 24 D26
variables
B1 1.111570061
B2 1.111300589
A1 107.9421139
B3 1.535301273
A2 107.7534593
D1 -116.7348992
B4 1.823832777
A3 112.0044535
D2 -61.17108693
B5 1.407122241
A4 93.84539099
D3 -116.7383075
B6 1.110297708
A5 109.9292907
D4 6.749194220
B7 1.109587311
A6 107.8349695
D5 122.4018307
B8 1.544624874
A7 109.3036920
D6 118.2593729
B9 1.111217800
A8 109.4694780
D7 60.08775718
B10 1.838254879
A9 110.3446871
D8 -121.6310266
B11 1.717704573
A10 94.06562115
D9 62.86796567
B12 0.990362055
A11 104.6172761
D10 -95.08780374
B13 1.542200376
A12 107.1813833
D11 118.9306590
B14 1.112498090
A13 108.9192921
D12 -59.30659160
B15 1.112252669
A14 108.2973829
D13 118.3621723
B16 1.538370567

A15 107.7214865
D14 -123.1669206
B17 1.111960881
A16 109.2499497
D15 -57.93655397
B18 1.110666467
A17 108.7319022
D16 -120.2369477
B19 1.534683355
A18 109.7414553
D17 121.2985287
B20 1.112367295
A19 109.5546902
D18 179.1836750
B21 1.113150933
A20 108.8742202
D19 118.7545101
B22 1.535303227
A21 109.2663957
D20 -122.2762208
B23 1.111963129
A22 109.2606628
D21 62.74340595
B24 1.110734442
A23 108.7285186
D22 -119.1815111
B25 1.507519817
A24 108.4811205
D23 123.5763376
B26 1.348927722
A25 119.0902574
D24 59.08641867
B27 0.967728268
A26 121.4731189
D25 179.4078181
B28 1.223103021
A27 121.1816502
D26 -121.3734015
End

AB4: DHLA-OH(S2) (Habs)

geometry
zmatrix
C
H 1 B1
H 1 B2 2 A1
C 1 B3 2 A2 3 D1
S 4 B4 1 A3 2 D2
O 5 B5 4 A4 1 D3
H 6 B6 5 A5 4 D4
H 4 B7 5 A6 6 D5
H 4 B8 5 A7 6 D6
C 1 B9 2 A8 3 D7
H 10 B10 1 A9 2 D8
S 10 B11 11 A10 1 D9
H 12 B12 10 A11 11 D10
C 10 B13 11 A12 1 D11
H 14 B14 10 A13 11 D12
H 14 B15 15 A14 10 D13
C 14 B16 15 A15 10 D14
H 17 B17 14 A16 15 D15
H 17 B18 18 A17 14 D16
C 17 B19 18 A18 14 D17
H 20 B20 17 A19 18 D18
H 20 B21 21 A20 17 D19
C 20 B22 21 A21 17 D20
H 23 B23 20 A22 21 D21
H 23 B24 24 A23 20 D22
C 23 B25 24 A24 20 D23
O 26 B26 23 A25 24 D24
H 27 B27 26 A26 23 D25
O 26 B28 23 A27 24 D26
variables
B1 1.113003594
B2 1.111964478
A1 107.8876025
B3 1.536743310
A2 108.1959130
D1 -116.7412538
B4 1.828312063
A3 111.7617391
D2 -61.24766123
B5 1.719188471
A4 94.08809019
D3 60.70668010

B6 0.991447931
A5 104.5694114
D4 127.9753876
B7 1.110367507
A6 110.7911832
D5 -176.9706758
B8 1.110987399
A7 107.9921375
D6 -59.24504923
B9 1.544322181
A8 109.1538065
D7 118.1071313
B10 1.112016187
A9 108.9146345
D8 -177.7678574
B11 1.834405898
A10 109.2260718
D9 -120.6816467
B12 1.408582266
A11 93.51483938
D10 8.008383477
B13 1.542439950
A12 107.7934693
D11 119.6815942
B14 1.112247275
A13 108.9896346
D12 -60.36462981
B15 1.111839017
A14 108.3248114
D13 118.3656321
B16 1.538427769
A15 108.0798440
D14 -123.1430866
B17 1.112347518
A16 109.3115602
D15 62.42998952
B18 1.110345442
A17 108.6943730
D16 -120.0476531
B19 1.534420086
A18 109.6846327
D17 121.7394422
B20 1.112088576
A19 109.5246611
D18 -61.18178972
B21 1.112124993

A20 108.9331992
D19 118.8972915
B22 1.536544825
A21 109.4915179
D20 -122.0233631
B23 1.111145355
A22 109.2990980
D21 62.71869240
B24 1.110849225
A23 108.7103205
D22 -119.0992037
B25 1.507442205
A24 108.4938932
D23 123.5982932
B26 1.350334033
A25 118.9178552
D24 59.14618553
B27 0.967641463
A26 121.4224216
D25 179.4339054
B28 1.221482706
A27 121.2723229
D26 -121.2853638
End

AB5: DHLA-OH(C1)

geometry
zmatrix
C
C 1 B1
C 2 B2 1 A1
C 3 B3 2 A2 1 D1
C 4 B4 3 A3 2 D2
C 5 B5 4 A4 3 D3
C 6 B6 5 A5 4 D4
C 7 B7 6 A6 5 D5
O 8 B8 7 A7 6 D6
H 9 B9 8 A8 7 D7
O 8 B10 7 A9 6 D8
H 7 B11 6 A10 5 D9
H 7 B12 6 A11 5 D10
H 6 B13 5 A12 4 D11
H 6 B14 5 A13 4 D12
H 5 B15 4 A14 3 D13
H 5 B16 4 A15 3 D14

H 4 B17 3 A16 2 D15
H 4 B18 3 A17 2 D16
S 3 B19 2 A18 1 D17
H 20 B20 3 A19 2 D18
H 3 B21 2 A20 1 D19
H 2 B22 1 A21 3 D20
H 2 B23 1 A22 3 D21
S 1 B24 2 A23 3 D22
H 25 B25 1 A24 2 D23
O 1 B26 2 A25 3 D24
H 27 B27 1 A26 2 D25
H 1 B28 2 A27 3 D26
H 1 B29 2 A28 3 D27
variables
B1 1.621718225
B2 1.565138333
A1 122.5105984
B3 1.549599626
A2 107.4707949
D1 -172.0863925
B4 1.531885766
A3 115.4806037
D2 -176.9588341
B5 1.537470000
A4 109.7114388
D3 177.1107991
B6 1.532907695
A5 110.9680664
D4 -178.0149820
B7 1.505967463
A6 113.3771630
D5 178.8081056
B8 1.348718280
A7 118.8650023
D6 -179.7872008
B9 0.967019131
A8 121.6468199
D7 179.7769280
B10 1.223101795
A9 121.3108123
D8 -0.052572028
B11 1.111332084
A10 108.9709064
D9 58.46540633
B12 1.110508442
A11 109.0062678

D10 -60.28480626
B13 1.113449146
A12 109.5913403
D11 60.69298639
B14 1.113696996
A13 109.1309784
D12 -58.08233359
B15 1.110236912
A14 109.6100737
D13 58.43117580
B16 1.111904222
A15 109.8640162
D14 -61.43264898
B17 1.113838857
A16 108.4943226
D15 61.32270271
B18 1.111802590
A17 108.5654867
D16 -56.09006822
B19 1.837965723
A18 109.9228181
D17 68.15396922
B20 1.407648038
A19 94.66031454
D18 -119.0289409
B21 1.112077335
A20 112.1227766
D19 -54.00291572
B22 1.117100264
A21 103.7874808
D20 -118.7716579
B23 1.130655120
A22 116.8943554
D21 123.0323231
B24 1.842924307
A23 105.0731589
D22 30.20358795
B25 1.417885045
A24 100.7226717
D23 -115.2272266
B26 1.414888335
A25 83.09471812
D24 -154.1578783
B27 0.997666778
A26 109.2122537
D25 -88.30034054

B28 1.100164079
A27 80.35470815
D26 -48.70014699
B29 1.111045454
A28 175.6958345
D27 63.23525379
End

AB6: DHLA-OH(C2)

geometry
zmatrix
C
C 1 B1
S 2 B2 1 A1
H 3 B3 2 A2 1 D1
H 2 B4 1 A3 3 D2
H 2 B5 1 A4 3 D3
C 1 B6 2 A5 3 D4
C 7 B7 1 A6 2 D5
C 8 B8 7 A7 1 D6
C 9 B9 8 A8 7 D7
C 10 B10 9 A9 8 D8
C 11 B11 10 A10 9 D9
O 12 B12 11 A11 10 D10
H 13 B13 12 A12 11 D11
O 12 B14 11 A13 10 D12
H 11 B15 10 A14 9 D13
H 11 B16 10 A15 9 D14
H 10 B17 9 A16 8 D15
H 10 B18 9 A17 8 D16
H 9 B19 8 A18 7 D17
H 9 B20 8 A19 7 D18
H 8 B21 7 A20 1 D19
H 8 B22 7 A21 1 D20
S 7 B23 1 A22 2 D21
H 24 B24 7 A23 1 D22
H 7 B25 1 A24 2 D23
O 1 B26 2 A25 3 D24
H 27 B27 1 A26 2 D25
H 1 B28 2 A27 3 D26
H 1 B29 2 A28 3 D27
variables
B1 1.567713622
B2 1.843008681

A1 114.0226385
B3 1.415910661
A2 93.53129527
D1 -70.03297933
B4 1.116803027
A3 110.2975082
D2 -117.7593317
B5 1.115399928
A4 113.6959922
D3 125.4561854
B6 1.579870881
A5 174.3110019
D4 55.36488446
B7 1.562987204
A6 118.6400084
D5 175.2808849
B8 1.546637643
A7 109.2956510
D6 172.7050499
B9 1.530055555
A8 114.9781653
D7 177.3456182
B10 1.542901487
A9 108.8821988
D8 -178.1840101
B11 1.501736994
A10 114.2621014
D9 177.2000185
B12 1.350724250
A11 118.7739959
D10 -178.4798898
B13 0.967667815
A12 121.7514866
D11 178.7499199
B14 1.222403370
A13 121.2957640
D12 0.744384844
B15 1.112343023
A14 108.9987751
D13 57.14748009
B16 1.112523708
A15 109.3901130
D14 -61.07863354
B17 1.112311108
A16 110.2490723
D15 60.95780594

B18 1.111460751
A17 109.1011881
D16 -58.96699122
B19 1.108312230
A18 109.4571180
D17 57.28108559
B20 1.112578087
A19 108.4576743
D18 -60.77777073
B21 1.111081455
A20 111.1363710
D19 53.89922743
B22 1.112280540
A21 109.7465844
D20 -65.63990050
B23 1.848470990
A22 108.0150932
D21 51.91562149
B24 1.408104044
A23 92.75085140
D22 -90.28672558
B25 1.119284146
A24 109.0516117
D23 -63.82721020
B26 1.418327889
A25 91.11752220
D24 -69.68160863
B27 0.997884763
A26 109.6273787
D25 91.85608626
B28 1.113820003
A27 90.92857212
D26 172.2216042
B29 1.110261231
A28 86.75751267
D27 51.57606885
End

AB7: DHLA-OH(C3)

geometry
zmatrix
C
C 1 B1
C 2 B2 1 A1
S 3 B3 2 A2 1 D1

H 4 B4 3 A3 2 D2
H 3 B5 2 A4 1 D3
H 3 B6 2 A5 1 D4
H 2 B7 3 A6 4 D5
H 2 B8 3 A7 4 D6
C 1 B9 2 A8 3 D7
C 10 B10 1 A9 2 D8
C 11 B11 10 A10 1 D9
C 12 B12 11 A11 10 D10
C 13 B13 12 A12 11 D11
O 14 B14 13 A13 12 D12
H 15 B15 14 A14 13 D13
O 14 B16 13 A15 12 D14
H 13 B17 12 A16 11 D15
H 13 B18 12 A17 11 D16
H 12 B19 11 A18 10 D17
H 12 B20 11 A19 10 D18
H 11 B21 10 A20 1 D19
H 11 B22 10 A21 1 D20
H 10 B23 1 A22 2 D21
H 10 B24 1 A23 2 D22
S 1 B25 2 A24 3 D23
H 26 B26 1 A25 2 D24
O 1 B27 2 A26 3 D25
H 28 B28 1 A27 2 D26
H 1 B29 2 A28 3 D27
variables
B1 1.616230491
B2 1.489942616
A1 127.4095218
B3 1.808572918
A2 108.9619394
D1 -179.2695115
B4 1.393347767
A3 88.81574382
D2 -143.4662233
B5 1.101047229
A4 110.6223798
D3 53.66593623
B6 1.122858851
A5 104.5272200
D4 -62.68300103
B7 1.156749325
A6 95.35596565
D5 36.63161272
B8 1.120972346

A7 103.4531593
D6 -69.77937328
B9 1.565456483
A8 161.5606736
D7 60.62654127
B10 1.494272398
A9 137.3723299
D8 60.83611912
B11 1.560541573
A10 104.9519425
D9 -179.3328035
B12 1.478232729
A11 108.6657572
D10 -179.3119643
B13 1.490093286
A12 112.3498877
D11 -59.26002277
B14 1.341498416
A13 117.4018421
D12 -178.1407373
B15 0.961884089
A14 121.1296645
D13 178.9776335
B16 1.225341177
A15 122.1761500
D14 1.154623992
B17 1.105773937
A16 106.5391574
D15 -179.2294372
B18 1.110205386
A17 107.5216394
D16 61.90516867
B19 1.127249307
A18 111.9937568
D17 60.31347117
B20 1.119987053
A19 110.1134846
D18 -57.18321966
B21 1.104744767
A20 108.1343120
D19 62.26781352
B22 1.114352278
A21 109.2532799
D20 -60.35864609
B23 1.104071103
A22 103.0525071

D21 -45.38022468
B24 1.120468206
A23 105.3332245
D22 -151.9613264
B25 1.893324061
A24 106.2808125
D23 -51.52019622
B26 1.403032787
A25 105.8357770
D24 71.85918301
B27 1.415862635
A26 75.18422672
D25 128.3707310
B28 1.001695563
A27 108.3975541
D26 -97.04103201
B29 1.124008007
A28 88.67659437
D27 -126.9770691
End

AB8: DHLA-OH(C1) (Habs)

geometry
zmatrix
C
C 1 B1
C 2 B2 1 A1
C 3 B3 2 A2 1 D1
C 4 B4 3 A3 2 D2
C 5 B5 4 A4 3 D3
C 6 B6 5 A5 4 D4
C 7 B7 6 A6 5 D5
O 8 B8 7 A7 6 D6
H 9 B9 8 A8 7 D7
O 8 B10 7 A9 6 D8
H 7 B11 6 A10 5 D9
H 7 B12 6 A11 5 D10
H 6 B13 5 A12 4 D11
H 6 B14 5 A13 4 D12
H 5 B15 4 A14 3 D13
H 5 B16 4 A15 3 D14
H 4 B17 3 A16 2 D15
H 4 B18 3 A17 2 D16
S 3 B19 2 A18 1 D17
H 20 B20 3 A19 2 D18

H 3 B21 2 A20 1 D19
H 2 B22 1 A21 3 D20
H 2 B23 1 A22 3 D21
S 1 B24 2 A23 3 D22
H 25 B25 1 A24 2 D23
H 1 B26 2 A25 3 D24
O 1 B27 2 A26 3 D25
H 28 B28 1 A27 2 D26
variables
B1 1.542524554
B2 1.545960543
A1 114.6304889
B3 1.541745439
A2 110.2859714
D1 -179.3108452
B4 1.537727544
A3 112.9401194
D2 -59.30797938
B5 1.533961538
A4 110.8985463
D3 -59.30228000
B6 1.536366167
A5 111.0873085
D4 -179.2242386
B7 1.507187447
A6 113.0954644
D5 -179.2753992
B8 1.349729973
A7 118.9817652
D6 -179.5276091
B9 0.967496770
A8 121.4341734
D7 179.5061167
B10 1.222060555
A9 121.1952487
D8 0.109639017
B11 1.111023402
A10 109.1941984
D9 60.41060683
B12 1.111276743
A11 109.2228426
D10 -58.33982258
B13 1.112036870
A12 109.5603004
D11 59.71383714
B14 1.113030548

A13 108.8244244
D12 -59.26433851
B15 1.110963996
A14 109.8803199
D13 -178.9980214
B16 1.112126791
A15 109.3546224
D14 61.79035095
B17 1.112374937
A16 108.9372220
D15 -179.3629324
B18 1.112176695
A17 108.9524905
D16 62.65444177
B19 1.833995638
A18 110.5527434
D17 58.57477009
B20 1.408685203
A19 93.53296718
D18 -110.7419890
B21 1.112040017
A20 108.8447346
D19 -61.39759087
B22 1.112002248
A21 108.4170783
D20 -121.6054760
B23 1.112266155
A22 108.1593548
D21 121.5330939
B24 1.829630017
A23 112.3667904
D22 60.73026194
B25 1.409029808
A24 93.58137985
D23 -132.4347343
B26 1.109892788
A25 108.4110118
D24 -58.66377694
B27 1.402525223
A26 110.6542291
D25 -176.0076668
B28 0.993481253
A27 107.1507017
D26 -66.67363975
End

AB9: DHLA-OH(C2) (Habs)

geometry
zmatrix
C
C 1 B1
C 2 B2 1 A1
C 3 B3 2 A2 1 D1
C 4 B4 3 A3 2 D2
C 5 B5 4 A4 3 D3
C 6 B6 5 A5 4 D4
C 7 B7 6 A6 5 D5
O 8 B8 7 A7 6 D6
H 9 B9 8 A8 7 D7
O 8 B10 7 A9 6 D8
H 7 B11 6 A10 5 D9
H 7 B12 6 A11 5 D10
H 6 B13 5 A12 4 D11
H 6 B14 5 A13 4 D12
H 5 B15 4 A14 3 D13
H 5 B16 4 A15 3 D14
H 4 B17 3 A16 2 D15
H 4 B18 3 A17 2 D16
S 3 B19 2 A18 1 D17
H 20 B20 3 A19 2 D18
H 3 B21 2 A20 1 D19
O 2 B22 1 A21 3 D20
H 23 B23 2 A22 1 D21
H 2 B24 1 A23 3 D22
S 1 B25 2 A24 3 D23
H 26 B26 1 A25 2 D24
H 1 B27 2 A26 3 D25
H 1 B28 2 A27 3 D26
variables
B1 1.536922249
B2 1.545786855
A1 114.9825420
B3 1.543189230
A2 110.1525654
D1 -179.2954135
B4 1.537775991
A3 113.1118095
D2 -179.3001510
B5 1.534224234
A4 110.9758343
D3 60.69604943

B6 1.538046163
A5 110.9711437
D4 -179.3124909
B7 1.505860883
A6 113.1420013
D5 -179.2903226
B8 1.350947075
A7 118.8836943
D6 -179.6261225
B9 0.967664198
A8 121.5673063
D7 179.6648398
B10 1.220626478
A9 121.3589060
D8 0.198384428
B11 1.111990558
A10 109.0331357
D9 60.45166766
B12 1.110195478
A11 109.2540770
D10 -58.26598046
B13 1.112641002
A12 109.5603318
D11 59.69703751
B14 1.112501236
A13 108.9365931
D12 -59.30262493
B15 1.110596686
A14 109.9517484
D13 -58.90819731
B16 1.112812653
A15 109.3201892
D14 -178.1586718
B17 1.112018435
A16 109.1875835
D15 60.09403926
B18 1.112565054
A17 108.6136366
D16 -57.80642596
B19 1.832952536
A18 110.8091568
D17 58.45123907
B20 1.409214675
A19 93.26851151
D18 -113.1682752
B21 1.111933901

A20 108.5179874
D19 -61.04746601
B22 1.113102421
A21 108.5456868
D20 -122.0001032
B23 0.969149627
A22 109.4541748
D21 64.04267717
B24 1.111561964
A23 107.2804855
D22 121.6097661
B25 1.822108669
A24 112.5517910
D23 -179.2663505
B26 1.411076894
A25 93.14177910
D24 -132.2831890
B27 1.109445808
A26 109.3873695
D25 59.05643418
B28 1.110978848
A27 109.8016416
D26 -58.11300932
End

AB10: DHLA-OH(C3) (Habs)

geometry
zmatrix
C
C 1 B1
C 2 B2 1 A1
C 3 B3 2 A2 1 D1
C 4 B4 3 A3 2 D2
C 5 B5 4 A4 3 D3
C 6 B6 5 A5 4 D4
C 7 B7 6 A6 5 D5
O 8 B8 7 A7 6 D6
O 8 B9 7 A8 6 D7
H 10 B10 8 A9 7 D8
H 7 B11 6 A10 5 D9
H 7 B12 6 A11 5 D10
H 6 B13 5 A12 4 D11
H 6 B14 5 A13 4 D12
H 5 B15 4 A14 3 D13
H 5 B16 4 A15 3 D14

H 4 B17 3 A16 2 D15
H 4 B18 3 A17 2 D16
S 3 B19 2 A18 1 D17
H 20 B20 3 A19 2 D18
O 3 B21 2 A20 1 D19
H 22 B22 3 A21 2 D20
H 2 B23 1 A22 3 D21
H 2 B24 1 A23 3 D22
S 1 B25 2 A24 3 D23
H 26 B26 1 A25 2 D24
H 1 B27 2 A26 3 D25
H 1 B28 2 A27 3 D26
variables
B1 1.532241483
B2 1.540064455
A1 113.7281927
B3 1.544244191
A2 112.5830966
D1 -68.64858334
B4 1.533879359
A3 115.3797365
D2 171.9632432
B5 1.537102063
A4 113.7335479
D3 -177.8373315
B6 1.531459596
A5 115.0442793
D4 -70.41899105
B7 1.514184230
A6 113.4184538
D5 -70.27274013
B8 1.209837974
A7 126.0996922
D6 -8.850183658
B9 1.355115341
A8 111.3965967
D7 172.2888048
B10 0.975287160
A9 105.8824568
D8 179.0035195
B11 1.104127291
A10 110.5439111
D9 170.3389822
B12 1.102006043
A11 112.8814245
D10 53.00367870

B13 1.101043364
A12 108.5795729
D11 168.2737294
B14 1.103678770
A13 109.4929909
D12 51.88234005
B15 1.101790379
A14 110.8227374
D13 58.70230473
B16 1.103926797
A15 108.5118233
D14 -58.01540664
B17 1.103458575
A16 107.0040549
D15 51.28125413
B18 1.102732480
A17 107.9694420
D16 -63.25305479
B19 1.892907044
A18 109.1636831
D17 173.4719240
B20 1.357985510
A19 94.69814622
D18 -59.09203136
B21 1.413654720
A20 106.2199830
D19 54.55832175
B22 0.968893825
A21 107.5796859
D20 169.6658480
B23 1.100643571
A22 110.5780197
D21 -122.8178353
B24 1.101349758
A23 108.4386867
D22 120.1757563
B25 1.852320332
A24 108.5597129
D23 -175.6300054
B26 1.358282421
A25 96.41179622
D24 177.2715356
B27 1.099517674
A26 111.5688309
D25 65.04091970
B28 1.097885805

A27 109.8444953
D26 -55.96636123
End

AC1: ALA-OH(S1)

geometry
zmatrix
C
H 1 B1
C 1 B2 2 A1
H 3 B3 1 A2 2 D1
C 3 B4 1 A3 2 D2
H 5 B5 3 A4 1 D3
C 5 B6 3 A5 1 D4
H 7 B7 5 A6 3 D5
C 7 B8 5 A7 3 D6
H 9 B9 7 A8 5 D7
C 9 B10 7 A9 5 D8
H 11 B11 9 A10 7 D9
C 11 B12 9 A11 7 D10
H 13 B13 11 A12 9 D11
C 13 B14 11 A13 9 D12
O 15 B15 13 A14 11 D13
H 16 B16 15 A15 13 D14
O 15 B17 13 A16 11 D15
H 13 B18 11 A17 9 D16
H 11 B19 9 A18 7 D17
H 9 B20 7 A19 5 D18
H 7 B21 5 A20 3 D19
S 5 B22 3 A21 1 D20
S 1 B23 2 A22 3 D21
O 23 B24 5 A23 3 D22
H 25 B25 23 A24 5 D23
H 3 B26 1 A25 2 D24
H 1 B27 2 A26 3 D25
variables
B1 1.111830922
B2 1.546103489
A1 110.0504262
B3 1.111410815
A2 111.3959080
D1 58.17234951
B4 1.531697751
A3 109.1007835
D2 -64.64694995
B5 1.112941148
A4 108.4852602
D3 68.24672637

B6 1.535197707
A5 113.1324119
D4 -170.0169948
B7 1.112551572
A6 108.3104972
D5 -59.64214766
B8 1.535779607
A7 111.0967286
D6 -179.2977367
B9 1.112095769
A8 109.2021481
D7 -179.6930753
B10 1.531977154
A9 111.4795209
D8 -59.31593826
B11 1.113223248
A10 109.0967979
D9 -58.79965661
B12 1.535872716
A11 110.6103820
D10 -179.2813245
B13 1.111611443
A12 109.3521667
D11 60.00349472
B14 1.509694671
A13 113.2483560
D12 -179.3133854
B15 1.349264244
A14 119.8162555
D13 179.5254772
B16 0.967737568
A15 121.4957809
D14 -0.100430345
B17 1.221663620
A16 121.0322670
D15 -0.443181617
B18 1.111915464
A17 109.1177589
D16 -58.68096403
B19 1.112467528
A18 109.3819709
D17 60.30225642
B20 1.111761665
A19 109.5044568
D18 61.35490156
B21 1.111880389

A20 110.0159530
D19 58.91909981
B22 1.798348409
A21 100.9781036
D20 -48.60934327
B23 1.848360895
A22 108.9071528
D21 -122.2258086
B24 1.719430720
A23 92.54918698
D22 116.9782643
B25 0.990615970
A24 104.2711785
D23 112.3869323
B26 1.114109959
A25 107.5784706
D24 176.5837599
B27 1.110203585
A26 109.1404688
D25 118.8492757
End

AC2: ALA-OH(S2)

geometry
zmatrix
C
H 1 B1
C 1 B2 2 A1
H 3 B3 1 A2 2 D1
C 3 B4 1 A3 2 D2
H 5 B5 3 A4 1 D3
C 5 B6 3 A5 1 D4
H 7 B7 5 A6 3 D5
C 7 B8 5 A7 3 D6
H 9 B9 7 A8 5 D7
C 9 B10 7 A9 5 D8
H 11 B11 9 A10 7 D9
C 11 B12 9 A11 7 D10
H 13 B13 11 A12 9 D11
C 13 B14 11 A13 9 D12
O 15 B15 13 A14 11 D13
H 16 B16 15 A15 13 D14
O 15 B17 13 A16 11 D15
H 13 B18 11 A17 9 D16
H 11 B19 9 A18 7 D17

H 9 B20 7 A19 5 D18
H 7 B21 5 A20 3 D19
S 5 B22 3 A21 1 D20
S 1 B23 2 A22 3 D21
O 24 B24 1 A23 2 D22
H 25 B25 24 A24 1 D23
H 3 B26 1 A25 2 D24
H 1 B27 2 A26 3 D25
variables
B1 1.111363577
B2 1.525813553
A1 109.7703302
B3 1.111545771
A2 110.0652954
D1 53.97018636
B4 1.556582475
A3 110.3438839
D2 -70.10028601
B5 1.112570897
A4 108.8259192
D3 63.94566029
B6 1.540672905
A5 108.8409766
D4 -176.9074489
B7 1.112816696
A6 108.4243726
D5 -59.26681299
B8 1.536244121
A7 113.3562382
D6 -179.3299756
B9 1.112685490
A8 109.4425498
D7 -179.7451827
B10 1.535361847
A9 110.4399270
D8 -59.24861513
B11 1.112858032
A10 109.1016497
D9 -58.52997782
B12 1.536036783
A11 111.4791559
D10 -179.3120196
B13 1.111183603
A12 109.3101653
D11 179.8581872
B14 1.510458540

A13 112.9443153
D12 -59.36758102
B15 1.349443589
A14 119.8903412
D13 179.4702207
B16 0.967178370
A15 121.5722439
D14 -0.314549050
B17 1.221586264
A16 121.0771104
D15 -0.517414020
B18 1.112157363
A17 109.0618093
D16 61.05728821
B19 1.112185686
A18 109.1402806
D17 60.33103211
B20 1.110999550
A19 109.8494395
D18 60.87461089
B21 1.112696275
A20 109.2220350
D19 58.57326439
B22 1.856643477
A21 110.1418281
D20 -55.03852635
B23 1.790643739
A22 111.5271391
D21 -111.4111979
B24 1.719419670
A23 92.61112771
D22 0.921508374
B25 0.991429776
A24 104.2895519
D23 -114.4720164
B26 1.113574874
A25 108.2512067
D24 171.7986923
B27 1.109607588
A26 109.8349674
D25 122.8535438
End

AC3: ALA-OH(C1)

geometry

zmatrix
C
C 1 B1
H 2 B2 1 A1
C 2 B3 1 A2 3 D1
H 4 B4 2 A3 1 D2
C 4 B5 2 A4 1 D3
H 6 B6 4 A5 2 D4
C 6 B7 4 A6 2 D5
H 8 B8 6 A7 4 D6
C 8 B9 6 A8 4 D7
H 10 B10 8 A9 6 D8
C 10 B11 8 A10 6 D9
H 12 B12 10 A11 8 D10
C 12 B13 10 A12 8 D11
O 14 B14 12 A13 10 D12
H 15 B15 14 A14 12 D13
O 14 B16 12 A15 10 D14
H 12 B17 10 A16 8 D15
H 10 B18 8 A17 6 D16
H 8 B19 6 A18 4 D17
H 6 B20 4 A19 2 D18
S 4 B21 2 A20 1 D19
S 1 B22 2 A21 3 D20
H 2 B23 1 A22 23 D21
O 1 B24 2 A23 3 D22
H 25 B25 1 A24 2 D23
H 1 B26 2 A25 3 D24
H 1 B27 2 A26 3 D25
variables
B1 1.596086777
B2 1.127640457
A1 116.5054359
B3 1.538057541
A2 111.9608438
D1 -123.1726998
B4 1.114677083
A3 110.8164925
D2 71.05739710
B5 1.539683409
A4 110.9396563
D3 -168.6661537
B6 1.112485955
A5 108.0186121
D4 -58.12256438
B7 1.535542575

A6 113.2468893
D5 -177.7538159
B8 1.113282534
A7 109.3057548
D6 58.09433178
B9 1.534343508
A8 109.8971767
D7 178.0823527
B10 1.112340775
A9 108.9434373
D8 -58.53763559
B11 1.535391155
A10 112.0157460
D9 -178.9502491
B12 1.111530027
A11 109.1956347
D10 59.26472240
B13 1.511022171
A12 112.6071420
D11 179.6474782
B14 1.349320570
A13 119.9922563
D12 -179.6853393
B15 0.966314649
A14 121.5970811
D13 0.069376894
B16 1.222476585
A15 121.0231339
D14 0.185215184
B17 1.110962196
A16 109.3618047
D15 -59.66141855
B18 1.112877801
A17 109.0194978
D16 60.18235566
B19 1.111719389
A18 110.1718231
D17 -61.31154562
B20 1.111924458
A19 109.5983306
D18 59.82417404
B21 1.803511575
A20 104.8023681
D19 -47.13486639
B22 1.835238132
A21 104.7333974

D20 127.7178767
B23 1.125024889
A22 108.9037028
D21 -109.8854737
B24 1.412518672
A23 81.48696329
D22 -57.16676504
B25 0.995949798
A24 107.6990164
D23 122.4229156
B26 1.115351962
A25 82.40355970
D24 52.07760862
B27 1.112031474
A26 172.9899665
D25 -173.6257876
End

AC4: ALA-OH(C2)

geometry
zmatrix
C
C 1 B1
H 2 B2 1 A1
H 2 B3 3 A2 1 D1
S 2 B4 3 A3 1 D2
S 5 B5 2 A4 3 D3
C 1 B6 2 A5 3 D4
H 7 B7 1 A6 2 D5
C 7 B8 1 A7 2 D6
H 9 B9 7 A8 1 D7
C 9 B10 7 A9 1 D8
H 11 B11 9 A10 7 D9
C 11 B12 9 A11 7 D10
H 13 B13 11 A12 9 D11
C 13 B14 11 A13 9 D12
H 15 B15 13 A14 11 D13
C 15 B16 13 A15 11 D14
O 17 B17 15 A16 13 D15
H 18 B18 17 A17 15 D16
O 17 B19 15 A18 13 D17
H 15 B20 13 A19 11 D18
H 13 B21 11 A20 9 D19
H 11 B22 9 A21 7 D20
H 9 B23 7 A22 1 D21

O 1 B24 2 A23 3 D22
H 25 B25 1 A24 2 D23
H 1 B26 2 A25 3 D24
H 1 B27 2 A26 3 D25
variables
B1 1.598979049
B2 1.113658835
A1 107.4236361
B3 1.118243265
A2 107.8969082
D1 123.1201622
B4 1.829475608
A3 106.0006797
D2 -127.6940068
B5 2.086042665
A4 92.57077437
D3 123.5769807
B6 1.580248398
A5 92.89329232
D4 -87.83153249
B7 1.120040178
A6 112.2359412
D5 60.60082394
B8 1.558931044
A7 111.6420504
D6 178.8810298
B9 1.112872859
A8 109.0323958
D7 -55.85885022
B10 1.539803884
A9 113.7007620
D8 -174.6262401
B11 1.112286384
A10 108.9285626
D9 59.65817278
B12 1.534603532
A11 109.9352558
D10 179.7206983
B13 1.112680547
A12 109.0890544
D11 -56.16027520
B14 1.536156568
A13 112.2286009
D12 -176.2371965
B15 1.112008093
A14 108.9311042

D13 60.03454643
B16 1.512534628
A15 112.5073368
D14 -179.8225981
B17 1.348423153
A16 120.0674834
D15 -178.4269724
B18 0.967187159
A17 121.6853709
D16 0.605045364
B19 1.221962356
A18 120.9692474
D17 1.399588660
B20 1.111390570
A19 109.7277852
D18 -58.83593386
B21 1.112578986
A20 108.8004956
D19 62.47308892
B22 1.111410815
A21 110.8671315
D20 -59.77609349
B23 1.111912766
A22 109.5166832
D21 62.11268028
B24 1.426027700
A23 90.49698092
D22 87.82716610
B25 1.004801971
A24 113.8831873
D23 -70.32445091
B26 1.111511134
A25 120.1397481
D24 177.4276452
B27 1.116377624
A26 120.6400683
D25 0.023016933
End

AC5: ALA-OH(C1) (Habs)

geometry
zmatrix
C
H 1 B1
C 1 B2 2 A1

H 3 B3 1 A2 2 D1
C 3 B4 1 A3 2 D2
H 5 B5 3 A4 1 D3
C 5 B6 3 A5 1 D4
H 7 B7 5 A6 3 D5
C 7 B8 5 A7 3 D6
H 9 B9 7 A8 5 D7
C 9 B10 7 A9 5 D8
H 11 B11 9 A10 7 D9
C 11 B12 9 A11 7 D10
H 13 B13 11 A12 9 D11
C 13 B14 11 A13 9 D12
O 15 B15 13 A14 11 D13
H 16 B16 15 A15 13 D14
O 15 B17 13 A16 11 D15
H 13 B18 11 A17 9 D16
H 11 B19 9 A18 7 D17
H 9 B20 7 A19 5 D18
H 7 B21 5 A20 3 D19
S 5 B22 3 A21 1 D20
S 1 B23 2 A22 3 D21
H 3 B24 1 A23 2 D22
O 1 B25 2 A24 3 D23
H 26 B26 1 A25 2 D24
variables
B1 1.114459510
B2 1.517891300
A1 111.2486744
B3 1.111427910
A2 110.6118912
D1 57.78977815
B4 1.521206758
A3 107.5557740
D2 -63.91675187
B5 1.113428040
A4 109.7365267
D3 62.77479012
B6 1.539364479
A5 110.0730870
D4 -176.8056291
B7 1.113287923
A6 108.3514755
D5 -59.39425990
B8 1.537162646
A7 112.5721180
D6 -179.2750285

B9 1.113113651
A8 109.4463045
D7 -179.8335323
B10 1.533402100
A9 110.8454200
D8 -59.31162714
B11 1.113040431
A10 109.1193487
D9 -58.48457937
B12 1.535689422
A11 111.1267325
D10 -179.2789235
B13 1.111686107
A12 109.3880091
D11 179.9353985
B14 1.510701493
A13 113.0381616
D12 -59.28846222
B15 1.349709969
A14 119.8171861
D13 179.3117649
B16 0.966948809
A15 121.5094172
D14 -0.394058415
B17 1.221682856
A16 121.0669428
D15 -0.685032468
B18 1.110837522
A17 109.0047891
D16 61.10964777
B19 1.112545729
A18 109.2374558
D17 60.41569008
B20 1.111529127
A19 109.5941657
D18 61.01493729
B21 1.112717844
A20 109.7154859
D19 58.80909118
B22 1.824507057
A21 106.9569007
D20 -55.19579451
B23 1.816927076
A22 107.8234234
D21 -118.1409951
B24 1.114412401

A23 109.1545761
D22 177.2886758
B25 1.401335791
A24 110.5781959
D23 122.6119439
B26 0.992920440
A25 106.5968605
D24 -48.02925788
End

AC6: ALA-OH(C2) (Habs)

geometry
zmatrix
C
H 1 B1
C 1 B2 2 A1
O 3 B3 1 A2 2 D1
H 4 B4 3 A3 1 D2
C 3 B5 1 A4 2 D3
H 6 B6 3 A5 1 D4
C 6 B7 3 A6 1 D5
H 8 B8 6 A7 3 D6
C 8 B9 6 A8 3 D7
H 10 B10 8 A9 6 D8
C 10 B11 8 A10 6 D9
H 12 B12 10 A11 8 D10
C 12 B13 10 A12 8 D11
H 14 B14 12 A13 10 D12
C 14 B15 12 A14 10 D13
O 16 B16 14 A15 12 D14
H 17 B17 16 A16 14 D15
O 16 B18 14 A17 12 D16
H 14 B19 12 A18 10 D17
H 12 B20 10 A19 8 D18
H 10 B21 8 A20 6 D19
H 8 B22 6 A21 3 D20
S 6 B23 3 A22 1 D21
S 1 B24 2 A23 3 D22
H 3 B25 1 A24 2 D23
H 1 B26 2 A25 3 D24
variables
B1 1.111051217
B2 1.519054288
A1 111.0987367

B3 1.405806229
A2 111.2461854
D1 58.38388462
B4 0.993539693
A3 107.7782247
D2 -62.56968296
B5 1.530658265
A4 107.8478145
D3 -65.24216017
B6 1.112450240
A5 109.8214287
D4 63.51123438
B7 1.541322123
A6 110.6988217
D5 -175.5548697
B8 1.112131217
A7 108.6013037
D6 -59.56122444
B9 1.536562744
A8 112.5018777
D7 -179.2934949
B10 1.112438775
A9 109.4327907
D8 -59.76715840
B11 1.533847476
A10 110.8987070
D9 60.73895028
B12 1.112955125
A11 109.0789671
D10 -58.58542688
B13 1.536727661
A12 111.0899286
D11 -179.2748834
B14 1.111031105
A13 109.3886349
D12 59.85204382
B15 1.509620710
A14 113.0597299
D13 -179.3181001
B16 1.349720763
A15 119.8542732
D14 179.2242352
B17 0.967763446
A16 121.5055008
D15 -0.281063158
B18 1.221759875

A17 121.0641115
D16 -0.694426702
B19 1.111835568
A18 109.0019988
D17 -58.85668835
B20 1.111497734
A19 109.2686929
D18 60.37686629
B21 1.111446958
A20 109.6736119
D19 -178.9346171
B22 1.112570699
A21 109.6808051
D20 58.78256992
B23 1.826279066
A22 106.8204422
D21 -53.98118738
B24 1.815451941
A23 108.8644786
D22 -118.8925081
B25 1.113562527
A24 108.2534031
D23 177.1220556
B26 1.110320083
A25 109.8425154
D24 120.6948303
End

AC7: ALA-OH(C3) (Habs)

geometry
zmatrix
C
H 1 B1
H 1 B2 2 A1
C 1 B3 2 A2 3 D1
H 4 B4 1 A3 2 D2
H 4 B5 1 A4 2 D3
C 4 B6 1 A5 2 D4
O 7 B7 4 A6 1 D5
H 8 B8 7 A7 4 D6
C 7 B9 4 A8 1 D7
H 10 B10 7 A9 4 D8
H 10 B11 7 A10 4 D9
C 10 B12 7 A11 4 D10

C 13 B13 10 A12 7 D11
C 14 B14 13 A13 10 D12
H 15 B15 14 A14 13 D13
H 15 B16 14 A15 13 D14
C 15 B17 14 A16 13 D15
O 18 B18 15 A17 14 D16
O 18 B19 15 A18 14 D17
H 20 B20 18 A19 15 D18
H 14 B21 13 A20 10 D19
H 14 B22 13 A21 10 D20
H 13 B23 10 A22 7 D21
H 13 B24 10 A23 7 D22
S 7 B25 4 A24 1 D23
S 1 B26 2 A25 3 D24
variables
B1 1.110245919
B2 1.109622458
A1 109.6200529
B3 1.514963036
A2 110.9366969
D1 -120.3462733
B4 1.113293313
A3 108.5746892
D2 175.5679957
B5 1.112144775
A4 110.5471031
D3 57.01008543
B6 1.530717805
A5 108.1547847
D4 -65.70787741
B7 1.407555683
A6 110.9203490
D5 62.73488728
B8 0.993507423
A7 107.7608231
D6 60.17542634
B9 1.549080695
A8 109.9905630
D7 -174.7174572
B10 1.112480562
A9 109.5353533
D8 58.92956954
B11 1.112478764
A10 108.5642310
D9 -58.84900154
B12 1.538644208

A11 113.0417009
D10 -179.3107440
B13 1.533131762
A12 111.0119413
D11 60.69282415
B14 1.536364866
A13 110.9690571
D12 -179.3104155
B15 1.112294026
A14 109.3239608
D13 60.02496484
B16 1.112126791
A15 109.0802654
D14 -58.63225359
B17 1.509384312
A16 113.2145298
D15 -179.3121061
B18 1.221828548
A17 121.0455428
D16 -0.455480768
B19 1.349253868
A18 119.8857043
D17 179.4771432
B20 0.967517442
A19 121.5175781
D18 -0.204918610
B21 1.112334932
A20 109.4285347
D19 60.28706827
B22 1.112757835
A21 109.1085597
D20 -58.79387326
B23 1.111397319
A22 109.5656006
D21 -59.51237139
B24 1.110525551
A23 109.6555599
D22 -178.7920448
B25 1.826969075
A24 106.1329492
D23 -54.89328273
B26 1.815518934
A25 109.1503901
D24 120.6499840
End

Appendix D: Side Products Following H Abstraction

AD1: H_2O

```
geometry
zmatrix
O
H 1 B1
H 1 B2 2 A1
variables
B1 1.050000000
B2 1.050000000
A1 109.4712206
End
```

AD2: CH_4

```
geometry
zmatrix
C
H 1 B1
H 1 B2 2 A1
H 1 B3 2 A2 3 D1
H 1 B4 2 A3 3 D2
variables
B1 1.112999513
B2 1.112999513
A1 109.4712206
B3 1.112999513
A2 109.4712206
D1 120.0000000
B4 1.112999513
A3 109.4712206
D2 -120.0000000
End
```

AD3: H_2O_2

```
geometry
zmatrix
O
O 1 B1
H 2 B2 1 A1
H 1 B3 2 A2 3 D1
variables
```

B1 1.427753993
B2 0.941376263
A1 98.50397771
B3 0.941376263
A2 98.50397771
D1 -118.5656522
End

AD4: CH_3OH

geometry
zmatrix
C
O 1 B1
H 2 B2 1 A1
H 1 B3 2 A2 3 D1
H 1 B4 2 A3 3 D2
H 1 B5 2 A4 3 D3
variables
B1 1.406998428
B2 0.942304043
A1 107.3762717
B3 1.114972412
A2 108.6937696
D1 -179.9999991
B4 1.114928887
A3 108.6973130
D2 -59.82522375
B5 1.114928887
A4 108.6973130
D3 59.82522375
End

AD5: $HOOCH_3$

geometry
zmatrix
C
O 1 B1
O 2 B2 1 A1
H 3 B3 2 A2 1 D1
H 1 B4 2 A3 3 D2
H 1 B5 2 A4 3 D3
H 1 B6 2 A5 3 D4

variables
B1 1.500000000
B2 1.460000000
A1 109.4712206
B3 1.050000000
A2 109.4712206
D1 25.46348938
B4 1.090000000
A3 109.4712206
D2 -180.0000000
B5 1.090000000
A4 109.4712206
D3 -60.00000000
B6 1.090000000
A5 109.4712206
D4 60.00000000
End

AD6: $HOOCH_2CH_3$

geometry
zmatrix
C
C 1 B1
H 2 B2 1 A1
H 2 B3 1 A2 3 D1
H 2 B4 1 A3 3 D2
O 1 B5 2 A4 3 D3
O 6 B6 1 A5 2 D4
H 7 B7 6 A6 1 D5
H 1 B8 2 A7 3 D6
H 1 B9 2 A8 3 D7
variables
B1 1.540000000
B2 1.090000000
A1 109.4712206
B3 1.090000000
A2 109.4712206
D1 120.0000000
B4 1.090000000
A3 109.4712206
D2 -120.0000000
B5 1.500000000
A4 109.4712206
D3 180.0000000

B6 1.460000000
A5 109.4712206
D4 -80.33025365
B7 1.050000000
A6 109.4712206
D5 19.66044547
B8 1.090000000
A7 109.4712206
D6 60.00000000
B9 1.090000000
A8 109.4712206
D7 -60.00000000
End

AD7: $HOOCCl_3$

geometry
zmatrix
C
O 1 B1
O 2 B2 1 A1
H 3 B3 2 A2 1 D1
Cl 1 B4 2 A3 3 D2
Cl 1 B5 2 A4 3 D3
Cl 1 B6 2 A5 3 D4
variables
B1 1.500000000
B2 1.460000000
A1 109.4712206
B3 1.050000000
A2 109.4712206
D1 -0.000000000
B4 1.760000000
A3 109.4712206
D2 -60.00000000
B5 1.760000000
A4 109.4712206
D3 -179.9999988
B6 1.760000000
A5 109.4712206
D4 60.00000000
End

Appendix E: DHLA Hydrogen Abstractions

AE1: DHLA HTC1

geometry
zmatrix
C
C 1 B1
S 2 B2 1 A1
H 3 B3 2 A2 1 D1
H 2 B4 1 A3 3 D2
C 1 B5 2 A4 3 D3
C 6 B6 1 A5 2 D4
C 7 B7 6 A6 1 D5
C 8 B8 7 A7 6 D6
C 9 B9 8 A8 7 D7
C 10 B10 9 A9 8 D8
O 11 B11 10 A10 9 D9
O 11 B12 10 A11 9 D10
H 13 B13 11 A12 10 D11
H 10 B14 9 A13 8 D12
H 10 B15 9 A14 8 D13
H 9 B16 8 A15 7 D14
H 9 B17 8 A16 7 D15
H 8 B18 7 A17 6 D16
H 8 B19 7 A18 6 D17
H 7 B20 6 A19 1 D18
H 7 B21 6 A20 1 D19
S 6 B22 1 A21 2 D20
H 23 B23 6 A22 1 D21
H 6 B24 1 A23 2 D22
H 1 B25 2 A24 3 D23
H 1 B26 2 A25 3 D24
variables
B1 1.542063877
B2 1.825719036
A1 116.0933397
B3 1.404434762
A2 95.13972859
D1 -99.18666997
B4 1.109878372
A3 110.0600894
D2 122.6033344
B5 1.552615213
A4 115.9378952
D3 -58.44872838
B6 1.548089145

A5 110.2160490
D4 -162.9968171
B7 1.541358492
A6 113.2192663
D5 -176.1448805
B8 1.534809760
A7 111.8543207
D6 -174.6878894
B9 1.539128325
A8 110.6065122
D7 -172.2321398
B10 1.509194818
A9 113.4278797
D8 -178.8579254
B11 1.218754692
A10 121.1653405
D9 2.338054165
B12 1.351529504
A11 119.7123665
D10 -177.5295065
B13 0.967231617
A12 121.5588199
D11 0.982158699
B14 1.111783252
A13 108.4682803
D12 61.19499452
B15 1.111547120
A14 109.8453733
D13 -57.41252416
B16 1.112485955
A15 109.0116501
D14 66.44533717
B17 1.111834970
A16 109.7379879
D15 -52.77929530
B18 1.110020270
A17 108.4495820
D16 65.88927861
B19 1.112072390
A18 110.4031697
D17 -53.27911809
B20 1.113887337
A19 107.8637323
D18 63.20313787
B21 1.110964446
A20 110.0364181

D19 -54.79739301
B22 1.841261253
A21 111.7524908
D20 73.36469215
B23 1.407057213
A22 96.85002006
D21 28.94697757
B24 1.112490000
A23 108.1520503
D22 -45.51414440
B25 1.112863873
A24 104.8237150
D23 -177.9987962
B26 1.112063847
A25 110.7184439
D24 67.26362824
End

AE2: DHLA HTC2

geometry
zmatrix
C
H 1 B1
H 1 B2 2 A1
C 1 B3 2 A2 3 D1
H 4 B4 1 A3 2 D2
C 4 B5 1 A4 2 D3
H 6 B6 4 A5 1 D4
C 6 B7 4 A6 1 D5
H 8 B8 6 A7 4 D6
H 8 B9 6 A8 4 D7
C 8 B10 6 A9 4 D8
H 11 B11 8 A10 6 D9
H 11 B12 8 A11 6 D10
C 11 B13 8 A12 6 D11
H 14 B14 11 A13 8 D12
H 14 B15 11 A14 8 D13
C 14 B16 11 A15 8 D14
H 17 B17 14 A16 11 D15
H 17 B18 14 A17 11 D16
C 17 B19 14 A18 11 D17
O 20 B20 17 A19 14 D18
O 20 B21 17 A20 14 D19
H 22 B22 20 A21 17 D20

S 6 B23 4 A22 1 D21
H 24 B24 6 A23 4 D22
S 1 B25 2 A24 3 D23
H 26 B26 1 A25 2 D24
variables
B1 1.110163051
B2 1.108812428
A1 105.9875913
B3 1.533018265
A2 108.8753729
D1 -118.7890169
B4 1.111649675
A3 111.8511250
D2 70.31003492
B5 1.541082087
A4 116.4094575
D3 -59.89728608
B6 1.111602897
A5 107.9714060
D4 177.8148037
B7 1.541131403
A6 109.6075845
D5 60.67709086
B8 1.112738963
A7 108.0378703
D6 60.57899916
B9 1.112863873
A8 109.7978319
D7 -57.33197014
B10 1.538214874
A9 112.8150222
D8 -179.2486061
B11 1.110175211
A10 109.1107202
D9 -179.3350149
B12 1.111126005
A11 109.8123246
D10 61.43270127
B13 1.534404771
A12 111.3468123
D11 -59.28748607
B14 1.112894424
A13 109.0836578
D12 59.65612786
B15 1.112063847
A14 109.4759803

D13 -59.44381373
B16 1.537432925
A15 110.7076633
D14 -179.2616992
B17 1.111464349
A16 108.6420243
D15 -59.49120579
B18 1.111261445
A17 109.6220146
D16 -178.1550806
B19 1.509507536
A18 113.3085809
D17 60.69716028
B20 1.221039311
A19 121.1328704
D18 1.818338198
B21 1.350123328
A20 119.7589110
D19 -178.0894972
B22 0.967699850
A21 121.5395726
D20 0.859092634
B23 1.833982279
A22 111.7031935
D21 -63.19350957
B24 1.407736126
A23 94.63282658
D22 49.30945825
B25 1.822906470
A24 107.8755816
D23 116.8117746
B26 1.406821950
A25 93.76659902
D24 34.00388077
End

AE3: DHLA HTC3

geometry
zmatrix
C
H 1 B1
H 1 B2 2 A1
C 1 B3 2 A2 3 D1
H 4 B4 1 A3 2 D2

H 4 B5 1 A4 2 D3
C 4 B6 1 A5 2 D4
C 7 B7 4 A6 1 D5
H 8 B8 7 A7 4 D6
H 8 B9 7 A8 4 D7
C 8 B10 7 A9 4 D8
H 11 B11 8 A10 7 D9
H 11 B12 8 A11 7 D10
C 11 B13 8 A12 7 D11
H 14 B14 11 A13 8 D12
H 14 B15 11 A14 8 D13
C 14 B16 11 A15 8 D14
H 17 B17 14 A16 11 D15
H 17 B18 14 A17 11 D16
C 17 B19 14 A18 11 D17
O 20 B20 17 A19 14 D18
O 20 B21 17 A20 14 D19
H 22 B22 20 A21 17 D20
S 7 B23 4 A22 1 D21
H 24 B24 7 A23 4 D22
S 1 B25 2 A24 3 D23
H 26 B26 1 A25 2 D24
variables
B1 1.111113856
B2 1.111083255
A1 106.0120541
B3 1.537057579
A2 108.9777452
D1 -118.9195612
B4 1.112036870
A3 105.1217647
D2 54.08710259
B5 1.111439157
A4 110.7311121
D3 -61.66397920
B6 1.545388301
A5 115.0171775
D4 172.0688108
B7 1.542302175
A6 111.2456921
D5 -162.0661651
B8 1.111527328
A7 107.9152846
D6 58.18346805
B9 1.111566012
A8 109.7361336

D7 -59.79751922
B10 1.537070265
A9 112.9234140
D8 177.9048617
B11 1.110565622
A10 109.2384221
D9 64.27565137
B12 1.111880389
A11 109.7965411
D10 -55.04854233
B13 1.533859511
A12 111.1161140
D11 -175.8233073
B14 1.112816696
A13 109.0486886
D12 63.45275806
B15 1.112552021
A14 109.4696953
D13 -55.56347791
B16 1.536061522
A15 111.0042551
D14 -175.4447309
B17 1.112187035
A16 108.7100810
D15 60.50329527
B18 1.111669015
A17 109.7087973
D16 -58.19077179
B19 1.510198331
A18 113.2795456
D17 -179.3947828
B20 1.222099832
A19 120.9872150
D18 1.817566150
B21 1.348816518
A20 119.9142845
D19 -178.0042384
B22 0.967737051
A21 121.5209432
D20 0.840041331
B23 1.833340394
A22 112.3602340
D21 72.05395045
B24 1.407610742
A23 93.86278639
D22 59.13828913

B25 1.823429187
A24 106.9936712
D23 116.3010267
B26 1.406904048
A25 93.67438484
D24 34.38851038
End

AE4: DHLA HTC4

geometry
zmatrix
C
H 1 B1
H 1 B2 2 A1
C 1 B3 2 A2 3 D1
H 4 B4 1 A3 2 D2
H 4 B5 1 A4 2 D3
C 4 B6 1 A5 2 D4
H 7 B7 4 A6 1 D5
C 7 B8 4 A7 1 D6
H 9 B9 7 A8 4 D7
C 9 B10 7 A9 4 D8
H 11 B11 9 A10 7 D9
H 11 B12 9 A11 7 D10
C 11 B13 9 A12 7 D11
H 14 B14 11 A13 9 D12
H 14 B15 11 A14 9 D13
C 14 B16 11 A15 9 D14
H 17 B17 14 A16 11 D15
H 17 B18 14 A17 11 D16
C 17 B19 14 A18 11 D17
O 20 B20 17 A19 14 D18
O 20 B21 17 A20 14 D19
H 22 B22 20 A21 17 D20
S 7 B23 4 A22 1 D21
H 24 B24 7 A23 4 D22
S 1 B25 2 A24 3 D23
H 26 B26 1 A25 2 D24
variables
B1 1.111766162
B2 1.109984234
A1 105.8911448
B3 1.539555780
A2 108.9026366

D1 -118.9246011
B4 1.112441459
A3 105.3320390
D2 -177.4584965
B5 1.111076505
A4 110.3054384
D3 66.87188034
B6 1.547163857
A5 115.5448401
D4 -59.38399729
B7 1.111346031
A6 107.8898611
D5 177.4338044
B8 1.539572018
A7 109.9120765
D6 60.72511049
B9 1.112820740
A8 110.7738773
D7 -55.34468520
B10 1.533506113
A9 113.4852910
D8 -179.3088247
B11 1.110993249
A10 109.0300101
D9 60.44384734
B12 1.112364149
A11 109.8763435
D10 -58.84358944
B13 1.531799595
A12 111.0038164
D11 -179.3125596
B14 1.113521441
A13 109.0761899
D12 179.5540517
B15 1.112748399
A14 109.5456040
D13 60.45835600
B16 1.536992518
A15 110.6159510
D14 -59.27422626
B17 1.112266155
A16 108.6342619
D15 60.55995337
B18 1.111749972
A17 109.6718667
D16 -58.06768416

B19 1.508953942
A18 113.4530503
D17 -179.3171910
B20 1.222261429
A19 121.0220609
D18 1.965252239
B21 1.348756464
A20 119.8862342
D19 -177.9002411
B22 0.968300573
A21 121.4730428
D20 0.889884767
B23 1.833033551
A22 112.6605256
D21 -62.97609419
B24 1.407228126
A23 94.25239256
D22 51.41896641
B25 1.823741484
A24 106.9988391
D23 116.1123189
B26 1.406607266
A25 93.94721948
D24 31.88013162
End

AE5: DHLA HTC5

geometry
zmatrix
C
H 1 B1
H 1 B2 2 A1
C 1 B3 2 A2 3 D1
H 4 B4 1 A3 2 D2
H 4 B5 1 A4 2 D3
C 4 B6 1 A5 2 D4
H 7 B7 4 A6 1 D5
C 7 B8 4 A7 1 D6
H 9 B9 7 A8 4 D7
H 9 B10 7 A9 4 D8
C 9 B11 7 A10 4 D9
H 12 B12 9 A11 7 D10
C 12 B13 9 A12 7 D11
H 14 B14 12 A13 9 D12

H 14 B15 12 A14 9 D13
C 14 B16 12 A15 9 D14
H 17 B17 14 A16 12 D15
H 17 B18 14 A17 12 D16
C 17 B19 14 A18 12 D17
O 20 B20 17 A19 14 D18
O 20 B21 17 A20 14 D19
H 22 B22 20 A21 17 D20
S 7 B23 4 A22 1 D21
H 24 B24 7 A23 4 D22
S 1 B25 2 A24 3 D23
H 26 B26 1 A25 2 D24
variables
B1 1.111109806
B2 1.110746596
A1 105.7713535
B3 1.539424893
A2 108.8668967
D1 -118.8686269
B4 1.111771559
A3 105.1217575
D2 -177.3330417
B5 1.112128590
A4 110.3368229
D3 67.16075947
B6 1.550545065
A5 115.6618979
D4 -59.19767965
B7 1.112495393
A6 107.9657646
D5 177.8441077
B8 1.543163634
A7 110.2741271
D6 60.67835109
B9 1.112705711
A8 108.1913164
D7 61.12772475
B10 1.112205467
A9 110.0569465
D8 -57.04106743
B11 1.535207152
A10 112.6313669
D9 -179.2937257
B12 1.110525101
A11 109.4141139
D10 -60.58697015

B13 1.530390146
A12 111.6942154
D11 60.71537017
B14 1.112942496
A13 108.8173560
D12 60.03964173
B15 1.112310658
A14 109.6102581
D13 -59.11443940
B16 1.534834845
A15 110.5264931
D14 -179.2998586
B17 1.112033273
A16 108.7344437
D15 60.57556819
B18 1.111756268
A17 109.6255617
D16 -58.09461880
B19 1.510269512
A18 113.2407488
D17 -179.2856414
B20 1.221745063
A19 121.0345341
D18 1.729838762
B21 1.349509911
A20 119.8545891
D19 -178.0854474
B22 0.967603741
A21 121.5113305
D20 0.824103150
B23 1.833938112
A22 112.1957247
D21 -63.00235214
B24 1.407905537
A23 94.25373865
D22 52.81965411
B25 1.822861761
A24 106.9203983
D23 116.2432138
B26 1.406915776
A25 93.80692072
D24 32.09098758
End

AE6: DHLA HTC6

geometry
zmatrix
C
H 1 B1
H 1 B2 2 A1
C 1 B3 2 A2 3 D1
H 4 B4 1 A3 2 D2
H 4 B5 1 A4 2 D3
C 4 B6 1 A5 2 D4
H 7 B7 4 A6 1 D5
C 7 B8 4 A7 1 D6
H 9 B9 7 A8 4 D7
H 9 B10 7 A9 4 D8
C 9 B11 7 A10 4 D9
H 12 B12 9 A11 7 D10
H 12 B13 9 A12 7 D11
C 12 B14 9 A13 7 D12
H 15 B15 12 A14 9 D13
C 15 B16 12 A15 9 D14
H 17 B17 15 A16 12 D15
H 17 B18 15 A17 12 D16
C 17 B19 15 A18 12 D17
O 20 B20 17 A19 15 D18
O 20 B21 17 A20 15 D19
H 22 B22 20 A21 17 D20
S 7 B23 4 A22 1 D21
H 24 B24 7 A23 4 D22
S 1 B25 2 A24 3 D23
H 26 B26 1 A25 2 D24
variables
B1 1.110846074
B2 1.110243667
A1 105.9028213
B3 1.540241864
A2 108.8069172
D1 -118.8539838
B4 1.112720989
A3 105.0870462
D2 -177.3770781
B5 1.111887135
A4 110.4075741
D3 67.17329344
B6 1.549468619
A5 115.6121126

D4 -59.25723869
B7 1.112049459
A6 107.8811734
D5 57.81595597
B8 1.545599560
A7 110.3780354
D6 -59.30292351
B9 1.112795579
A8 108.3702224
D7 60.92008369
B10 1.112475168
A9 109.7916805
D8 -57.13045578
B11 1.536610230
A10 112.8910125
D9 -179.3110832
B12 1.110900086
A11 109.6536065
D10 60.38131933
B13 1.111914565
A12 109.6836169
D11 -59.18851930
B14 1.530701147
A13 111.0151333
D12 -179.3016518
B15 1.112259862
A14 110.2020757
D13 61.66672642
B16 1.533500897
A15 111.1537257
D14 -59.31272399
B17 1.111462550
A16 108.7496206
D15 -179.7753718
B18 1.111108456
A17 109.6012075
D16 61.42910860
B19 1.507680006
A18 112.8811507
D17 -59.26455924
B20 1.221554747
A19 120.9993227
D18 1.897239914
B21 1.348888431
A20 119.8330554
D19 -178.1908630

B22 0.968070762
A21 121.5276492
D20 0.916468500
B23 1.833688632
A22 112.2096166
D21 177.0237531
B24 1.408037997
A23 94.26337491
D22 52.41122942
B25 1.823895282
A24 106.9555110
D23 116.2459828
B26 1.407143916
A25 93.84430469
D24 31.68547867
End

AE7: DHLA HTC7

geometry
zmatrix
C
H 1 B1
H 1 B2 2 A1
C 1 B3 2 A2 3 D1
H 4 B4 1 A3 2 D2
H 4 B5 1 A4 2 D3
C 4 B6 1 A5 2 D4
H 7 B7 4 A6 1 D5
C 7 B8 4 A7 1 D6
H 9 B9 7 A8 4 D7
H 9 B10 7 A9 4 D8
C 9 B11 7 A10 4 D9
H 12 B12 9 A11 7 D10
H 12 B13 9 A12 7 D11
C 12 B14 9 A13 7 D12
H 15 B15 12 A14 9 D13
H 15 B16 12 A15 9 D14
C 15 B17 12 A16 9 D15
H 18 B18 15 A17 12 D16
C 18 B19 15 A18 12 D17
O 20 B20 18 A19 15 D18
O 20 B21 18 A20 15 D19
H 22 B22 20 A21 18 D20
S 7 B23 4 A22 1 D21

H 24 B24 7 A23 4 D22
S 1 B25 2 A24 3 D23
H 26 B26 1 A25 2 D24
variables
B1 1.110954094
B2 1.110490432
A1 105.7838702
B3 1.539431713
A2 108.8074664
D1 -118.8165490
B4 1.112550673
A3 105.0284608
D2 -177.3832312
B5 1.111126005
A4 110.3914804
D3 67.13831076
B6 1.549802891
A5 115.6296961
D4 -59.31486503
B7 1.112865670
A6 107.8790603
D5 -62.17144349
B8 1.545260172
A7 110.3103471
D6 -179.2705922
B9 1.112291778
A8 108.1349166
D7 -59.12460541
B10 1.112230642
A9 109.7372266
D8 -177.1258616
B11 1.538421594
A10 113.0543901
D9 60.71110708
B12 1.110244568
A11 109.2693088
D10 60.53006296
B13 1.113039981
A12 109.8300424
D11 -58.69122513
B14 1.531960182
A13 111.1747346
D12 -179.2559044
B15 1.112288182
A14 109.0550943
D13 -59.87300688

B16 1.112628420
A15 109.7936905
D14 -179.2537794
B17 1.532951728
A16 110.3801684
D15 60.70670529
B18 1.111178204
A17 109.0844716
D16 59.33285975
B19 1.507786789
A18 113.7473095
D17 -179.2956903
B20 1.222967293
A19 121.0391292
D18 1.099976853
B21 1.348320808
A20 119.8115214
D19 -178.7842371
B22 0.967733951
A21 121.4716590
D20 0.907036224
B23 1.833841324
A22 112.2081763
D21 56.97875705
B24 1.406986141
A23 94.29545028
D22 52.13113580
B25 1.823385313
A24 106.9960783
D23 116.2584029
B26 1.406943496
A25 93.85515254
D24 31.30974884
End

AE8: DHLA HTS1

geometry
zmatrix
C
C 1 B1
C 2 B2 1 A1
C 3 B3 2 A2 1 D1
C 4 B4 3 A3 2 D2
C 5 B5 4 A4 3 D3

C 6 B6 5 A5 4 D4
C 7 B7 6 A6 5 D5
O 8 B8 7 A7 6 D6
O 8 B9 7 A8 6 D7
H 10 B10 8 A9 7 D8
H 7 B11 6 A10 5 D9
H 7 B12 6 A11 5 D10
H 6 B13 5 A12 4 D11
H 6 B14 5 A13 4 D12
H 5 B15 4 A14 3 D13
H 5 B16 4 A15 3 D14
H 4 B17 3 A16 2 D15
H 4 B18 3 A17 2 D16
S 3 B19 2 A18 1 D17
H 3 B20 2 A19 1 D18
H 2 B21 1 A20 3 D19
H 2 B22 1 A21 3 D20
S 1 B23 2 A22 3 D21
H 24 B24 1 A23 2 D22
H 1 B25 2 A24 3 D23
H 1 B26 2 A25 3 D24
variables
B1 1.538463519
B2 1.548008398
A1 115.4731453
B3 1.542717732
A2 109.8256141
D1 60.66217277
B4 1.538444344
A3 112.6343928
D2 -179.3151872
B5 1.533436011
A4 111.1048261
D3 -59.22534748
B6 1.536247701
A5 110.8737306
D4 -179.3431946
B7 1.509739381
A6 113.1998998
D5 -59.30740614
B8 1.221855147
A7 121.0380225
D6 0.318785134
B9 1.349329463
A8 119.8839663
D7 -179.6793301

B10 0.968136870
A9 121.5040393
D8 0.112936472
B11 1.111024752
A10 109.1035338
D9 -179.8997181
B12 1.111950538
A11 109.2885186
D10 61.37701542
B13 1.112576290
A12 109.1217571
D11 60.04693377
B14 1.112270201
A13 109.3189454
D12 -59.05392507
B15 1.112084979
A14 108.9093060
D13 -179.5889995
B16 1.110994599
A15 110.1770758
D14 61.25221016
B17 1.112924526
A16 109.6531681
D15 57.88511664
B18 1.112408648
A17 108.7387628
D16 -60.26530215
B19 1.829563882
A18 111.9062222
D17 -177.5434303
B20 1.111950538
A19 108.1678779
D18 -57.13562656
B21 1.111665867
A20 110.4664635
D19 -126.7924774
B22 1.112642350
A21 104.9704433
D20 117.5390272
B23 1.822566597
A22 114.7337352
D21 60.74310165
B24 1.408869760
A23 93.33351425
D22 -101.8768780
B25 1.110885683

A24 110.5741630
D23 -64.49579345
B26 1.110484579
A25 109.0545728
D24 179.4645422
End

AE9: DHLA HTS2

geometry
zmatrix
C
C 1 B1
C 2 B2 1 A1
C 3 B3 2 A2 1 D1
C 4 B4 3 A3 2 D2
C 5 B5 4 A4 3 D3
C 6 B6 5 A5 4 D4
C 7 B7 6 A6 5 D5
O 8 B8 7 A7 6 D6
H 9 B9 8 A8 7 D7
O 8 B10 7 A9 6 D8
H 7 B11 6 A10 5 D9
H 7 B12 6 A11 5 D10
H 6 B13 5 A12 4 D11
H 6 B14 5 A13 4 D12
H 5 B15 4 A14 3 D13
H 5 B16 4 A15 3 D14
H 4 B17 3 A16 2 D15
H 4 B18 3 A17 2 D16
S 3 B19 2 A18 1 D17
H 20 B20 3 A19 2 D18
H 3 B21 2 A20 1 D19
H 2 B22 1 A21 3 D20
H 2 B23 1 A22 3 D21
S 1 B24 2 A23 3 D22
H 1 B25 2 A24 3 D23
H 1 B26 2 A25 3 D24
variables
B1 1.538779386
B2 1.550313839
A1 116.0107626
B3 1.544497653
A2 109.8490132
D1 60.69129963

B4 1.538039661
A3 113.4938754
D2 60.73677715
B5 1.534729618
A4 110.8233416
D3 60.65790184
B6 1.535601511
A5 111.2002972
D4 -179.2616030
B7 1.510296660
A6 113.1115585
D5 60.71124145
B8 1.349161962
A7 119.8939681
D6 -178.1963285
B9 0.967500904
A8 121.5084209
D7 0.837789201
B10 1.222132971
A9 121.0040307
D8 1.730501151
B11 1.111609194
A10 108.7498031
D9 -59.42434359
B12 1.110937442
A11 109.6916494
D10 -178.1435028
B13 1.112960916
A12 109.0064910
D11 59.54567587
B14 1.112249972
A13 109.3121259
D12 -59.34058477
B15 1.110654762
A14 109.3965163
D13 -59.19769249
B16 1.111919511
A15 109.9146432
D14 -178.6431044
B17 1.113232231
A16 108.3439565
D15 -59.45396079
B18 1.112109707
A17 109.4751027
D16 -177.2864485
B19 1.832946808

A18 112.4773348
D17 -62.88886242
B20 1.407205031
A19 94.13947208
D18 54.68322648
B21 1.110976597
A20 108.0233929
D19 177.9609513
B22 1.113003594
A21 105.2808674
D20 -118.0654973
B23 1.112205467
A22 110.0164405
D21 126.4994982
B24 1.819589514
A23 114.3744891
D22 60.72303260
B25 1.110687175
A24 108.0046626
D23 -57.10336112
B26 1.110773604
A25 110.3027971
D24 -174.7675809
End

Appendix F: DHLA Adducts with Various Radicals

AF1: DHLA-CH_3

geometry
zmatrix
C
C 1 B1
C 2 B2 1 A1
C 3 B3 2 A2 1 D1
C 4 B4 3 A3 2 D2
C 5 B5 4 A4 3 D3
C 6 B6 5 A5 4 D4
C 7 B7 6 A6 5 D5
O 8 B8 7 A7 6 D6
H 9 B9 8 A8 7 D7
O 8 B10 7 A9 6 D8
H 7 B11 6 A10 5 D9
H 7 B12 6 A11 5 D10
H 6 B13 5 A12 4 D11
H 6 B14 5 A13 4 D12
H 5 B15 4 A14 3 D13
H 5 B16 4 A15 3 D14
H 4 B17 3 A16 2 D15
H 4 B18 3 A17 2 D16
S 3 B19 2 A18 1 D17
C 20 B20 3 A19 2 D18
H 21 B21 20 A20 3 D19
H 21 B22 20 A21 3 D20
H 21 B23 20 A22 3 D21
H 3 B24 2 A23 1 D22
H 2 B25 1 A24 3 D23
H 2 B26 1 A25 3 D24
S 1 B27 2 A26 3 D25
H 28 B28 1 A27 2 D26
H 1 B29 2 A28 3 D27
H 1 B30 2 A29 3 D28
variables
B1 1.543411157
B2 1.551211462
A1 117.3777485
B3 1.549758046
A2 111.8004060
D1 -59.27385010
B4 1.544437762
A3 117.1855721
D2 60.69136770

B5 1.536329717
A4 115.0962720
D3 60.71972445
B6 1.535841789
A5 111.4789034
D4 -179.2883810
B7 1.507510199
A6 112.6925118
D5 -59.32429598
B8 1.349782946
A7 119.1132503
D6 -179.7278960
B9 0.967585138
A8 121.3481459
D7 179.8105662
B10 1.223418980
A9 121.2129375
D8 0.126128129
B11 1.111044104
A10 109.2270920
D9 -179.8252882
B12 1.111072005
A11 109.3784296
D10 61.27940493
B13 1.112696275
A12 109.0121784
D11 60.37944430
B14 1.101347357
A13 110.6738672
D12 -60.21363503
B15 1.111781453
A14 109.9424489
D13 -64.92388857
B16 1.113186867
A15 106.2819584
D14 178.5830493
B17 1.112944743
A16 106.2090813
D15 -56.53619188
B18 1.110886583
A17 110.7615892
D16 -173.1117561
B19 1.839725251
A18 110.3352185
D17 173.1495205
B20 1.824555562

A19 96.83872495
D18 -59.29631111
B21 1.108480040
A20 108.3505974
D19 -171.0634839
B22 1.108809271
A21 110.2711949
D20 70.09097605
B23 1.110489081
A22 110.7988618
D21 -53.93986321
B24 1.112588423
A23 104.8967302
D22 56.22687914
B25 1.111470198
A24 109.4702110
D23 -125.4484207
B26 1.113363822
A25 105.8950932
D24 119.5011224
B27 1.822317481
A26 114.7639499
D25 -59.30281683
B28 1.408716792
A27 93.23478281
D26 -94.81236377
B29 1.109549007
A28 111.5780607
D27 175.0456579
B30 1.110181967
A29 108.7340398
D28 59.53454272
End

AF2: DHLA-OOH

geometry
zmatrix
C
C 1 B1
C 2 B2 1 A1
C 3 B3 2 A2 1 D1
C 4 B4 3 A3 2 D2
C 5 B5 4 A4 3 D3
C 6 B6 5 A5 4 D4

C 7 B7 6 A6 5 D5
O 8 B8 7 A7 6 D6
H 9 B9 8 A8 7 D7
O 8 B10 7 A9 6 D8
H 7 B11 6 A10 5 D9
H 7 B12 6 A11 5 D10
H 6 B13 5 A12 4 D11
H 6 B14 5 A13 4 D12
H 5 B15 4 A14 3 D13
H 5 B16 4 A15 3 D14
H 4 B17 3 A16 2 D15
H 4 B18 3 A17 2 D16
S 3 B19 2 A18 1 D17
O 20 B20 3 A19 2 D18
O 21 B21 20 A20 3 D19
H 22 B22 21 A21 20 D20
H 3 B23 2 A22 1 D21
H 2 B24 1 A23 3 D22
H 2 B25 1 A24 3 D23
S 1 B26 2 A25 3 D24
H 27 B27 1 A26 2 D25
H 1 B28 2 A27 3 D26
H 1 B29 2 A28 3 D27
variables
B1 1.540049773
B2 1.548708290
A1 115.7190979
B3 1.544824560
A2 109.9381072
D1 60.74735766
B4 1.539248737
A3 113.0170730
D2 60.68575858
B5 1.534388538
A4 111.0146404
D3 -179.2896122
B6 1.535631091
A5 110.9903482
D4 -59.30739529
B7 1.510012318
A6 113.2451028
D5 60.78431560
B8 1.348140614
A7 119.9610334
D6 -179.2156744
B9 0.967889498

A8 121.4698654
D7 0.319986434
B10 1.222217352
A9 120.9764322
D8 0.666558351
B11 1.111631988
A10 109.0622217
D9 -59.67551002
B12 1.112081564
A11 109.3628054
D10 -178.3740226
B13 1.112594489
A12 109.1988011
D11 179.8721625
B14 1.112406467
A13 109.1995914
D12 60.91834202
B15 1.110394339
A14 109.7997431
D13 60.55157262
B16 1.111764205
A15 109.3732786
D14 -58.73289382
B17 1.112326042
A16 108.5904886
D15 -59.00044283
B18 1.112592522
A17 109.4483046
D16 -177.0115767
B19 1.837177127
A18 111.8618390
D17 -61.21114362
B20 1.718893467
A19 94.04691877
D18 -59.31591571
B21 1.316711620
A20 104.4972403
D19 -179.2874272
B22 0.991261449
A21 104.7258301
D20 -149.8061096
B23 1.113193751
A22 107.7304307
D21 177.1822733
B24 1.112921687
A23 105.1383457

D22 -117.7368936
B25 1.111695184
A24 110.3225988
D23 126.6719302
B26 1.821031727
A25 113.9411800
D24 60.67847451
B27 1.407959310
A26 92.64142904
D25 173.1699290
B28 1.111001589
A27 107.5842161
D26 -57.16205784
B29 1.110725080
A28 109.0527993
D27 -175.9213931
End

AF3: DHLA-OCH_3

geometry
zmatrix
C
C 1 B1
C 2 B2 1 A1
C 3 B3 2 A2 1 D1
C 4 B4 3 A3 2 D2
C 5 B5 4 A4 3 D3
C 6 B6 5 A5 4 D4
C 7 B7 6 A6 5 D5
O 8 B8 7 A7 6 D6
H 9 B9 8 A8 7 D7
O 8 B10 7 A9 6 D8
H 7 B11 6 A10 5 D9
H 7 B12 6 A11 5 D10
H 6 B13 5 A12 4 D11
H 6 B14 5 A13 4 D12
H 5 B15 4 A14 3 D13
H 5 B16 4 A15 3 D14
H 4 B17 3 A16 2 D15
H 4 B18 3 A17 2 D16
S 3 B19 2 A18 1 D17
O 20 B20 3 A19 2 D18
C 21 B21 20 A20 3 D19
H 22 B22 21 A21 20 D20

H 22 B23 21 A22 20 D21
H 22 B24 21 A23 20 D22
H 3 B25 2 A24 1 D23
H 2 B26 1 A25 3 D24
H 2 B27 1 A26 3 D25
S 1 B28 2 A27 3 D26
H 29 B29 1 A28 2 D27
H 1 B30 2 A29 3 D28
H 1 B31 2 A30 3 D29
variables
B1 1.542642862
B2 1.552193609
A1 117.2015867
B3 1.551783812
A2 111.7093572
D1 -59.31485936
B4 1.543810869
A3 117.1475888
D2 -179.2683423
B5 1.536750468
A4 114.6877831
D3 -179.2614498
B6 1.535723282
A5 111.4660436
D4 -179.3297431
B7 1.507972811
A6 112.7205608
D5 -59.28378723
B8 1.350175174
A7 119.0467064
D6 -179.6013375
B9 0.966886239
A8 121.3520762
D7 179.7535758
B10 1.222332197
A9 121.2250770
D8 0.246718723
B11 1.111023402
A10 109.1142794
D9 -179.6993450
B12 1.111338382
A11 109.4361959
D10 61.38536867
B13 1.112809957
A12 108.9451649
D11 60.27603505

B14 1.099251564
A13 111.1164065
D12 -59.88393296
B15 1.111305539
A14 110.0289550
D13 54.35152953
B16 1.112513371
A15 106.4088211
D14 -62.19376203
B17 1.112737166
A16 105.6040909
D15 63.55252453
B18 1.109488621
A17 111.4225404
D16 -52.96411956
B19 1.834556350
A18 110.2830029
D17 171.6158452
B20 1.727999421
A19 93.69096848
D18 -179.2925049
B21 1.401514181
A20 107.1670299
D19 60.66155733
B22 1.108574761
A21 108.3866459
D20 171.6300042
B23 1.113000449
A22 111.7257474
D21 54.36199668
B24 1.111435558
A23 110.4579295
D22 -70.35527754
B25 1.111977518
A24 104.6033336
D23 56.91189801
B26 1.111441406
A25 109.5161330
D24 -125.2507773
B27 1.112646395
A26 105.9765829
D25 119.6371159
B28 1.821667643
A27 114.7546406
D26 60.73825795
B29 1.409123841

A28 93.09711876
D27 -91.80739799
B30 1.109440399
A29 111.6545866
D28 -64.73743502
B31 1.110288701
A30 108.7653414
D29 179.8416217
End

AF4: DHLA-$OOCH_3$

geometry
zmatrix
C
C 1 B1
C 2 B2 1 A1
C 3 B3 2 A2 1 D1
C 4 B4 3 A3 2 D2
C 5 B5 4 A4 3 D3
C 6 B6 5 A5 4 D4
C 7 B7 6 A6 5 D5
O 8 B8 7 A7 6 D6
H 9 B9 8 A8 7 D7
O 8 B10 7 A9 6 D8
H 7 B11 6 A10 5 D9
H 7 B12 6 A11 5 D10
H 6 B13 5 A12 4 D11
H 6 B14 5 A13 4 D12
H 5 B15 4 A14 3 D13
H 5 B16 4 A15 3 D14
H 4 B17 3 A16 2 D15
H 4 B18 3 A17 2 D16
S 3 B19 2 A18 1 D17
O 20 B20 3 A19 2 D18
O 21 B21 20 A20 3 D19
C 22 B22 21 A21 20 D20
H 23 B23 22 A22 21 D21
H 23 B24 22 A23 21 D22
H 23 B25 22 A24 21 D23
H 3 B26 2 A25 1 D24
H 2 B27 1 A26 3 D25
H 2 B28 1 A27 3 D26
S 1 B29 2 A28 3 D27

H 30 B30 1 A29 2 D28
H 1 B31 2 A30 3 D29
H 1 B32 2 A31 3 D30
variables
B1 1.540619681
B2 1.547248526
A1 115.6447555
B3 1.544470783
A2 110.1764660
D1 -59.26067577
B4 1.536053384
A3 112.3441259
D2 -59.32579110
B5 1.531592962
A4 111.7845476
D3 -179.2593005
B6 1.536237286
A5 110.4172064
D4 60.67149610
B7 1.508797203
A6 113.3971076
D5 -59.28037752
B8 1.349051519
A7 119.7953535
D6 -179.3867125
B9 0.967952995
A8 121.5043089
D7 0.369279855
B10 1.221815862
A9 121.0322962
D8 0.686352620
B11 1.112193329
A10 109.0187121
D9 -179.8513939
B12 1.112313355
A11 109.3300061
D10 61.54413531
B13 1.112820291
A12 109.1465683
D11 -59.78884640
B14 1.112070591
A13 109.4408779
D12 -178.9673847
B15 1.110723638
A14 109.6652396
D13 60.17225620

B16 1.112667965
A15 108.9197417
D14 -59.14759559
B17 1.113053458
A16 108.6014733
D15 -178.4735125
B18 1.111957283
A17 109.8016097
D16 63.28769656
B19 1.838241007
A18 111.4188838
D17 178.9217594
B20 1.720865480
A19 94.11373634
D18 -59.26899027
B21 1.321334553
A20 104.9059300
D19 -59.30008781
B22 1.405281822
A21 106.9363284
D20 -59.31060052
B23 1.109274988
A22 108.5339768
D21 144.9747880
B24 1.114425861
A23 113.0621697
D22 26.90021834
B25 1.108254935
A24 109.8824849
D23 -96.57740200
B26 1.113031895
A25 108.0099497
D24 57.09170939
B27 1.113140153
A26 104.8220663
D25 -118.0344869
B28 1.111719839
A27 110.5243127
D26 126.4467555
B29 1.822494444
A28 115.2000075
D27 -179.2934471
B30 1.405815422
A29 93.31379262
D28 -61.93342113
B31 1.110824018

A30 109.4354495
D29 60.12173160
B32 1.111300589
A31 109.5008909
D30 -56.46112056
End

AF5: DHLA-$OOCH_2CH_3$

geometry
zmatrix
C
C 1 B1
C 2 B2 1 A1
C 3 B3 2 A2 1 D1
C 4 B4 3 A3 2 D2
C 5 B5 4 A4 3 D3
C 6 B6 5 A5 4 D4
C 7 B7 6 A6 5 D5
O 8 B8 7 A7 6 D6
H 9 B9 8 A8 7 D7
O 8 B10 7 A9 6 D8
H 7 B11 6 A10 5 D9
H 7 B12 6 A11 5 D10
H 6 B13 5 A12 4 D11
H 6 B14 5 A13 4 D12
H 5 B15 4 A14 3 D13
H 5 B16 4 A15 3 D14
H 4 B17 3 A16 2 D15
H 4 B18 3 A17 2 D16
S 3 B19 2 A18 1 D17
O 20 B20 3 A19 2 D18
O 21 B21 20 A20 3 D19
C 22 B22 21 A21 20 D20
C 23 B23 22 A22 21 D21
H 24 B24 23 A23 22 D22
H 24 B25 23 A24 22 D23
H 24 B26 23 A25 22 D24
H 23 B27 22 A26 21 D25
H 23 B28 22 A27 21 D26
H 3 B29 2 A28 1 D27
H 2 B30 1 A29 3 D28
H 2 B31 1 A30 3 D29
S 1 B32 2 A31 3 D30
H 33 B33 1 A32 2 D31

H 1 B34 2 A33 3 D32
H 1 B35 2 A34 3 D33
variables
B1 1.535120191
B2 1.546193390
A1 114.7569990
B3 1.545320032
A2 109.2530522
D1 -177.9489576
B4 1.534074966
A3 113.0560796
D2 175.6153370
B5 1.532176883
A4 111.7543384
D3 -176.7719294
B6 1.536938515
A5 110.3083156
D4 -179.5920911
B7 1.507987400
A6 113.4306229
D5 179.8316337
B8 1.349792947
A7 119.7690275
D6 -179.6699004
B9 0.967878608
A8 121.4311632
D7 0.065836483
B10 1.221218244
A9 121.0666745
D8 0.201743732
B11 1.111195302
A10 109.0820561
D9 59.21754751
B12 1.111963129
A11 109.1664439
D10 -59.35093603
B13 1.112002248
A12 109.4064937
D11 59.89274634
B14 1.113021563
A13 109.2745717
D12 -59.32500926
B15 1.108901258
A14 109.7326142
D13 63.39321251
B16 1.111378423

A15 109.0385159
D14 -56.53119481
B17 1.113181926
A16 108.1928301
D15 56.26144019
B18 1.112184337
A17 109.7730622
D16 -61.66431249
B19 1.842117532
A18 109.5434318
D17 59.34146601
B20 1.723140737
A19 95.35039224
D18 -155.3866295
B21 1.320476051
A20 105.5180801
D19 84.72613951
B22 1.409736855
A21 106.5823785
D20 -143.4067690
B23 1.522858825
A22 110.0865009
D21 -100.4377057
B24 1.110334634
A23 110.0485075
D22 -58.82968062
B25 1.111257846
A24 109.6957373
D23 -178.5399921
B26 1.110506641
A25 110.2193413
D24 61.69845956
B27 1.109967117
A26 108.4407751
D25 139.6913778
B28 1.115282027
A27 112.9699297
D26 22.11187565
B29 1.110417489
A28 107.5997561
D27 -59.60780870
B30 1.112560111
A29 107.7901300
D28 -122.0104330
B31 1.112316951
A30 108.0529320

D29 121.7110864
B32 1.822141872
A31 112.3460049
D30 62.34195588
B33 1.408668165
A32 93.23581035
D31 -97.54289418
B34 1.110011261
A33 111.6450492
D32 -61.42588584
B35 1.111149855
A34 109.5366151
D33 -178.1249952
End

AF6: DHLA-$OOCCl_3$

geometry
zmatrix
C
H 1 B1
H 1 B2 2 A1
C 1 B3 2 A2 3 D1
H 4 B4 1 A3 2 D2
H 4 B5 1 A4 2 D3
C 4 B6 1 A5 2 D4
H 7 B7 4 A6 1 D5
C 7 B8 4 A7 1 D6
H 9 B9 7 A8 4 D7
H 9 B10 7 A9 4 D8
C 9 B11 7 A10 4 D9
H 12 B12 9 A11 7 D10
H 12 B13 9 A12 7 D11
C 12 B14 9 A13 7 D12
H 15 B15 12 A14 9 D13
H 15 B16 12 A15 9 D14
C 15 B17 12 A16 9 D15
H 18 B18 15 A17 12 D16
H 18 B19 15 A18 12 D17
C 18 B20 15 A19 12 D18
O 21 B21 18 A20 15 D19
H 22 B22 21 A21 18 D20

O 21 B23 18 A22 15 D21
S 7 B24 4 A23 1 D22
O 25 B25 7 A24 4 D23
O 26 B26 25 A25 7 D24
C 27 B27 26 A26 25 D25
Cl 28 B28 27 A27 26 D26
Cl 28 B29 27 A28 26 D27
Cl 28 B30 27 A29 26 D28
S 1 B31 2 A30 3 D29
H 32 B32 1 A31 2 D30
variables
B1 1.110914938
B2 1.109800883
A1 105.9227712
B3 1.535953775
A2 111.1942712
D1 -119.1872137
B4 1.112013489
A3 107.8089145
D2 177.1141898
B5 1.111543521
A4 108.2308788
D3 60.55755420
B6 1.544592503
A5 114.5229952
D4 -61.08701353
B7 1.111260995
A6 107.3398704
D5 -59.47354231
B8 1.542907321
A7 110.0095747
D6 -177.3790351
B9 1.112310209
A8 108.2894088
D7 56.08344217
B10 1.112450448
A9 109.7715325
D8 -62.15432201
B11 1.536376256
A10 112.5532816
D9 175.3827862
B12 1.109631921
A11 109.8945248
D10 62.49985990
B13 1.109931980
A12 108.8395069

D11 -56.93861870
B14 1.532096929
A13 111.6168594
D12 -176.7298158
B15 1.112795579
A14 109.1725564
D13 59.39474124
B16 1.112516966
A15 109.4663620
D14 -59.87816342
B17 1.537114830
A16 110.4259004
D15 179.5391031
B18 1.111632133
A17 109.0694052
D16 60.06999732
B19 1.111254246
A18 109.1478502
D17 -58.58041338
B20 1.508093498
A19 113.3711422
D18 -179.1843270
B21 1.348236626
A20 119.8372960
D19 179.9813443
B22 0.968643381
A21 121.4649412
D20 0.103165633
B23 1.222900241
A22 121.0446310
D21 0.147802581
B24 1.840107606
A23 109.9086542
D22 59.89363369
B25 1.721482501
A24 94.53527334
D23 -145.4394416
B26 1.320893637
A25 104.8629510
D24 83.79767421
B27 1.407213559
A26 107.0803249
D25 -165.1924136
B28 1.783004767
A27 110.5712701
D26 -70.77561208

B29 1.777783733
A28 108.1173042
D27 170.9001347
B30 1.790061451
A29 112.5008103
D28 52.76712953
B31 1.823481560
A30 109.7624114
D29 115.9808681
B32 1.405952346
A31 93.45161874
D30 16.94160717
End

AG1: •OH

geometry
zmatrix
O
H 1 B1
variables
B1 0.974454000
End

AG2: •CH_3

geometry
zmatrix
C
H 1 B1
H 1 B2 2 A1
H 1 B3 2 A2 3 D1
variables
B1 1.089993270
B2 1.089993270
A1 120.0000000
B3 1.089993270
A2 120.0000000
D1 180.0000000
End

AG3: •OOH

geometry
zmatrix
O
O 1 B1
H 1 B2 2 A1
variables
B1 1.462206886
B2 0.941970347
A1 108.8570969
End

AG4: •OCH_3

geometry
zmatrix
C
O 1 B1
H 1 B2 2 A1
H 1 B3 2 A2 3 D1
H 1 B4 2 A3 3 D2
variables
B1 1.500000000
B2 1.090000000
A1 109.4712206
B3 1.090000000
A2 109.4712206
D1 120.0000000
B4 1.090000000
A3 109.4712206
D2 -120.0000000
End

AG5: •$OOCH_3$

geometry
zmatrix
C
O 1 B1
O 2 B2 1 A1
H 1 B3 2 A2 3 D1
H 1 B4 2 A3 3 D2
H 1 B5 2 A4 3 D3
variables
B1 1.501655127
B2 1.462091300
A1 111.3803608
B3 1.112931979
A2 110.2453232
D1 0.000000000
B4 1.112959068
A3 109.5365628
D2 120.1348991
B5 1.112959068
A4 109.5365628
D3 -120.1348991
End

AG6: •$OOCH_2CH_3$

geometry
zmatrix
C
O 1 B1
O 2 B2 1 A1
C 1 B3 2 A2 3 D1
H 4 B4 1 A3 2 D2
H 4 B5 1 A4 2 D3
H 4 B6 1 A5 2 D4
H 1 B7 2 A6 3 D5
H 1 B8 2 A7 3 D6
variables
B1 1.501260593
B2 1.460531437
A1 109.8832803
B3 1.528914860
A2 108.9068436
D1 -54.56286889
B4 1.114682287
A3 111.4525949
D2 -179.4171236
B5 1.113905143
A4 110.2607915
D3 -58.91178529
B6 1.113906093
A5 110.3461515
D4 60.10712325
B7 1.114747112
A6 108.9185636
D5 66.38638885
B8 1.114752101
A7 108.8438734
D6 -175.4299883
End

AG7: •$OOCCl_3$

geometry
zmatrix
C
O 1 B1
O 2 B2 1 A1
Cl 1 B3 2 A2 3 D1

Cl 1 B4 2 A3 3 D2
Cl 1 B5 2 A4 3 D3
variables
B1 1.503119058
B2 1.460728681
A1 110.1226209
B3 1.796990920
A2 108.0617856
D1 -54.28713494
B4 1.796976017
A3 107.7293273
D2 -174.2376453
B5 1.796989978
A4 107.9811182
D3 65.85367634
End

Appendix H: ALA Explicitly Solvated by Water

AH1: 1 water

NO.	ATOM	X	Y	Z
1	C	0.0000	0.0000	0.0000
2	C	1.3448	0.7120	0.2194
3	C	2.4918	-0.2658	0.5514
4	C	3.8548	0.4037	0.3410
5	C	5.0683	-0.3805	0.8684
6	C	6.3743	0.3629	0.5113
7	C	7.6185	-0.5384	0.3862
8	C	8.6242	-0.0033	-0.6252
9	O	8.3811	0.6273	-1.6240
10	O	9.8938	-0.3269	-0.3254
11	H	10.3775	0.0766	-1.0638
12	H	7.3311	-1.5479	0.0115
13	H	8.0936	-0.6699	1.3868
14	H	6.5651	1.1820	1.2488
15	H	6.2144	0.8859	-0.4589
16	H	5.0552	-1.3959	0.4099
17	H	4.9949	-0.5137	1.9738
18	H	3.8556	1.4153	0.8109
19	H	3.9649	0.5331	-0.7617
20	S	2.3091	-1.6333	-0.5915
21	S	0.3369	-1.4252	-1.0295
22	H	2.3824	-0.6489	1.5937
23	H	1.2475	1.4878	1.0156
24	H	1.5951	1.2288	-0.7358
25	H	-0.7423	0.6660	-0.5030
26	H	-0.4255	-0.3474	0.9702
27	H	6.5234	0.6217	-2.7095
28	O	6.2074	-0.2647	-2.7572
29	H	6.9183	-0.7635	-2.3895

AH2: 2 water

NO.	ATOM	X	Y	Z
1	C	0.0000	0.0000	0.0000
2	C	1.4194	0.5511	0.1867
3	C	2.4384	-0.5931	0.3268
4	C	3.8601	-0.0418	0.2355
5	C	4.9233	-1.0786	0.6061
6	C	6.3034	-0.4064	0.5999

7	C	7.3627	-1.3000	1.2552
8	C	8.6167	-0.5145	1.6032
9	O	8.9703	-0.2994	2.7439
10	O	9.2874	-0.0891	0.4827
11	H	9.9308	0.1995	1.1542
12	H	7.5990	-2.1677	0.5962
13	H	6.9608	-1.7078	2.2130
14	H	6.2504	0.5594	1.1565
15	H	6.5936	-0.1576	-0.4498
16	H	4.9097	-1.9368	-0.1065
17	H	4.6983	-1.4849	1.6210
18	H	3.9416	0.8265	0.9318
19	H	4.0436	0.3247	-0.8015
20	S	2.1013	-1.7331	-1.0114
21	S	0.1247	-1.3088	-1.2162
22	H	2.2747	-1.1263	1.2937
23	H	1.4708	1.2381	1.0646
24	H	1.6836	1.1364	-0.7245
25	H	-0.6944	0.7930	-0.3611
26	H	-0.3871	-0.4207	0.9574
27	H	7.4878	1.1496	3.2887
28	O	6.6287	1.1397	3.6747
29	H	6.7392	1.5704	4.5037
30	H	5.3752	-0.7895	4.3219
31	O	4.5677	-0.3470	4.1251
32	H	4.8603	0.3736	3.5920

AH3: 3 water

NO.	ATOM	X	Y	Z
1	C	0.0000	0.0000	0.0000
2	C	1.3130	0.6897	-0.4085
3	C	2.5250	-0.1357	0.0580
4	C	3.8567	0.3302	-0.5395
5	C	4.9860	-0.6128	-0.1037
6	C	6.3588	-0.2083	-0.6618
7	C	7.4539	-1.1847	-0.2019
8	C	8.8352	-0.8106	-0.7016
9	O	9.1364	0.1178	-1.4105
10	O	9.7768	-1.6599	-0.2540
11	H	10.5870	-1.2965	-0.6490
12	H	7.2170	-2.2121	-0.5664
13	H	7.4840	-1.2103	0.9129
14	H	6.6076	0.8227	-0.3140

15	H	6.3164	-0.1872	-1.7770
16	H	4.7408	-1.6464	-0.4442
17	H	5.0404	-0.6245	1.0104
18	H	4.0747	1.3731	-0.2094
19	H	3.7801	0.3284	-1.6515
20	S	2.1971	-1.8227	-0.4455
21	S	0.1680	-1.7213	-0.4629
22	H	2.5759	-0.1151	1.1725
23	H	1.3604	1.7287	-0.0036
24	H	1.3352	0.7493	-1.5216
25	H	-0.8817	0.4506	-0.5118
26	H	-0.1505	0.0605	1.1026
27	H	3.9135	-1.2936	3.7081
28	O	3.6767	-1.9972	3.1308
29	H	4.3351	-2.6575	3.2701
30	H	4.7825	-4.1532	1.3593
31	O	5.2749	-3.4257	1.6995
32	H	4.6945	-2.7114	1.4906
33	H	2.7560	-2.8134	1.7369
34	O	2.9233	-3.3810	1.0030
35	H	2.0901	-3.4800	0.5795

AH4: 4 water

NO.	ATOM	X	Y	Z
1	C	0.0000	0.0000	0.0000
2	C	1.2132	0.9398	0.0906
3	C	2.4967	0.1413	0.3853
4	C	3.7687	0.9744	0.1994
5	C	5.0300	0.1632	0.5318
6	C	6.2925	1.0386	0.5030
7	C	7.5569	0.2485	0.8728
8	C	8.7136	1.1614	1.2310
9	O	8.7064	2.0672	2.0302
10	O	9.8241	0.8773	0.5293
11	H	10.4530	1.5400	0.8584
12	H	7.8292	-0.4360	0.0348
13	H	7.3693	-0.3952	1.7619
14	H	6.1541	1.8824	1.2169

15	H	6.4235	1.4917	-0.5080
16	H	5.1338	-0.6824	-0.1892
17	H	4.9226	-0.2763	1.5511
18	H	3.7109	1.8802	0.8476
19	H	3.8238	1.3185	-0.8597
20	S	2.4993	-1.2312	-0.7647
21	S	0.4929	-1.3558	-1.0603
22	H	2.4439	-0.2694	1.4224
23	H	1.0492	1.7269	0.8645
24	H	1.3285	1.4464	-0.8959
25	H	-0.8944	0.5142	-0.4224
26	H	-0.2529	-0.4077	1.0058
27	H	3.5242	-1.1703	4.5114
28	O	4.2879	-0.7223	4.1937
29	H	3.9670	0.1128	3.8982
30	H	4.7578	2.7545	3.8099
31	O	4.5081	1.8653	3.6316
32	H	5.2800	1.5541	3.1875
33	H	5.8663	0.7632	4.6375
34	O	6.5434	0.3545	4.1231
35	H	6.2350	-0.5332	4.0735
36	H	7.4495	3.4134	3.1508
37	O	6.7917	2.8864	3.5676
38	H	7.1806	2.0268	3.5470

AH5: 5 water

NO.	ATOM	X	Y	Z
1	C	0.0000	0.0000	0.0000
2	C	1.2988	0.7040	0.4249
3	C	2.5309	-0.1197	0.0052
4	C	3.8381	0.6662	0.1358
5	C	5.0422	-0.1415	-0.3715
6	C	6.2926	0.7444	-0.4846
7	C	7.5307	-0.0240	-0.9706
8	C	8.6548	0.9052	-1.3844
9	O	8.6199	2.1114	-1.4367
10	O	9.7482	0.2291	-1.7777
11	H	10.2847	0.9292	-2.1854
12	H	7.2674	-0.6518	-1.8538
13	H	7.8943	-0.7000	-0.1619
14	H	6.5163	1.2116	0.5039

15	H	6.0677	1.5732	-1.1945
16	H	4.7999	-0.5715	-1.3721
17	H	5.2426	-0.9956	0.3171
18	H	4.0002	0.9667	1.1979
19	H	3.7398	1.5989	-0.4654
20	S	2.2580	-0.5590	-1.7095
21	S	0.2273	-0.4868	-1.7078
22	H	2.5790	-1.0603	0.6042
23	H	1.3057	0.8985	1.5237
24	H	1.3347	1.6855	-0.1028
25	H	-0.8869	0.6696	0.0937
26	H	-0.1654	-0.9154	0.6136
27	H	6.0132	1.8452	-3.7644
28	O	6.4210	1.0153	-3.9487
29	H	5.6781	0.4463	-3.8568
30	H	6.4856	3.9507	-3.3773
31	O	5.7941	3.6061	-2.8400
32	H	5.9952	4.0006	-2.0101
33	H	8.3320	3.9249	-2.5767
34	O	8.0492	4.5735	-1.9543
35	H	8.3446	4.2144	-1.1363
36	H	7.8778	2.2342	-4.7366
37	O	8.0377	2.8003	-4.0034
38	H	7.6421	2.3129	-3.3001
39	H	3.1839	1.5697	-3.2949
40	O	4.1222	1.5428	-3.2461
41	H	4.3737	2.3712	-2.8719

AH6: 6 water

NO.	ATOM	X	Y	Z
1	C	0.0000	0.0000	0.0000
2	C	1.3088	0.7489	0.3043
3	C	2.5298	-0.1732	0.1193
4	C	3.8626	0.5835	0.1531
5	C	5.0651	-0.3501	-0.0627
6	C	6.3991	0.3709	0.1768
7	C	7.6206	-0.5542	0.0433
8	C	8.8878	0.0795	0.6059
9	O	8.9326	1.1821	1.1133
10	O	9.9237	-0.8217	0.5904
11	H	10.2868	-0.1736	1.2188
12	H	7.7634	-0.8447	-1.0252
13	H	7.4556	-1.4957	0.6171
14	H	6.3837	0.7983	1.2047

15	H	6.4951	1.2244	-0.5356
16	H	5.0421	-0.7590	-1.1003
17	H	4.9978	-1.2117	0.6408
18	H	3.9503	1.0998	1.1375
19	H	3.8568	1.3692	-0.6389
20	S	2.2975	-0.9649	-1.4704
21	S	0.2680	-0.8741	-1.5397
22	H	2.5115	-0.9634	0.9074
23	H	1.2804	1.1884	1.3299
24	H	1.3972	1.5870	-0.4243
25	H	-0.8632	0.6989	-0.1007
26	H	-0.2235	-0.7424	0.8014
27	H	5.5237	-1.9303	3.4902
28	O	4.8831	-1.2404	3.4184
29	H	5.3978	-0.4787	3.2127
30	H	2.7066	2.7611	3.6535
31	O	3.6346	2.6606	3.5324
32	H	3.7423	1.7238	3.5955
33	H	5.5178	2.0299	4.2674
34	O	5.7933	1.4582	3.5715
35	H	5.4887	1.9153	2.8051
36	H	8.0659	0.5049	2.9431
37	O	7.7579	-0.2885	3.3465
38	H	6.9957	0.0074	3.8155
39	H	2.4104	2.9773	-2.5525
40	O	1.9913	2.2597	-2.9967
41	H	2.3823	1.4844	-2.6302
42	H	1.8593	-0.3794	3.3132
43	O	2.4818	0.2645	3.6048
44	H	3.2607	-0.2314	3.8009

AH7: 7 water

NO.	ATOM	X	Y	Z
1	C	0.0000	0.0000	0.0000
2	C	1.2575	0.8635	0.1995
3	C	2.5185	-0.0188	0.2783
4	C	3.8314	0.7687	0.2071
5	C	5.0523	-0.1640	0.2658
6	C	6.3720	0.6264	0.2897
7	C	7.5957	-0.2779	0.5111
8	C	8.8868	0.4935	0.7699
9	O	8.9396	1.6059	1.2517
10	O	9.9858	-0.2094	0.3283

11	H	10.4421	0.6030	0.6043
12	H	7.7305	-0.9198	-0.3911
13	H	7.4156	-0.9561	1.3786
14	H	6.3075	1.3822	1.1044
15	H	6.4988	1.1856	-0.6682
16	H	5.0456	-0.8581	-0.6085
17	H	4.9781	-0.7894	1.1868
18	H	3.8674	1.4944	1.0540
19	H	3.8620	1.3504	-0.7428
20	S	2.4120	-1.1484	-1.1070
21	S	0.3901	-1.1516	-1.3137
22	H	2.4871	-0.6200	1.2181
23	H	1.1556	1.5033	1.1071
24	H	1.3500	1.5396	-0.6811
25	H	-0.8919	0.6095	-0.2755
26	H	-0.2324	-0.5776	0.9242
27	H	4.0279	-2.4671	3.6610
28	O	4.4643	-1.6487	3.8200
29	H	4.3319	-1.4749	4.7373
30	H	2.7299	0.1254	3.6937
31	O	2.1302	0.8548	3.6574
32	H	1.3818	0.5792	4.1554
33	H	6.4764	1.9170	3.6241
34	O	6.8415	2.6356	3.1327
35	H	7.5413	2.2363	2.6566
36	H	5.4339	0.2560	3.9516
37	O	6.3388	0.0637	3.7685
38	H	6.3270	-0.8748	3.7217
39	H	2.0185	2.5819	-2.9233
40	O	2.3507	1.7636	-3.2542
41	H	2.9649	1.9668	-2.5687
42	H	3.6320	2.1491	3.3704
43	O	4.4846	2.0894	3.7670
44	H	5.0183	2.6792	3.2645
45	H	3.5903	0.6919	6.3211
46	O	3.8005	0.1410	5.5887
47	H	3.8538	0.7476	4.8704

AH8: 8 water

NO.	ATOM	X	Y	Z
1	C	0.0000	0.0000	0.0000
2	C	1.2460	0.8968	-0.0441
3	C	2.5219	0.0411	0.0370

4	C	3.7937	0.8471	-0.2428
5	C	5.0534	-0.0088	-0.0498
6	C	6.3463	0.7987	-0.2503
7	C	7.5940	-0.0504	0.0407
8	C	8.9026	0.7056	-0.1476
9	O	8.9860	1.8480	-0.5460
10	O	9.9719	-0.0657	0.2496
11	H	10.4498	0.7590	0.0457
12	H	7.5980	-0.9398	-0.6332
13	H	7.5527	-0.4189	1.0932
14	H	6.3408	1.6868	0.4252
15	H	6.3819	1.1742	-1.3005
16	H	5.0316	-0.8614	-0.7699
17	H	5.0466	-0.4378	0.9795
18	H	3.8283	1.7308	0.4365
19	H	3.7549	1.2212	-1.2918
20	S	2.3224	-1.2419	-1.1958
21	S	0.2915	-1.3159	-1.1787
22	H	2.5709	-0.4468	1.0392
23	H	1.2145	1.6569	0.7724
24	H	1.2506	1.4317	-1.0214
25	H	-0.9246	0.5596	-0.2713
26	H	-0.1179	-0.4398	1.0169
27	H	3.7743	-3.1140	3.3501
28	O	4.6192	-3.0615	3.7602
29	H	4.4249	-2.5373	4.5200
30	H	2.7331	1.4947	3.3926
31	O	3.5803	1.1460	3.1695
32	H	4.0481	1.8810	2.8163
33	H	6.9237	0.8689	3.3369
34	O	6.2208	1.4928	3.2914
35	H	5.4872	0.9669	3.5626
36	H	6.0229	-1.7308	4.0571
37	O	5.9455	-0.9290	3.5706
38	H	5.4405	-1.1969	2.8215
39	H	1.6406	1.9206	-3.6962
40	O	2.2560	2.5168	-3.3044
41	H	2.6721	2.9595	-4.0240
42	H	0.1732	0.7093	4.0920
43	O	1.0443	0.6785	3.7386
44	H	1.0843	-0.1048	3.2151
45	H	5.3424	3.1563	3.4490
46	O	4.5910	3.6263	3.1268
47	H	4.9140	4.4852	2.9227
48	H	2.6393	-0.3739	4.3338
49	O	3.1281	-1.1152	4.0266

50	H	3.8335	-0.6765	3.5794

AH9: 9 water

NO.	ATOM	X	Y	Z
1	C	0.0000	0.0000	0.0000
2	C	1.2661	0.8166	0.3041
3	C	2.5276	-0.0302	0.0586
4	C	3.8195	0.7916	0.0824
5	C	5.0543	-0.1034	-0.0993
6	C	6.3515	0.7199	-0.1118
7	C	7.5988	-0.1765	-0.1536
8	C	8.8859	0.6119	-0.0111
9	O	8.9982	1.7697	0.2988
10	O	9.9712	-0.1391	-0.2642
11	H	10.6998	0.4901	-0.1274
12	H	7.6167	-0.7434	-1.1139
13	H	7.5652	-0.9134	0.6828
14	H	6.3827	1.3595	0.8007
15	H	6.3511	1.4049	-0.9927
16	H	4.9646	-0.6842	-1.0484
17	H	5.0976	-0.8405	0.7368
18	H	3.8963	1.3425	1.0487
19	H	3.7793	1.5476	-0.7353
20	S	2.3098	-0.7801	-1.5533
21	S	0.2780	-0.7825	-1.5858
22	H	2.5718	-0.8468	0.8169
23	H	1.2436	1.2058	1.3491
24	H	1.2882	1.6888	-0.3890
25	H	-0.9085	0.6439	-0.0420
26	H	-0.1507	-0.7927	0.7685
27	H	3.2350	-1.7161	2.7355
28	O	3.9908	-1.3451	3.1533
29	H	4.6493	-1.9681	2.8969
30	H	4.1597	0.6519	3.2512
31	O	3.3653	0.9436	3.6647
32	H	3.0646	0.1359	4.0426
33	H	6.5406	0.5189	2.6510
34	O	6.2451	0.8873	3.4680
35	H	6.4299	1.8085	3.4106
36	H	7.1773	-1.2335	3.8339
37	O	6.4327	-1.5038	3.3275
38	H	5.7556	-0.9236	3.6432
39	H	2.5886	1.1203	-3.5831

40	O	2.2243	1.9338	-3.2712
41	H	2.2147	1.8453	-2.3349
42	H	3.0201	3.7412	3.3031
43	O	2.5217	3.3096	2.6281
44	H	2.4266	2.4268	2.9401
45	H	3.4011	-3.4616	0.8081
46	O	3.7206	-3.3066	1.6802
47	H	4.0582	-4.1349	1.9773
48	H	5.4647	0.9866	-3.4053
49	O	4.5238	1.0180	-3.3808
50	H	4.2996	1.9350	-3.3884
51	H	4.3800	2.8472	2.7252
52	O	4.8685	3.0386	3.5086
53	H	4.7421	2.2597	4.0269

AH10: 10 water

NO.	ATOM	X	Y	Z
1	C	0.0000	0.0000	0.0000
2	C	1.3301	0.7692	-0.0474
3	C	2.5187	-0.1743	0.2326
4	C	3.8816	0.4858	-0.0238
5	C	5.0887	-0.3821	0.3773
6	C	6.3986	0.4339	0.3434
7	C	7.6400	-0.4041	0.7053
8	C	8.8981	0.4343	0.9253
9	O	8.9667	1.3548	1.6996
10	O	9.8773	0.1157	0.0422
11	H	10.5170	0.8546	0.0734
12	H	7.8289	-1.1883	-0.0667
13	H	7.4441	-0.9310	1.6653
14	H	6.3058	1.2519	1.0962
15	H	6.5352	0.8978	-0.6647
16	H	5.1632	-1.2643	-0.3008
17	H	4.9203	-0.7866	1.4021
18	H	3.9221	1.4502	0.5360
19	H	3.9585	0.7184	-1.1117
20	S	2.2762	-1.5605	-0.8758
21	S	0.2485	-1.4745	-0.9848
22	H	2.4524	-0.5433	1.2845
23	H	1.3232	1.6329	0.6583
24	H	1.4487	1.1753	-1.0773
25	H	-0.8464	0.5966	-0.4121
26	H	-0.2434	-0.3010	1.0445

27	H	5.6667	-2.9988	2.6718
28	O	4.7717	-3.1943	2.8904
29	H	4.7582	-2.9948	3.8092
30	H	2.8226	1.1387	2.8281
31	O	2.1877	1.6698	3.2789
32	H	2.2707	1.3828	4.1711
33	H	4.7084	-4.6006	1.1747
34	O	4.4065	-3.9576	0.5563
35	H	4.0360	-3.3012	1.1209
36	H	6.7709	4.0379	2.8865
37	O	6.9593	3.1196	2.9700
38	H	7.5446	2.9155	2.2643
39	H	6.6588	1.3471	4.4038
40	O	6.9390	0.6617	3.8242
41	H	7.4425	1.1302	3.1802
42	H	1.9011	2.1442	-2.8488
43	O	2.6632	1.9947	-3.3810
44	H	3.2405	2.7149	-3.1925
45	H	2.8037	3.1581	1.9624
46	O	3.6206	3.5324	2.2487
47	H	3.4750	3.6129	3.1757
48	H	4.1204	1.9013	3.9157
49	O	4.8093	2.2692	4.4448
50	H	5.4159	2.6067	3.8179
51	H	4.7625	-0.0149	4.1834
52	O	3.9219	-0.2736	3.8390
53	H	4.5069	-0.8827	3.4289
54	H	6.4105	-1.0876	3.2599
55	O	6.2944	-1.6463	4.0084
56	H	6.7896	-1.1688	4.6477

AH11: 20 water

NO.	ATOM	X	Y	Z
1	C	0.0000	0.0000	0.0000
2	C	1.1070	1.0658	-0.0460
3	C	2.4705	0.4097	0.2334
4	C	3.6582	1.3385	-0.0204
5	C	4.9760	0.6605	0.3681
6	C	6.1885	1.5925	0.3099
7	C	7.4761	0.7769	0.4857
8	C	8.6929	1.6249	0.8028
9	O	8.6406	2.8011	1.0691
10	O	9.8400	0.8643	0.7467

11	H	10.2286	1.7268	0.9617
12	H	7.6632	0.1686	-0.4302
13	H	7.3624	0.0901	1.3523
14	H	6.0949	2.3545	1.1169
15	H	6.2073	2.1453	-0.6576
16	H	5.1677	-0.2061	-0.2976
17	H	4.9020	0.2523	1.4000
18	H	3.5246	2.2851	0.5513
19	H	3.6703	1.5958	-1.1018
20	S	2.5635	-0.9951	-0.8728
21	S	0.5686	-1.3421	-1.0402
22	H	2.4899	0.0334	1.2832
23	H	0.8952	1.8913	0.6744
24	H	1.1291	1.5003	-1.0727
25	H	-0.9749	0.3953	-0.3679
26	H	-0.1295	-0.3847	1.0381
27	H	6.0400	-2.9520	1.3583
28	O	6.5687	-2.3952	0.8100
29	H	7.4141	-2.4509	1.2231
30	H	3.7035	-2.8730	1.5169
31	O	4.2693	-2.3521	2.0609
32	H	4.6506	-1.7835	1.4121
33	H	5.1421	-2.2833	-0.3885
34	O	4.2373	-2.5440	-0.4025
35	H	3.9742	-2.2886	-1.2695
36	H	5.7057	3.2333	4.5632
37	O	5.1495	3.9564	4.3178
38	H	5.1991	3.9790	3.3738
39	H	7.6231	2.2016	2.8634
40	O	7.1031	2.3129	3.6388
41	H	7.5311	1.7131	4.2258
42	H	6.2666	1.7066	-2.7302
43	O	6.7755	0.9398	-2.9287
44	H	7.6367	1.1841	-2.6370
45	H	6.7790	4.3290	3.2837
46	O	6.6904	4.6782	2.4101
47	H	7.4798	4.3906	1.9823
48	H	5.1750	-0.3548	-2.7721
49	O	4.4213	-0.8754	-2.5429
50	H	3.7323	-0.4438	-3.0168
51	H	5.3148	1.3336	-4.2044
52	O	5.0686	0.5504	-4.6695
53	H	5.8544	0.0352	-4.6079
54	H	3.7065	2.5070	-2.8512
55	O	4.5710	2.7214	-3.1639
56	H	4.6747	3.6064	-2.8591

57	H	7.1235	-1.8989	3.9581
58	O	7.3083	-2.0046	3.0412
59	H	6.6804	-1.4076	2.6637
60	H	4.1631	1.6199	6.1563
61	O	4.6053	1.3254	5.3812
62	H	3.9384	0.8820	4.8859
63	H	7.9886	-0.2633	3.6031
64	O	8.6831	0.3744	3.5809
65	H	9.4199	-0.1050	3.2474
66	H	3.7402	2.5122	3.7082
67	O	4.2290	2.0834	3.0266
68	H	5.0858	2.0239	3.4095
69	H	4.0197	-0.0897	3.1988
70	O	3.4871	-0.5150	3.8534
71	H	3.1287	-1.2557	3.4015
72	H	3.4776	1.3929	-4.2101
73	O	2.7077	1.1223	-3.7334
74	H	2.3822	0.4022	-4.2431
75	H	5.8740	0.7886	4.1043
76	O	5.9957	-0.1256	3.9182
77	H	5.4078	-0.5378	4.5306
78	H	3.1089	5.0885	-1.1481
79	O	3.7637	4.4872	-1.4576
80	H	4.0829	4.0608	-0.6811
81	H	5.7225	-3.1632	3.8194
82	O	5.3115	-2.6424	4.4907
83	H	4.5716	-2.2659	4.0390
84	H	8.3242	3.1826	-0.9983
85	O	8.4838	2.7063	-1.7948
86	H	9.1452	3.2011	-2.2415

Appendix I: DHLA Explicitly Solvated by Water

AI1: 1 water

NO.	ATOM	X	Y	Z
1	C	0.0000	0.0000	0.0000
2	C	1.2736	0.7280	-0.4751
3	C	2.6027	-0.0464	-0.3259
4	C	3.8118	0.9070	-0.4403
5	C	5.1611	0.2311	-0.1398
6	C	6.3277	1.2303	-0.1906
7	C	7.6654	0.5421	0.1169
8	C	8.8306	1.5074	0.1817
9	O	8.8337	2.6845	-0.0867
10	O	9.9539	0.9022	0.6041
11	H	10.5987	1.6291	0.5872
12	H	7.8853	-0.2203	-0.6666
13	H	7.5890	0.0187	1.0984
14	H	6.1492	2.0439	0.5529
15	H	6.3698	1.7003	-1.2024
16	H	5.3626	-0.5862	-0.8691
17	H	5.1198	-0.2395	0.8707
18	H	3.6869	1.7325	0.2998
19	H	3.8349	1.3892	-1.4460
20	S	2.7488	-1.3224	-1.6353
21	H	1.9975	-2.2742	-1.0556
22	H	2.6406	-0.5168	0.6854
23	H	1.3631	1.6252	0.1830
24	H	1.1565	1.1408	-1.5054
25	S	-0.7117	-1.0758	-1.2978
26	H	-1.0444	-0.1169	-2.1816
27	H	-0.7730	0.7529	0.2841
28	H	0.2205	-0.5927	0.9171
29	H	4.8031	-1.2816	-3.2839
30	O	5.1343	-0.4397	-3.5471
31	H	4.4895	0.1699	-3.2322

AI2: 2 water

NO.	ATOM	X	Y	Z
1	C	0.0000	0.0000	0.0000

2	C	1.2401	0.6274	-0.6672
3	C	2.5690	-0.1524	-0.5446
4	C	3.7821	0.7952	-0.6912
5	C	5.1383	0.1269	-0.3968
6	C	6.2962	1.1401	-0.3516
7	C	7.6355	0.4596	-0.0206
8	C	8.7943	1.4349	0.0998
9	O	8.7535	2.6139	-0.1665
10	O	9.8997	0.8068	0.5564
11	H	9.6981	-0.1360	0.6684
12	H	7.8881	-0.2796	-0.8166
13	H	7.5391	-0.0911	0.9443
14	H	6.0826	1.9160	0.4225
15	H	6.3704	1.6593	-1.3370
16	H	5.3656	-0.6415	-1.1722
17	H	5.0797	-0.4037	0.5822
18	H	3.6661	1.6343	0.0346
19	H	3.7934	1.2589	-1.7064
20	S	2.6843	-1.4309	-1.8625
21	H	2.0424	-2.4329	-1.2364
22	H	2.6219	-0.6238	0.4651
23	H	1.3875	1.5943	-0.1301
24	H	1.0375	0.9164	-1.7256
25	S	-0.7127	-1.3587	-0.9861
26	H	-1.0797	-0.6264	-2.0535
27	H	-0.7873	0.7814	0.1213
28	H	0.2566	-0.3574	1.0240
29	H	4.5111	0.2177	2.7751
30	O	5.3008	0.6620	3.0334
31	H	5.0339	1.5632	2.9757
32	H	2.4985	1.4871	3.4989
33	O	2.9273	1.3352	2.6745
34	H	2.3421	1.6791	2.0232

AI3: 3 water

NO.	ATOM	X	Y	Z
1	C	0.0000	0.0000	0.0000
2	C	1.4210	0.6000	-0.1170
3	C	2.6860	-0.1590	0.3530
4	C	3.9260	0.7930	0.3200
5	C	5.3090	0.1230	0.4680
6	C	6.4750	1.1240	0.5160
7	C	7.8290	0.3980	0.5120

8	C	9.0050	1.3490	0.5440
9	O	8.9300	2.5680	0.5460
10	O	10.1940	0.7010	0.5690
11	H	10.1170	-0.2720	0.5600
12	H	7.9200	-0.2100	-0.3960
13	H	7.8990	-0.2570	1.3880
14	H	6.3940	1.7500	1.4120
15	H	6.4240	1.7970	-0.3480
16	H	5.4900	-0.5370	-0.3870
17	H	5.3240	-0.4950	1.3730
18	H	3.8070	1.5360	1.1210
19	H	3.9180	1.3610	-0.6200
20	S	2.9880	-1.6240	-0.7070
21	H	1.8150	-2.2270	-0.4440
22	H	2.5420	-0.5040	1.3840
23	H	1.3810	1.5550	0.4270
24	H	1.5650	0.8930	-1.1670
25	S	-0.2580	-1.7880	0.1710
26	H	-1.1110	-1.9300	-0.8580
27	H	-0.5750	0.3200	-0.8770
28	H	-0.5040	0.4530	0.8610
29	H	5.0280	-2.6120	4.2830
30	O	4.0350	-2.6770	4.3840
31	H	3.6740	-1.8020	4.7060
32	H	4.8090	-2.8000	1.7370
33	O	4.1110	-2.2570	2.2040
34	H	3.2720	-2.7920	2.2870
35	H	2.4100	2.2890	4.3840
36	O	2.2800	1.3310	4.6410
37	H	2.1660	0.7770	3.8170

AI4: 4 water

NO.	ATOM	X	Y	Z
1	C	0.0000	0.0000	0.0000
2	C	1.1770	0.3294	-0.9380
3	C	2.4911	-0.4326	-0.6515
4	C	3.7230	0.4572	-0.9224
5	C	5.0632	-0.1870	-0.5259
6	C	6.2260	0.8168	-0.6179
7	C	7.5633	0.1573	-0.2460
8	C	8.7312	1.1274	-0.2340
9	O	8.6952	2.2866	-0.5860
10	O	9.8407	0.5134	0.2291

11	H	9.6012	-0.3955	0.4780
12	H	7.7998	-0.6515	-0.9780
13	H	7.4813	-0.2993	0.7693
14	H	6.0306	1.6738	0.0723
15	H	6.2830	1.2255	-1.6559
16	H	5.2847	-1.0589	-1.1864
17	H	4.9964	-0.5647	0.5219
18	H	3.6188	1.3916	-0.3203
19	H	3.7484	0.7654	-1.9949
20	S	2.5953	-1.9302	-1.7156
21	H	2.0420	-2.8208	-0.8725
22	H	2.5210	-0.7217	0.4245
23	H	1.3755	1.4158	-0.7804
24	H	0.8783	0.2581	-2.0112
25	S	-0.6872	-1.6600	-0.3163
26	H	-1.0832	-1.4451	-1.5836
27	H	-0.8069	0.7586	-0.1332
28	H	0.3259	0.0689	1.0627
29	H	1.4047	-1.3624	2.8946
30	O	2.1400	-0.8015	3.0614
31	H	1.7990	0.0768	3.0016
32	H	4.6600	1.1196	4.0752
33	O	3.7629	1.2626	3.8331
34	H	3.5989	0.5774	3.2013
35	H	3.9397	-1.0852	3.8432
36	O	4.5831	-1.1182	3.1549
37	H	4.0411	-1.2904	2.4032
38	H	2.3353	2.0528	2.9721
39	O	1.9791	1.8389	2.1269
40	H	2.4290	2.4225	1.5410

AI5: 5 water

NO.	ATOM	X	Y	Z
1	C	0.0000	0.0000	0.0000
2	C	1.2344	0.9221	-0.0309
3	C	2.6263	0.2482	-0.0073
4	C	3.7264	1.2935	0.2713
5	C	5.1600	0.7463	0.4369
6	C	6.1393	1.9275	0.4827
7	C	7.6236	1.5531	0.5478
8	C	8.4878	2.7960	0.4113
9	O	8.0642	3.9124	0.2117
10	O	9.7913	2.4785	0.5720

11	H	9.8805	1.5101	0.6385
12	H	7.8764	0.8628	-0.2895
13	H	7.8556	1.0443	1.5129
14	H	5.8780	2.5916	1.3410
15	H	5.9927	2.5061	-0.4567
16	H	5.4571	0.0895	-0.4128
17	H	5.2380	0.1334	1.3653
18	H	3.4789	1.8555	1.2038
19	H	3.7115	2.0475	-0.5488
20	S	3.0115	-0.5070	-1.6370
21	H	2.5278	-1.7404	-1.4214
22	H	2.6482	-0.5100	0.8103
23	H	1.1684	1.5235	0.9090
24	H	1.1626	1.6659	-0.8610
25	S	-0.3467	-0.7779	-1.6164
26	H	-0.5041	0.3498	-2.3333
27	H	-0.8981	0.6003	0.2798
28	H	0.1316	-0.7792	0.7851
29	H	2.1238	0.9458	-3.2870
30	O	1.8708	1.7439	-3.7190
31	H	2.5167	1.8189	-4.4011
32	H	3.3348	4.2447	-2.0670
33	O	3.5548	3.5184	-2.6294
34	H	2.6816	3.2453	-2.8277
35	H	5.7108	4.5910	-0.3896
36	O	4.8631	4.6557	-0.8116
37	H	4.9869	4.2368	-1.6518
38	H	4.1007	1.5253	-2.8284
39	O	4.5752	1.4795	-3.6437
40	H	4.8042	2.3877	-3.7647
41	H	1.1830	5.3041	-1.5497
42	O	1.3930	4.4986	-1.9878
43	H	0.5689	4.1433	-2.2644

AI6: 6 water

NO.	ATOM	X	Y	Z
1	C	0.0000	0.0000	0.0000
2	C	1.5244	0.1020	-0.2217
3	C	2.3790	-0.9133	0.5635
4	C	2.2436	-0.8680	2.1034
5	C	2.1761	0.5042	2.8011
6	C	3.5028	1.2792	2.8548
7	C	4.6916	0.5814	3.5423

8	C	4.5154	0.1996	4.9954
9	O	3.6387	0.5688	5.7328
10	O	5.5053	-0.6430	5.3756
11	H	6.0910	-0.8027	4.6191
12	H	5.5728	1.2668	3.5272
13	H	4.9708	-0.3452	2.9897
14	H	3.3338	2.2771	3.3222
15	H	3.8031	1.5099	1.8102
16	H	1.7978	0.3718	3.8426
17	H	1.4047	1.1446	2.3144
18	H	3.0560	-1.4695	2.5728
19	H	1.3076	-1.4165	2.3715
20	S	4.1581	-0.7927	0.0703
21	H	4.2945	0.5370	-0.0632
22	H	2.0770	-1.9374	0.2377
23	H	1.8495	1.1278	0.0734
24	H	1.7441	0.0199	-1.3145
25	S	-0.6708	-1.5575	-0.6921
26	H	-0.4211	-1.3162	-1.9925
27	H	-0.5080	0.8690	-0.4822
28	H	-0.2440	0.0573	1.0855
29	H	3.4676	-1.5223	6.3734
30	O	2.6735	-1.8617	5.9939
31	H	2.3195	-1.1236	5.5280
32	H	1.3652	2.6688	4.4057
33	O	1.2786	3.5887	4.2101
34	H	0.9201	3.9384	5.0077
35	H	4.2356	2.7129	6.3392
36	O	4.5412	3.3384	5.6888
37	H	3.9195	4.0541	5.7289
38	H	8.1339	0.7301	5.1584
39	O	8.0168	0.1523	4.4242
40	H	8.8318	0.1804	3.9540
41	H	0.9205	3.7288	-1.3062
42	O	1.4691	3.1096	-1.7651
43	H	0.9764	2.8639	-2.5317
44	H	2.3529	1.8317	6.7856
45	O	2.2143	2.6140	6.2817
46	H	2.7021	2.4818	5.4823

AI7: 7 water

NO.	ATOM	X	Y	Z
1	C	0.0000	0.0000	0.0000

2	C	1.2778	0.0479	-0.8585
3	C	2.5510	-0.5652	-0.2415
4	C	3.8225	0.1526	-0.7417
5	C	5.0959	-0.2802	0.0018
6	C	6.2914	0.6435	-0.2718
7	C	7.5190	0.2208	0.5518
8	C	8.4684	1.3674	0.8294
9	O	8.1472	2.5381	0.8106
10	O	9.6878	0.9178	1.1936
11	H	9.7344	-0.0451	1.0484
12	H	8.0382	-0.6234	0.0412
13	H	7.2180	-0.1376	1.5611
14	H	5.9949	1.6880	-0.0199
15	H	6.5427	0.6461	-1.3597
16	H	5.3748	-1.3302	-0.2445
17	H	4.8915	-0.2663	1.0930
18	H	3.6986	1.2494	-0.5787
19	H	3.9494	0.0098	-1.8401
20	S	2.6633	-2.3444	-0.6947
21	H	2.9537	-2.8428	0.5210
22	H	2.4960	-0.4384	0.8632
23	H	1.4800	1.1358	-0.9965
24	H	1.0936	-0.3584	-1.8807
25	S	-0.6311	-1.6959	0.2499
26	H	-0.7931	-2.0278	-1.0456
27	H	-0.7946	0.6057	-0.4974
28	H	0.1898	0.4787	0.9884
29	H	4.9368	-2.3624	2.4111
30	O	4.1190	-2.5199	2.8489
31	H	4.3680	-2.3368	3.7397
32	H	1.4974	-1.3321	3.7630
33	O	1.3452	-0.5308	3.2923
34	H	0.4597	-0.6026	2.9770
35	H	6.4819	2.1808	3.3009
36	O	6.1180	1.3351	3.5029
37	H	5.1985	1.5241	3.6228
38	H	5.4279	-0.3967	3.3669
39	O	6.0432	-1.0657	3.6013
40	H	6.7256	-0.5193	3.9520
41	H	1.6732	2.8994	-3.9651
42	O	1.4025	2.1587	-3.4507
43	H	1.3465	1.4420	-4.0585
44	H	5.7294	2.6538	1.5331
45	O	4.9318	2.7328	2.0361
46	H	4.6152	1.8458	2.1233
47	H	2.9385	0.6999	3.2287

48	O	3.7352	0.2314	3.0558
49	H	3.4056	-0.6327	2.8796

AI8: 8 water

NO.	ATOM	X	Y	Z
1	C	0.0000	0.0000	0.0000
2	C	1.3004	0.6417	-0.5208
3	C	2.6152	-0.0030	-0.0331
4	C	3.8247	0.8792	-0.4055
5	C	5.1702	0.3543	0.1241
6	C	6.2970	1.3826	-0.0633
7	C	7.6520	0.8435	0.4195
8	C	8.7825	1.8387	0.2387
9	O	8.6639	2.9751	-0.1674
10	O	9.9618	1.2860	0.5899
11	H	9.8047	0.3762	0.8922
12	H	7.9043	-0.0850	-0.1452
13	H	7.5883	0.5846	1.5022
14	H	6.0492	2.3142	0.4992
15	H	6.3690	1.6515	-1.1439
16	H	5.4516	-0.5865	-0.4036
17	H	5.0712	0.1048	1.2051
18	H	3.6629	1.8949	0.0269
19	H	3.8825	1.0135	-1.5117
20	S	2.8357	-1.6662	-0.7746
21	H	1.9582	-2.3419	-0.0110
22	H	2.5864	-0.0896	1.0783
23	H	1.3054	1.6895	-0.1372
24	H	1.2943	0.7427	-1.6315
25	S	-0.6486	-1.2514	-1.1670
26	H	-0.8998	-0.4266	-2.2005
27	H	-0.7798	0.7843	0.1439
28	H	0.1698	-0.4553	1.0019
29	H	4.9843	-2.5582	3.4941
30	O	4.6644	-1.6925	3.6738
31	H	5.3582	-1.3180	4.1943
32	H	1.2245	2.6378	2.4739
33	O	2.1557	2.5002	2.4746
34	H	2.2190	1.5633	2.5745
35	H	5.9749	1.4252	3.7085
36	O	5.8567	0.4934	3.7142
37	H	5.0889	0.4075	3.1729
38	H	7.3246	-0.8484	3.9927

39	O	7.1749	-1.6027	3.4481
40	H	6.5433	-1.2669	2.8325
41	H	1.4244	3.3980	-3.4859
42	O	1.8464	3.2590	-2.6550
43	H	2.5376	3.0727	-3.2667
44	H	1.2892	1.1205	3.8673
45	O	0.4876	1.0200	3.3779
46	H	0.2471	0.1219	3.5132
47	H	4.0913	2.9056	2.2179
48	O	4.5561	2.3959	2.8569
49	H	3.8368	2.0589	3.3631
50	H	3.5806	-0.1270	4.3566
51	O	3.0662	0.1501	3.6182
52	H	3.1721	-0.5930	3.0477

AI9: 9 water

NO.	ATOM	X	Y	Z
1	C	0.0000	0.0000	0.0000
2	C	1.2550	0.4852	-0.7488
3	C	2.5212	-0.3847	-0.5802
4	C	3.7876	0.4940	-0.5282
5	C	5.1029	-0.2806	-0.3471
6	C	6.2796	0.6477	-0.0064
7	C	7.6142	-0.1172	0.0397
8	C	8.6540	0.5483	0.9246
9	O	8.4014	1.2517	1.8735
10	O	9.9097	0.2513	0.5297
11	H	9.8658	-0.3432	-0.2385
12	H	8.0011	-0.2376	-0.9993
13	H	7.4616	-1.1389	0.4526
14	H	6.0547	1.1255	0.9754
15	H	6.3623	1.4700	-0.7586
16	H	5.3595	-0.8474	-1.2715
17	H	4.9699	-1.0194	0.4770
18	H	3.6814	1.1888	0.3384
19	H	3.8566	1.1369	-1.4378
20	S	2.6398	-1.5364	-2.0141
21	H	3.4284	-2.4748	-1.4618
22	H	2.4448	-0.9505	0.3786
23	H	1.4697	1.5044	-0.3481
24	H	1.0266	0.6511	-1.8281
25	S	-0.4860	-1.6944	-0.4700
26	H	-0.7167	-1.4524	-1.7714

27	H	-0.8418	0.7032	-0.1988
28	H	0.1850	0.0245	1.0962
29	H	5.3062	-1.3213	3.4845
30	O	5.3109	-2.2471	3.2988
31	H	4.5560	-2.5462	3.7728
32	H	1.1086	0.2815	3.1548
33	O	1.1681	-0.6442	3.3188
34	H	0.3339	-0.9950	3.0628
35	H	7.4353	-0.3299	2.9901
36	O	6.6544	0.0485	3.3535
37	H	6.8045	0.9716	3.2472
38	H	7.3267	-2.0028	3.5550
39	O	7.7461	-2.2781	2.7564
40	H	7.0175	-2.6830	2.3168
41	H	2.0967	1.7015	-4.4698
42	O	2.6252	0.9865	-4.1619
43	H	2.0198	0.3005	-3.9374
44	H	2.7895	1.7674	2.2808
45	O	1.9403	1.8732	2.6722
46	H	1.8597	2.7998	2.8114
47	H	2.6121	-0.8259	4.7028
48	O	3.4194	-0.8901	4.2258
49	H	3.1057	-0.8864	3.3371
50	H	4.1982	-0.1148	-3.3894
51	O	4.9638	0.2319	-3.8163
52	H	4.5764	0.9057	-4.3487
53	H	3.5873	1.1369	3.8423
54	O	4.3387	1.3450	3.3100
55	H	4.9174	0.6308	3.5109

AI10: 10 water

NO.	ATOM	X	Y	Z
1	C	0.0000	0.0000	0.0000
2	C	1.1450	0.0642	-1.0287
3	C	2.4870	-0.5628	-0.5798
4	C	3.6884	0.3848	-0.8012
5	C	5.0325	-0.1815	-0.3012
6	C	6.1776	0.8459	-0.3469
7	C	7.5211	0.2345	0.0880
8	C	8.5983	1.2658	0.3975
9	O	8.4316	2.4459	0.6342
10	O	9.8202	0.7105	0.3169
11	H	9.7116	-0.2391	0.1459

12	H	7.8793	-0.4362	-0.7289
13	H	7.3736	-0.4198	0.9789
14	H	5.9104	1.7029	0.3129
15	H	6.2823	1.2542	-1.3806
16	H	5.3310	-1.0698	-0.9044
17	H	4.9066	-0.5282	0.7500
18	H	3.4945	1.3333	-0.2450
19	H	3.7756	0.6557	-1.8804
20	S	2.7808	-2.1176	-1.5274
21	H	1.9884	-2.9431	-0.8207
22	H	2.4516	-0.7764	0.5130
23	H	1.3123	1.1482	-1.2334
24	H	0.8029	-0.3534	-2.0057
25	S	-0.3487	-1.7122	0.5351
26	H	-0.7603	-2.1948	-0.6512
27	H	-0.9223	0.4501	-0.4367
28	H	0.2672	0.6246	0.8836
29	H	5.3462	-2.5536	2.5813
30	O	5.5312	-3.3645	3.0308
31	H	6.1192	-3.0602	3.6995
32	H	0.7006	-0.9829	2.7491
33	O	1.3913	-0.4061	3.0227
34	H	1.9714	-0.9810	3.4937
35	H	4.5137	-3.3341	-0.0241
36	O	4.2837	-3.3204	0.8900
37	H	4.8619	-3.9330	1.3153
38	H	6.1427	1.8954	3.2020
39	O	6.8431	1.4138	2.8079
40	H	7.0886	2.0224	2.1404
41	H	5.9442	-0.4913	2.6394
42	O	6.3059	-1.0719	3.2891
43	H	6.8733	-0.4830	3.7535
44	H	1.7660	2.9730	-3.9960
45	O	1.7202	2.0516	-3.8073
46	H	2.3639	1.6482	-4.3646
47	H	2.7031	1.3970	3.3153
48	O	2.2984	1.9376	2.6601
49	H	1.4709	1.5047	2.5517
50	H	4.2877	1.7880	2.3397
51	O	4.6034	2.6667	2.4690
52	H	3.7970	3.1525	2.4739
53	H	3.6018	-3.1063	2.8973
54	O	3.0228	-2.3734	2.7836
55	H	2.9178	-2.3703	1.8458
56	H	3.2937	-0.2690	2.5976
57	O	4.0320	0.0518	3.0884

58	H	4.3812	-0.7337	3.4704

AI11: 20 water

NO.	ATOM	X	Y	Z
1	C	0.0000	0.0000	0.0000
2	C	1.0744	0.8242	-0.7360
3	C	2.5267	0.2914	-0.6750
4	C	3.5406	1.4566	-0.6068
5	C	5.0263	1.0546	-0.5726
6	C	5.9593	2.2548	-0.3383
7	C	7.4377	1.8397	-0.2629
8	C	8.3749	2.9664	0.1232
9	O	8.1040	4.1514	0.1168
10	O	9.5673	2.4691	0.5126
11	H	9.5167	1.5013	0.4878
12	H	7.7814	1.4306	-1.2419
13	H	7.5427	1.0252	0.4888
14	H	5.6691	2.7491	0.6164
15	H	5.8266	2.9979	-1.1588
16	H	5.3202	0.5641	-1.5280
17	H	5.1832	0.3090	0.2379
18	H	3.3294	2.0391	0.3187
19	H	3.3692	2.1599	-1.4515
20	S	2.8878	-0.7225	-2.1681
21	H	2.5559	-1.9303	-1.6829
22	H	2.6590	-0.3259	0.2424
23	H	1.0620	1.8166	-0.2276
24	H	0.7640	1.0592	-1.7819
25	S	-0.2992	-1.6163	-0.7832
26	H	-0.6712	-1.1421	-1.9849
27	H	-0.9609	0.5673	0.0090
28	H	0.2953	-0.1376	1.0648
29	H	8.2525	-0.8016	2.3312
30	O	7.7965	-1.3012	1.6756
31	H	6.8977	-1.0966	1.8793
32	H	4.5218	0.1820	2.3022
33	O	4.9843	-0.6036	2.5480
34	H	5.5693	-0.2860	3.2156
35	H	3.2452	-1.6813	2.1979
36	O	2.3646	-1.8699	2.4796
37	H	2.2283	-2.7210	2.1067
38	H	4.0556	4.5014	4.1870
39	O	4.8983	4.5030	3.7636

40	H	4.6806	4.1837	2.9010
41	H	7.3614	3.8560	2.1219
42	O	7.2283	3.1902	2.7758
43	H	6.3224	3.3137	3.0121
44	H	6.1234	2.6843	-3.4905
45	O	6.8304	2.1519	-3.8143
46	H	7.6066	2.6130	-3.5556
47	H	5.9660	5.5157	2.4572
48	O	5.9037	5.1284	1.6000
49	H	6.6790	5.3949	1.1372
50	H	5.1262	1.1348	-3.7430
51	O	4.4043	1.7379	-3.7449
52	H	3.6687	1.2089	-3.4844
53	H	5.9863	0.9340	-5.3290
54	O	6.1607	0.1016	-4.9217
55	H	6.8363	0.3273	-4.3038
56	H	3.8083	3.5316	-3.8876
57	O	3.2894	3.9916	-3.2527
58	H	2.6740	3.3247	-3.0000
59	H	7.1144	-1.9742	0.0750
60	O	6.3704	-2.3246	-0.3835
61	H	6.7332	-2.8723	-1.0574
62	H	2.1439	2.2379	3.9302
63	O	2.5949	3.0599	3.8339
64	H	2.4477	3.2995	2.9338
65	H	6.4812	1.2875	2.9179
66	O	7.2100	0.7459	3.1675
67	H	7.8571	1.4109	3.3299
68	H	4.1949	4.5406	1.2510
69	O	3.3876	4.2438	1.6317
70	H	2.7712	4.5285	0.9847
71	H	1.8785	0.1255	2.4167
72	O	2.6139	0.5274	2.8406
73	H	3.0026	-0.2141	3.2763
74	H	1.1957	2.0820	-4.7667
75	O	1.9491	1.7948	-4.2811
76	H	2.6519	1.7391	-4.9098
77	H	3.8929	1.9540	2.7421
78	O	4.7857	1.9993	3.0391
79	H	4.7002	2.5428	3.8038
80	H	3.0104	5.1707	-1.7193
81	O	3.3215	4.8734	-0.8803
82	H	4.0253	4.3080	-1.1455
83	H	4.9513	-2.1972	1.2224
84	O	4.1759	-2.5052	0.7798
85	H	4.5149	-2.6788	-0.0806

86	H	7.4209	4.4508	-1.8810
87	O	7.9766	4.1219	-2.5675
88	H	8.7380	4.6677	-2.4980

Appendix J: DHLA-OH Explicitly Solvated by Varying Number of Water Molecules

AJ1: 1 water

NO.	ATOM	X	Y	Z
1	C	0.0000	0.0000	0.0000
2	C	1.3700	0.6220	-0.1930
3	C	2.4750	-0.4240	-0.3540
4	C	3.8630	0.2150	-0.3630
5	C	4.9870	-0.8280	-0.3030
6	C	6.3630	-0.1520	-0.2410
7	C	7.5020	-1.1750	-0.1690
8	C	7.5790	-1.8150	1.1840
9	O	7.9940	-3.1250	1.0490
10	H	8.0790	-3.5960	1.9190
11	O	7.3640	-1.3730	2.2870
12	H	8.4770	-0.6830	-0.3820
13	H	7.3890	-1.9520	-0.9580
14	H	6.4160	0.5260	0.6380
15	H	6.5100	0.4910	-1.1320
16	H	4.9340	-1.4980	-1.1860
17	H	4.8500	-1.4820	0.5810
18	H	3.9550	0.8990	0.5080
19	H	3.9920	0.8610	-1.2530
20	S	2.2200	-1.3770	-1.9010
21	H	2.1240	-0.3630	-2.7860
22	H	2.4050	-1.1860	0.4620
23	H	1.6180	1.2740	0.6720
24	H	1.3480	1.3120	-1.0700
25	S	-1.3310	1.3170	-0.0150
26	H	-0.7530	2.2560	0.7660
27	O	-0.7560	2.1730	-1.4440
28	H	-1.3100	1.8580	-2.1780
29	H	-0.2610	-0.7090	-0.8050
30	H	-0.1000	-0.5310	0.9600
31	H	5.0920	-2.1390	-4.7000
32	O	5.1240	-1.1460	-4.8080
33	H	4.2630	-0.7480	-4.4920

AJ2: 2 water

NO.	ATOM	X	Y	Z
1	C	0.0000	0.0000	0.0000
2	C	1.3700	0.6220	-0.1930
3	C	2.4750	-0.4240	-0.3540
4	C	3.8630	0.2150	-0.3630
5	C	4.9870	-0.8280	-0.3030
6	C	6.3630	-0.1520	-0.2410
7	C	7.5020	-1.1750	-0.1690
8	C	7.5790	-1.8150	1.1840
9	O	7.9940	-3.1250	1.0490
10	H	8.0790	-3.5960	1.9190
11	O	7.3640	-1.3730	2.2870
12	H	8.4770	-0.6830	-0.3820
13	H	7.3890	-1.9520	-0.9580
14	H	6.4160	0.5260	0.6380
15	H	6.5100	0.4910	-1.1320
16	H	4.9340	-1.4980	-1.1860
17	H	4.8500	-1.4820	0.5810
18	H	3.9550	0.8990	0.5080
19	H	3.9920	0.8610	-1.2530
20	S	2.2200	-1.3770	-1.9010
21	H	2.1240	-0.3630	-2.7860
22	H	2.4050	-1.1860	0.4620
23	H	1.6180	1.2740	0.6720
24	H	1.3480	1.3120	-1.0700
25	S	-1.3310	1.3170	-0.0150
26	H	-0.7530	2.2560	0.7660
27	O	-0.7560	2.1730	-1.4440
28	H	-1.3100	1.8580	-2.1780
29	H	-0.2610	-0.7090	-0.8050
30	H	-0.1000	-0.5310	0.9600
31	H	1.0790	-0.6430	4.1050
32	O	1.9700	-0.2330	3.9090
33	H	2.1180	0.5480	4.5150
34	H	4.7890	-0.1410	4.1650
35	O	4.7280	0.8510	4.2780
36	H	4.0710	1.2210	3.6220

AJ3: 3 water

NO.	ATOM	X	Y	Z
1	C	0.0000	0.0000	0.0000
2	C	1.3700	0.6220	-0.1930
3	C	2.4750	-0.4240	-0.3540
4	C	3.8630	0.2150	-0.3630
5	C	4.9870	-0.8280	-0.3030
6	C	6.3630	-0.1520	-0.2410
7	C	7.5020	-1.1750	-0.1690
8	C	7.5790	-1.8150	1.1840
9	O	7.9940	-3.1250	1.0490
10	H	8.0790	-3.5960	1.9190
11	O	7.3640	-1.3730	2.2870
12	H	8.4770	-0.6830	-0.3820
13	H	7.3890	-1.9520	-0.9580
14	H	6.4160	0.5260	0.6380
15	H	6.5100	0.4910	-1.1320
16	H	4.9340	-1.4980	-1.1860
17	H	4.8500	-1.4820	0.5810
18	H	3.9550	0.8990	0.5080
19	H	3.9920	0.8610	-1.2530
20	S	2.2200	-1.3770	-1.9010
21	H	2.1240	-0.3630	-2.7860
22	H	2.4050	-1.1860	0.4620
23	H	1.6180	1.2740	0.6720
24	H	1.3480	1.3120	-1.0700
25	S	-1.3310	1.3170	-0.0150
26	H	-0.7530	2.2560	0.7660
27	O	-0.7560	2.1730	-1.4440
28	H	-1.3100	1.8580	-2.1780
29	H	-0.2610	-0.7090	-0.8050
30	H	-0.1000	-0.5310	0.9600
31	H	3.8430	-2.1730	3.8130
32	O	2.9790	-2.6750	3.8610
33	H	2.2950	-2.1170	4.3280
34	H	3.7330	-3.6190	1.4280
35	O	2.9850	-3.0130	1.6970
36	H	2.1320	-3.5330	1.7390
37	H	2.1260	1.1260	4.4130
38	O	2.6330	0.2840	4.5950
39	H	2.9030	-0.1370	3.7300

AJ4: 4 water

NO.	ATOM	X	Y	Z
1	C	0.0000	0.0000	0.0000
2	C	1.3700	0.6220	-0.1930
3	C	2.4750	-0.4240	-0.3540
4	C	3.8630	0.2150	-0.3630
5	C	4.9870	-0.8280	-0.3030
6	C	6.3630	-0.1520	-0.2410
7	C	7.5020	-1.1750	-0.1690
8	C	7.5790	-1.8150	1.1840
9	O	7.9940	-3.1250	1.0490
10	H	8.0790	-3.5960	1.9190
11	O	7.3640	-1.3730	2.2870
12	H	8.4770	-0.6830	-0.3820
13	H	7.3890	-1.9520	-0.9580
14	H	6.4160	0.5260	0.6380
15	H	6.5100	0.4910	-1.1320
16	H	4.9340	-1.4980	-1.1860
17	H	4.8500	-1.4820	0.5810
18	H	3.9550	0.8990	0.5080
19	H	3.9920	0.8610	-1.2530
20	S	2.2200	-1.3770	-1.9010
21	H	2.1240	-0.3630	-2.7860
22	H	2.4050	-1.1860	0.4620
23	H	1.6180	1.2740	0.6720
24	H	1.3480	1.3120	-1.0700
25	S	-1.3310	1.3170	-0.0150
26	H	-0.7530	2.2560	0.7660
27	O	-0.7560	2.1730	-1.4440
28	H	-1.3100	1.8580	-2.1780
29	H	-0.2610	-0.7090	-0.8050
30	H	-0.1000	-0.5310	0.9600
31	H	0.5200	-0.5530	3.2230
32	O	1.1590	-1.3220	3.2300
33	H	0.6490	-2.1810	3.2310
34	H	3.5490	2.3020	4.1010
35	O	3.3730	3.0800	3.4980
36	H	2.4970	2.9500	3.0330
37	H	4.6640	-1.1950	4.6190
38	O	3.6830	-1.0070	4.5590
39	H	3.5270	-0.0230	4.6380
40	H	2.6510	-4.0210	1.7480
41	O	2.4960	-3.1310	2.1770
42	H	3.3110	-2.5620	2.0690

AJ5: 5 water

NO.	ATOM	X	Y	Z
1	C	0.0000	0.0000	0.0000
2	C	1.3700	0.6220	-0.1930
3	C	2.4750	-0.4240	-0.3540
4	C	3.8630	0.2150	-0.3630
5	C	4.9870	-0.8280	-0.3030
6	C	6.3630	-0.1520	-0.2410
7	C	7.5020	-1.1750	-0.1690
8	C	7.5790	-1.8150	1.1840
9	O	7.9940	-3.1250	1.0490
10	H	8.0790	-3.5960	1.9190
11	O	7.3640	-1.3730	2.2870
12	H	8.4770	-0.6830	-0.3820
13	H	7.3890	-1.9520	-0.9580
14	H	6.4160	0.5260	0.6380
15	H	6.5100	0.4910	-1.1320
16	H	4.9340	-1.4980	-1.1860
17	H	4.8500	-1.4820	0.5810
18	H	3.9550	0.8990	0.5080
19	H	3.9920	0.8610	-1.2530
20	S	2.2200	-1.3770	-1.9010
21	H	2.1240	-0.3630	-2.7860
22	H	2.4050	-1.1860	0.4620
23	H	1.6180	1.2740	0.6720
24	H	1.3480	1.3120	-1.0700
25	S	-1.3310	1.3170	-0.0150
26	H	-0.7530	2.2560	0.7660
27	O	-0.7560	2.1730	-1.4440
28	H	-1.3100	1.8580	-2.1780
29	H	-0.2610	-0.7090	-0.8050
30	H	-0.1000	-0.5310	0.9600
31	H	0.3140	-3.0620	-2.2730
32	O	0.7690	-2.8010	-3.1250
33	H	0.5140	-1.8640	-3.3650
34	H	3.6530	4.3270	-1.5510
35	O	3.3890	4.2180	-2.5100
36	H	4.0380	3.6110	-2.9670
37	H	4.5840	3.7150	0.8310
38	O	3.8260	3.3130	0.3160
39	H	3.0010	3.8600	0.4530
40	H	4.6960	-0.8180	-3.8670
41	O	5.6600	-0.5710	-3.9740
42	H	6.1330	-0.6870	-3.1020

43	H	1.5390	3.1370	-3.0890
44	O	1.9900	2.2920	-3.3770
45	H	1.3280	1.5430	-3.3750

AJ6: 6 water

NO.	ATOM	X	Y	Z
1	C	0.0000	0.0000	0.0000
2	C	1.3769	0.5116	-0.4337
3	C	2.4809	-0.5550	-0.3473
4	C	3.8813	0.0646	-0.5175
5	C	5.0199	-0.9301	-0.2415
6	C	6.4056	-0.2649	-0.2326
7	C	7.5245	-1.2897	0.0166
8	C	7.4235	-1.9576	1.3755
9	O	7.9133	-3.2095	1.3627
10	H	7.7435	-3.5085	2.2722
11	O	6.9619	-1.4931	2.3860
12	H	8.5218	-0.7928	-0.0339
13	H	7.4979	-2.0587	-0.7908
14	H	6.4437	0.5293	0.5509
15	H	6.5799	0.2363	-1.2148
16	H	5.0107	-1.7391	-1.0081
17	H	4.8364	-1.4150	0.7436
18	H	3.9797	0.9093	0.2043
19	H	3.9974	0.5052	-1.5358
20	S	2.1886	-1.8394	-1.6208
21	H	2.4284	-1.0748	-2.7002
22	H	2.4294	-1.0261	0.6604
23	H	1.6247	1.3595	0.2459
24	H	1.3161	0.9461	-1.4593
25	S	-1.1031	1.4074	0.0461
26	H	-1.4233	1.9571	1.2249
27	O	-1.3619	2.3037	-1.4343
28	H	-0.8357	1.9172	-2.1129
29	H	-0.4093	-0.7474	-0.7166
30	H	0.0441	-0.4604	1.0142
31	H	4.2106	0.3396	-4.6566
32	O	3.3677	0.7205	-4.4780
33	H	3.2088	1.3166	-5.1889
34	H	5.1968	-1.6614	3.5587
35	O	4.6340	-0.9450	3.3270
36	H	5.2129	-0.3526	2.8797
37	H	2.6906	-1.3375	2.9939

38	O	2.2292	-0.5567	3.2506
39	H	2.9491	-0.0654	3.6115
40	H	2.6356	-3.3816	0.4673
41	O	3.3823	-3.8032	0.8586
42	H	3.2476	-3.6241	1.7737
43	H	1.2002	-1.9719	2.5206
44	O	1.5627	-2.8243	2.3415
45	H	1.0362	-3.4150	2.8493
46	H	2.0690	1.3846	3.2354
47	O	2.7376	1.8392	2.7510
48	H	2.5193	1.1152	2.1902

AJ7: 7 water

NO.	ATOM	X	Y	Z
1	C	0.0000	0.0000	0.0000
2	C	1.3700	0.6220	-0.1930
3	C	2.4750	-0.4240	-0.3540
4	C	3.8630	0.2150	-0.3630
5	C	4.9870	-0.8280	-0.3030
6	C	6.3630	-0.1520	-0.2410
7	C	7.5020	-1.1750	-0.1690
8	C	7.5790	-1.8150	1.1840
9	O	7.9940	-3.1250	1.0490
10	H	8.0790	-3.5960	1.9190
11	O	7.3640	-1.3730	2.2870
12	H	8.4770	-0.6830	-0.3820
13	H	7.3890	-1.9520	-0.9580
14	H	6.4160	0.5260	0.6380
15	H	6.5100	0.4910	-1.1320
16	H	4.9340	-1.4980	-1.1860
17	H	4.8500	-1.4820	0.5810
18	H	3.9550	0.8990	0.5080
19	H	3.9920	0.8610	-1.2530
20	S	2.2200	-1.3770	-1.9010
21	H	2.1240	-0.3630	-2.7860
22	H	2.4050	-1.1860	0.4620
23	H	1.6180	1.2740	0.6720
24	H	1.3480	1.3120	-1.0700
25	S	-1.3310	1.3170	-0.0150
26	H	-0.7530	2.2560	0.7660
27	O	-0.7560	2.1730	-1.4440
28	H	-1.3100	1.8580	-2.1780
29	H	-0.2610	-0.7090	-0.8050

30	H	-0.1000	-0.5310	0.9600
31	H	4.4650	-3.7950	-0.2880
32	O	3.7030	-3.1630	-0.4340
33	H	2.9260	-3.6600	-0.8180
34	H	3.2320	1.9210	2.4410
35	O	2.9200	0.9710	2.4620
36	H	3.6640	0.3830	2.7760
37	H	5.2660	4.0600	1.6910
38	O	5.8370	3.2410	1.6250
39	H	5.2550	2.4330	1.5530
40	H	-0.0460	0.5090	3.0810
41	O	0.7940	0.1590	3.4950
42	H	0.9060	-0.8060	3.2580
43	H	1.4270	3.0680	2.9470
44	O	0.8170	2.9260	2.1680
45	H	1.1540	3.4430	1.3820
46	H	4.4390	-1.2450	4.5290
47	O	3.7110	-0.6200	4.8120
48	H	2.8610	-0.8650	4.3460
49	H	5.0140	0.1420	-3.6970
50	O	4.0330	0.3170	-3.7790
51	H	3.8260	1.2290	-3.4270

AJ8: 8 water

NO.	ATOM	X	Y	Z
1	C	0.0000	0.0000	0.0000
2	C	1.4391	0.5266	0.0508
3	C	2.4862	-0.5992	0.0100
4	C	3.9242	-0.1120	0.2710
5	C	4.9314	-1.2726	0.3698
6	C	6.2331	-0.8826	1.0850
7	C	7.2182	-2.0602	1.2030
8	C	6.7937	-3.1671	2.1595
9	O	7.8150	-3.9857	2.4866
10	H	7.3895	-4.6214	3.0840
11	O	5.7068	-3.3646	2.6350
12	H	8.1987	-1.6579	1.5532
13	H	7.3629	-2.5014	0.1882
14	H	6.0120	-0.4790	2.1022
15	H	6.7056	-0.0570	0.4992
16	H	5.1725	-1.6415	-0.6541
17	H	4.4650	-2.1221	0.9148
18	H	3.9302	0.4473	1.2352

19	H	4.2512	0.6163	-0.5088
20	S	2.4002	-1.4754	-1.5984
21	H	2.7542	-0.4498	-2.3930
22	H	2.2267	-1.3129	0.8249
23	H	1.5351	1.0873	1.0095
24	H	1.5982	1.2713	-0.7651
25	S	-1.0918	1.3373	0.4669
26	H	-1.3617	1.5535	1.7616
27	O	-1.4777	2.5577	-0.7257
28	H	-2.3448	2.3928	-1.0557
29	H	-0.2756	-0.3527	-1.0200
30	H	-0.1512	-0.8406	0.7159
31	H	2.4629	-3.0313	5.2456
32	O	1.6605	-2.7438	4.8374
33	H	1.3715	-3.4952	4.3506
34	H	2.5709	-0.4528	3.2596
35	O	3.2789	-1.0315	3.4665
36	H	2.9657	-1.4531	4.2488
37	H	3.8649	-3.2759	-2.3773
38	O	4.4222	-3.4400	-3.1192
39	H	4.0864	-4.2307	-3.4992
40	H	1.4423	-4.4493	1.2971
41	O	1.3343	-4.0829	0.4360
42	H	2.0813	-3.5099	0.3864
43	H	3.5946	-3.9083	2.8054
44	O	2.8032	-3.6388	2.3684
45	H	2.6983	-2.7461	2.6450
46	H	3.1565	1.0900	3.8208
47	O	2.2360	1.3029	3.7900
48	H	2.2019	2.2216	3.5873
49	H	4.3933	-2.4129	3.9771
50	O	4.2521	-3.0531	4.6571
51	H	5.0838	-3.4910	4.7090
52	H	5.5277	-1.8980	-2.7628
53	O	5.5933	-1.3165	-3.5003
54	H	5.1080	-1.8072	-4.1404

AJ9: 9 water

NO.	ATOM	X	Y	Z
1	C	0.0000	0.0000	0.0000
2	C	1.3700	0.6220	-0.1930
3	C	2.4750	-0.4240	-0.3540
4	C	3.8630	0.2150	-0.3630

5	C	4.9870	-0.8280	-0.3030
6	C	6.3630	-0.1520	-0.2410
7	C	7.5020	-1.1750	-0.1690
8	C	7.5790	-1.8150	1.1840
9	O	7.9940	-3.1250	1.0490
10	H	8.0790	-3.5960	1.9190
11	O	7.3640	-1.3730	2.2870
12	H	8.4770	-0.6830	-0.3820
13	H	7.3890	-1.9520	-0.9580
14	H	6.4160	0.5260	0.6380
15	H	6.5100	0.4910	-1.1320
16	H	4.9340	-1.4980	-1.1860
17	H	4.8500	-1.4820	0.5810
18	H	3.9550	0.8990	0.5080
19	H	3.9920	0.8610	-1.2530
20	S	2.2200	-1.3770	-1.9010
21	H	2.1240	-0.3630	-2.7860
22	H	2.4050	-1.1860	0.4620
23	H	1.6180	1.2740	0.6720
24	H	1.3480	1.3120	-1.0700
25	S	-1.3310	1.3170	-0.0150
26	H	-0.7530	2.2560	0.7660
27	O	-0.7560	2.1730	-1.4440
28	H	-1.3100	1.8580	-2.1780
29	H	-0.2610	-0.7090	-0.8050
30	H	-0.1000	-0.5310	0.9600
31	H	1.8070	-2.8810	3.4690
32	O	2.8060	-2.9330	3.4300
33	H	3.0810	-3.4990	2.6540
34	H	1.2830	0.1630	2.5360
35	O	0.9420	1.0780	2.7520
36	H	-0.0520	1.0500	2.8480
37	H	5.0000	3.4580	-0.9150
38	O	5.1530	4.0690	-0.1380
39	H	4.3780	4.6920	-0.0450
40	H	1.3060	-1.6630	-4.4420
41	O	2.3030	-1.7130	-4.5090
42	H	2.6350	-0.9720	-5.0910
43	H	0.2180	-3.0510	-0.3440
44	O	0.5640	-3.1740	0.5860
45	H	1.5130	-3.4860	0.5510
46	H	2.1310	0.5820	4.5180
47	O	2.7420	1.2310	4.0640
48	H	2.3300	2.1410	4.0750
49	H	3.5560	-1.2720	4.7660
50	O	3.9610	-0.5990	4.1470

51	H	3.5680	-0.7060	3.2340
52	H	3.8600	1.6130	-3.8610
53	O	4.1900	0.7670	-4.2800
54	H	4.6460	0.2070	-3.5890
55	H	3.0850	2.4700	1.7770
56	O	3.8000	2.2850	2.4520
57	H	4.6950	2.3260	2.0100

AJ10: 10 water

NO.	ATOM	X	Y	Z
1	C	0.0000	0.0000	0.0000
2	C	1.3700	0.6220	-0.1930
3	C	2.4750	-0.4240	-0.3540
4	C	3.8630	0.2150	-0.3630
5	C	4.9870	-0.8280	-0.3030
6	C	6.3630	-0.1520	-0.2410
7	C	7.5020	-1.1750	-0.1690
8	C	7.5790	-1.8150	1.1840
9	O	7.9940	-3.1250	1.0490
10	H	8.0790	-3.5960	1.9190
11	O	7.3640	-1.3730	2.2870
12	H	8.4770	-0.6830	-0.3820
13	H	7.3890	-1.9520	-0.9580
14	H	6.4160	0.5260	0.6380
15	H	6.5100	0.4910	-1.1320
16	H	4.9340	-1.4980	-1.1860
17	H	4.8500	-1.4820	0.5810
18	H	3.9550	0.8990	0.5080
19	H	3.9920	0.8610	-1.2530
20	S	2.2200	-1.3770	-1.9010
21	H	2.1240	-0.3630	-2.7860
22	H	2.4050	-1.1860	0.4620
23	H	1.6180	1.2740	0.6720
24	H	1.3480	1.3120	-1.0700
25	S	-1.3310	1.3170	-0.0150
26	H	-0.7530	2.2560	0.7660
27	O	-0.7560	2.1730	-1.4440
28	H	-1.3100	1.8580	-2.1780
29	H	-0.2610	-0.7090	-0.8050
30	H	-0.1000	-0.5310	0.9600
31	H	1.9940	-0.2630	4.1780
32	O	2.3530	-0.0800	3.2620
33	H	3.2800	0.2850	3.3340

34	H	4.8610	-2.5600	2.5420
35	O	3.9060	-2.6100	2.2490
36	H	3.4920	-1.7020	2.3000
37	H	1.2550	-3.6040	2.5860
38	O	0.7400	-2.7470	2.5660
39	H	1.3750	-1.9750	2.5590
40	H	5.7470	2.8360	-2.1930
41	O	5.3170	2.7130	-3.0880
42	H	4.7090	1.9210	-3.0600
43	H	-0.4230	0.9760	2.5280
44	O	0.2230	0.4430	3.0750
45	H	-0.1240	-0.4870	3.1880
46	H	4.1810	2.2760	4.0780
47	O	3.4270	2.4780	3.4530
48	H	3.7850	2.6100	2.5290
49	H	3.8240	-1.3490	4.7000
50	O	3.7530	-2.3080	4.4240
51	H	2.8000	-2.5260	4.2160
52	H	4.7840	-1.9460	-3.4360
53	O	4.0800	-2.5270	-3.0270
54	H	4.1510	-3.4510	-3.4000
55	H	1.7730	-4.0840	0.5010
56	O	0.8660	-3.6680	0.4220
57	H	0.4540	-3.9300	-0.4500
58	H	1.8230	3.6060	2.3780
59	O	1.5040	2.6580	2.3670
60	H	1.2350	2.3860	3.2910

AJ11: 20 water

NO.	ATOM	X	Y	Z
1	C	0.0000	0.0000	0.0000
2	C	1.3591	0.6915	-0.1575
3	C	2.5402	-0.2894	-0.2810
4	C	3.9090	0.3955	-0.1300
5	C	5.0657	-0.5838	0.1358
6	C	6.3609	0.1549	0.5215
7	C	7.3971	-0.7749	1.1721
8	C	6.9987	-1.2278	2.5629
9	O	7.4167	-2.4733	2.8396
10	H	6.9054	-2.6698	3.6389
11	O	6.3213	-0.6373	3.3707
12	H	8.3677	-0.2437	1.3050
13	H	7.5659	-1.6420	0.4889

14	H	6.1345	0.9911	1.2253
15	H	6.7964	0.6223	-0.3941
16	H	5.2323	-1.2423	-0.7448
17	H	4.7876	-1.2860	0.9494
18	H	3.8433	1.0715	0.7504
19	H	4.1433	1.0406	-1.0087
20	S	2.4732	-1.1537	-1.8972
21	H	2.4600	-0.0777	-2.7040
22	H	2.4471	-1.0349	0.5391
23	H	1.4836	1.3271	0.7499
24	H	1.3277	1.3928	-1.0239
25	S	-1.2461	1.2541	0.2842
26	H	-1.4468	1.7342	1.5191
27	O	-2.0738	1.9858	-1.0759
28	H	-2.1328	1.3521	-1.7695
29	H	-0.2744	-0.5820	-0.9083
30	H	-0.0002	-0.6886	0.8755
31	H	4.6812	-1.6899	4.3996
32	O	5.1158	-1.8371	5.2220
33	H	5.9247	-2.2021	4.9098
34	H	3.1255	-3.5880	0.7860
35	O	3.4068	-4.2119	1.4396
36	H	3.1785	-3.7859	2.2537
37	H	2.1321	-4.7034	0.0136
38	O	1.5483	-4.0555	-0.3385
39	H	1.9482	-3.8944	-1.1775
40	H	4.9990	1.9096	4.4009
41	O	4.6491	1.7713	3.5373
42	H	4.8238	0.8637	3.3580
43	H	6.6493	1.5450	3.2257
44	O	7.5401	1.6415	3.5221
45	H	7.5324	1.0856	4.2836
46	H	6.4851	-0.1372	5.5701
47	O	5.9315	0.6173	5.4707
48	H	5.1985	0.2268	5.0163
49	H	4.1081	3.6888	2.3540
50	O	3.3976	3.2623	1.9061
51	H	3.5206	2.3640	2.1612
52	H	1.4461	-3.7690	1.7047
53	O	1.4603	-2.8349	1.8558
54	H	1.1041	-2.5189	1.0452
55	H	1.8711	-3.1155	3.6040
56	O	2.3393	-3.7277	4.1426
57	H	2.2696	-3.2864	4.9721
58	H	4.3494	-3.5875	4.0267
59	O	4.8697	-3.2555	3.3160

60	H	4.8395	-3.9395	2.6742
61	H	1.8504	-0.5830	5.0733
62	O	1.7695	-1.3528	4.5358
63	H	1.3670	-0.9897	3.7633
64	H	5.0349	0.9943	-3.2542
65	O	5.8821	0.5900	-3.3123
66	H	6.4312	1.2096	-3.7609
67	H	2.8776	0.7028	3.8946
68	O	2.0002	0.8880	3.5904
69	H	2.0875	1.7665	3.2662
70	H	4.3841	-4.2862	-1.8345
71	O	3.9191	-4.1483	-1.0286
72	H	4.5767	-4.3468	-0.3825
73	H	4.1107	0.3662	6.4602
74	O	3.4456	0.1850	5.8173
75	H	3.6453	-0.6854	5.5078
76	H	4.3366	-2.6212	-2.6075
77	O	4.6753	-3.1333	-3.3250
78	H	5.5405	-3.3733	-3.0308
79	H	6.8399	-0.8530	-2.7234
80	O	6.5916	-1.7528	-2.8245
81	H	5.9569	-1.6948	-3.5201
82	H	-0.2074	-3.9211	-1.2887
83	O	-0.0771	-3.2225	-1.9067
84	H	0.5809	-2.6935	-1.4870
85	H	2.9658	-1.0118	3.0972
86	O	3.8341	-0.6534	3.0595
87	H	4.3652	-1.3507	2.7280
88	H	6.5985	-3.1203	-1.4051
89	O	6.3930	-4.0349	-1.3113
90	H	7.2050	-4.4794	-1.4851

VITA

MATTHEW GLENN BONFIELD

Education:	M.S. Chemistry, East Tennessee State University, Johnson City, Tennessee, 2021
	B.A. Chemistry, University of North Carolina at Charlotte, Charlotte, North Carolina, 2019
Professional Experience:	Lab Technician, Eastman Chemical Company; Kingsport, Tennessee, 2021-present
	Graduate Assistant, East Tennessee State University, College of Arts and Sciences, 2019-2021
Publications:	Zuczek, J.; Bonfield, M.; Elathram, N.; R. Hixson, W.; Kongruengkit, T.; B. Mitchell, J.; Zelenka, N.; D. Popov, L.; Morozov, A.; N. Shcherbakov, I.; C. Poler, J. Characterization of Molecular Spacer-Functionalized Nanostructured Carbons for Electrical Energy Storage Supercapacitor Materials. *C* **2020**, *6* (4), 66.

Conference Presentation:	"Computational Analysis of the Spin Trapping Properties of Lipoic Acid and Dihydrolipoic Acid." Oral presentation at SERMACS 2021, Birmingham, AL
Research Funding:	Matthew G. Bonfield and Scott J. Kirkby, "Computational Studies of alpha-Lipoic Acid as a Spin Trap Under Explicit Solvation," ETSU School of Graduate Studies Graduate Student Research Grants, $670, 2020